THE *C. ELEGANS* HOMOLOG OF *DROSOPHILA* LETHAL GIANT LARVAE FUNCTIONS REDUNDANTLY WITH PAR-2 TO MAINTAIN POLARITY IN THE EARLY EMBRYO

A Dissertation

Presented to the Faculty of the Graduate School

of Cornell University

In Partial Fulfillment of the Requirements for the Degree of

Doctor of Philosophy

by

Alexander Beatty

January 2012

THE *C. ELEGANS* HOMOLOG OF *DROSOPHILA* LETHAL GIANT LARVAE FUNCTIONS REDUNDANTLY WITH PAR-2 TO MAINTAIN POLARITY IN THE EARLY EMBRYO

Alexander Beatty, Ph. D.

Cornell University 2012

Polarity is essential for generating cell diversity. The one-cell *C. elegans* embryo serves as a model for studying the establishment and maintenance of polarity. In the early embryo, a myosin II-dependent contraction of the cortical meshwork asymmetrically distributes the highly conserved PDZ proteins PAR-3 and PAR-6 as well as an atypical protein kinase C (PKC-3) to the anterior. The RING-finger protein PAR-2 becomes enriched on the posterior cortex and prevents these three proteins from returning to the posterior. In addition to the PARs, other proteins are required for polarity in many metazoans. One example is the conserved *Drosophila* tumor-suppressor protein Lethal (2) giant larvae (Lgl). In *Drosophila* and mammals, Lgl contributes to the maintenance of cell polarity and plays a role in asymmetric cell division. We have found that the *C. elegans* homolog of Lgl, LGL-1, has a role in polarity but is not essential. It localizes asymmetrically to the posterior of the early embryo in a PKC-3-dependent manner, and functions redundantly with PAR-2 to maintain polarity. Furthermore, over-expression of LGL-1 is sufficient to rescue loss of PAR-2 function. LGL-1 negatively regulates the accumulation of myosin (NMY-2) on the posterior cortex in an anterior PAR-dependent manner.

BIOGRAPHICAL SKETCH

Alexander Beatty was born in eastern Pennsylvania in June of 1983. He was an energetic and inquisitive child. In fact, he needed to have a lid attached to his crib to prevent him from escaping to explore the neighborhood in the middle of the night. His parents encouraged him to start playing sports at an early age to positively channel his energy. With the addition of sports and outdoor activities, Alex had an easier time focusing, and was able to do fairly well in grade school and high school. Science always came most naturally to him.

After graduating high school, he was fortunate enough to have the opportunity to attend Ursinus College. During his time at Ursinus, he was inspired by a number of excellent mentors who not only educated him, but also gave him the confidence to pursue science as a career. In addition, Ursinus is where he got his start in research. He chose to study the early *C. elegans* embryo in Rebecca Lyzcak's lab. He graduated in 2005 with a BS in Biochemistry and Molecular Biology and a minor in Chemistry. In August of 2005, Alex began graduate school at Cornell University. He joined the Kemphues Lab in spring of 2006, where he has worked happily for the past six years.

ACKNOWLEDGMENTS

A tremendous number of people have helped me develop as a scientist and as a person. First and foremost, I would like to thank Kenneth Kemphues for giving me the opportunity to work his laboratory and for being an excellent mentor. I truly appreciate the guidance and the scientific freedom he afforded me during my time in the lab. I would also like to thank my committee members, Sylvia Lee and Tony Bretscher as well as members of the Kemphues Lab past and present, particularly Diane Morton, Bingsi Li, Heon Kim, Rich McCloskey, Wendy Hoose, Mona Hassab, Julia Rosenburg, Jin Li, and Melissa Beers. I am also grateful to all of the members of the Cornell Worm Group and Deborah Nero for her guidance.

During my time at Ursinus I was lucky enough to have several excellent mentors that inspired me. I am very grateful to Rebecca Lyczak and Christopher Shelton for teaching me how to approach scientific research, and showing me how much fun research can be. I would like to thank Tom Ruttledge for pushing me to excel in the classroom, and giving me lots of great advice.

I would also like to thank my friends including my best friends Joel and Amy Keeler, and all of the friends I have had the pleasure of meeting during my time at Cornell. Special thanks to Srich Murugesan, Gizem Rizki, Aaron Plys, Yin He, Rajni Singh, Damien Garbett, and Songeun Lee. I am also very grateful to my training partners Ken Kawamoto and James Brooks.

And last but not least, I would like to thank my family, especially my Mother and Father, Maryann and Lance for giving me unconditional supportive and love.

TABLE OF CONTENTS

LIST OF FIGURES

CHAPTER THREE

APPENDIX

LIST OF TABLES

CHAPTER ONE

INTRODUCTION

I. CELL POLARITY

Cell polarity refers to the asymmetric distribution of molecular components within a cell, and is critical feature of numerous cell types. The establishment and maintenance of polarity are required for essentially every stage of development as well as many physiological processes. In embryos and stem cells, cell polarity directs the partitioning of cell fate determinants, which facilitates asymmetric cell division (Gonczy, 2008; Knoblich, 2008). Polarity is also coordinated across tissues during morphogenesis to direct the orientation of common cellular structures (Goodrich and Strutt, 2011). After differentiation, cell polarity is necessary for a number of processes such as neuronal signaling, polarized membrane trafficking, cell migration, and wound healing (Suzuki and Ohno, 2006). In addition to being required for many developmental and physiological processes, failure to establish or maintain cell polarity is associated with a number of pathologies. Perhaps most notably, loss of polarity and tissue architecture is hallmark of cancerous cells, and emerging evidence suggests that loss of polarity plays a causal role in tumor formation (Lee and Vasioukhin, 2008).

Because of its fundamental role in biology, substantial effort has been made to understand the basis of cell polarity. For more than two decades, the embryo of the nematode *Caenorhabditis elegans* has served as a fruitful model system for studying cell polarity and asymmetric cell division. The one-cell *C. elegans* embryo establishes an anterior-posterior axis shortly after fertilization, and studies using this model have led to key mechanistic insights and the identification of conserved molecules central to

the processes (Goldstein and Macara, 2007; Nance and Zallen, 2011; St Johnston and Ahringer, 2010).

II. POLARITY IN THE EARLY *C. ELEGANS* EMBRYO

Shortly after fertilization, the one-cell *C. elegans* embryo establishes anterior-posterior polarity, which results in the formation of distinct cortical domains and the asymmetric distribution of cytoplasmic cell fate determinants (Munro and Bowerman, 2009; Nance and Zallen, 2010; Schneider and Bowerman, 2003). The establishment and maintenance of polarity are mediated by a group of conserved polarity regulators collectively known as the PAR (*par*titioning-defective) proteins (Goldstein and Macara, 2007). There are two antagonistic sets of PAR proteins: one includes the PDZ-containing proteins PAR-3 and PAR-6 as well as a serine/threonine kinase, PKC-3, while the other is composed of another kinase PAR-1 and the putative E3 ubiquitin ligase PAR-2 (or the WD40-repeat protein Lethal giant larvae (Lgl) in other polarity systems) (Goldstein and Macara, 2007; Nance and Zallen, 2010; St Johnston and Ahringer, 2010). Consistent with their antagonistic relationship, the two sets of PAR proteins localize to reciprocal asymmetric cortical domains in the early embryo (Boyd et al., 1996; Etemad-Moghadam et al., 1995; Guo and Kemphues, 1995; Hung and Kemphues, 1999; Tabuse et al., 1998). Furthermore, two additional PAR proteins, the 14-3-3 protein PAR-5 and another serine/threonine kinase PAR-4, contribute to cell polarity but are not asymmetrically localized (Morton et al., 2002; Watts et al., 2000).

2.1 Polarity Establishment

Prior to fertilization, the oocyte is arrested in prophase of meiosis I and lacks specified body axes. Sperm entry triggers the completion of meiosis and provides a positional cue for anterior-posterior axis formation. The pole of the oblong oocyte closest to the point of sperm entry becomes the posterior pole of the zygote. In the early embryo, the completion of meiosis II coincides with the onset of a phenomenon known as cortical ruffling. During this time, a non-muscle myosin II heavy chain, NMY-2, and F-actin are organized into an extensive network of large foci interconnected by finer filaments (Munro et al., 2004; Velarde et al., 2007). The actomyosin network provides uniform cortical tension throughout the embryo, and the cortical ruffling results from transient contractions of the actomyosin network with no net directionality (Munro et al., 2004).

As the zygote enters the first mitotic interphase, a transient cue associated with the sperm centrosome/microtubule organizing center positioned in the posterior pole breaks the symmetry of the ruffling embryo, and initiates smoothing along the posterior cortex (Goldstein and Hird, 1996). The exact nature of the cue that initiates symmetry breaking remains a point of contention (Motegi and Seydoux, 2007). Evidence suggests that the trigger is either the interaction of astral microtubules with cortex or a diffusible signal from the centrosome. In mutants defective for centrosome maturation, the remnant of the acentrosomal meiotic spindle is sufficient to initiate the formation of distinct cortical domains (Wallenfang and Seydoux, 2000), indicating that microtubules may be sufficient to break symmetry. Furthermore, in embryos depleted for tubulin, anterior-posterior polarity is only established in embryos that formed observable asters (Tsai and Ahringer, 2007). However, strong depletion of

microtubules using RNAi targeted against γ-/β-tubulin combined with nocodazole treatment does not prevent polarity establishment, suggesting that it is the centrosome, and not the associated aster, that initiates polarity (Cowan and Hyman, 2004). Thus, the symmetry-breaking cue appears to be associated with the sperm centrosome/microtubule organizing center, but definitively separating the requirement for the centrosome or the associated microtubule aster has proved challenging.

Although the precise nature of the initial cue that breaks symmetry in the early embryo remains mysterious, the downstream events that lead to the establishment of polarity are better understood. Polarity establishment is thought to proceed via an asymmetric contraction of the actomyosin network, which serves to generate cortical flows that partition cortical polarity components (Munro et al., 2004). The contraction is initiated by precise spatial and temporal regulation of the rho GTPase RHO-1 (Jenkins et al., 2006; Motegi and Sugimoto, 2006; Schonegg and Hyman, 2006). Prior to establishment, RHO-1 and its primary GEF, ECT-2 (Jenkins et al., 2006; Motegi and Sugimoto, 2006; Schonegg and Hyman, 2006), are symmetrically distributed on the cortex of the embryo (Motegi and Sugimoto, 2006). In response to the symmetry-breaking cue, the level of cortical ECT-2 on the posterior cortex near the centrosome decreases. The cortical clearing of ECT-2 requires a functional centrosome, but not RHO-1 or myosin contractility (Motegi and Sugimoto, 2006). As a result of the decrease in ECT-2, cortical RHO-1 levels, and presumably activity, near the posterior pole are reduced (Motegi and Sugimoto, 2006). Additionally, a paternally derived rho-GAP, CYK-4, localized in the vicinity of the centrosome may also contribute to lessening the amount of active RHO-1 on the posterior cortex (Jenkins et al., 2006).

Active RHO-1 likely promotes the activating phosphorylation of the regulatory

myosin light chain MLC-4 (Jenkins et al., 2006; Kumfer et al., 2010; Zonies et al., 2010), enabling myosin to interact with cortical actin and facilitating contractility (Riento and Ridley, 2003). Thus, the overall result of the asymmetry in the RHO-1 distribution and activity is the formation of a contractility gradient with a local down regulation of contractile forces in the posterior, which triggers an NMY-2-dependent contraction of the actomyosin cytoskeleton toward the anterior (Fig. 1.1D; Motegi and Sugimoto, 2006; Munro et al., 2004). The contractility gradient coupled with the high viscosity of the cortex generates polarizing cortical flows in the direction of the anterior (Cheeks et al., 2004; Mayer et al.; Munro et al., 2004).

Prior to the onset of the cortical flows, PAR-3, PAR-6 and PKC-3 are cortical and symmetrical, but coincidently with the onset of the flows, these proteins begin to clear from the posterior cortex and become enriched on the anterior cortex (Fig. 1.1 A; Cheeks et al., 2004; Cuenca et al., 2003; Munro et al., 2004). While it is not clear whether the anterior PAR proteins are directly associated with the cortical meshwork or whether the polarity regulators are passively transported to the anterior by the cortical flows, the boundary of the anterior cortical domain coincides with posterior edge of the contracting actomyosin network (Munro et al., 2004). As the anterior PAR proteins, PAR-3, PAR-6, and PKC-3, become enriched on the anterior cortex, the posterior PAR proteins, PAR-1 and PAR-2, become enriched in the reciprocal cortical domain (Fig 1.1C; Cuenca et al., 2003).

The anterior domain contracts and the posterior domain expands until each of the domains occupies approximately half of the cortical area. The mechanism by which the contraction is halted is not well understood, but the attenuation of the RHO-1-mediated contractility appears to be regulated, at least in part, by the redundant Rho-

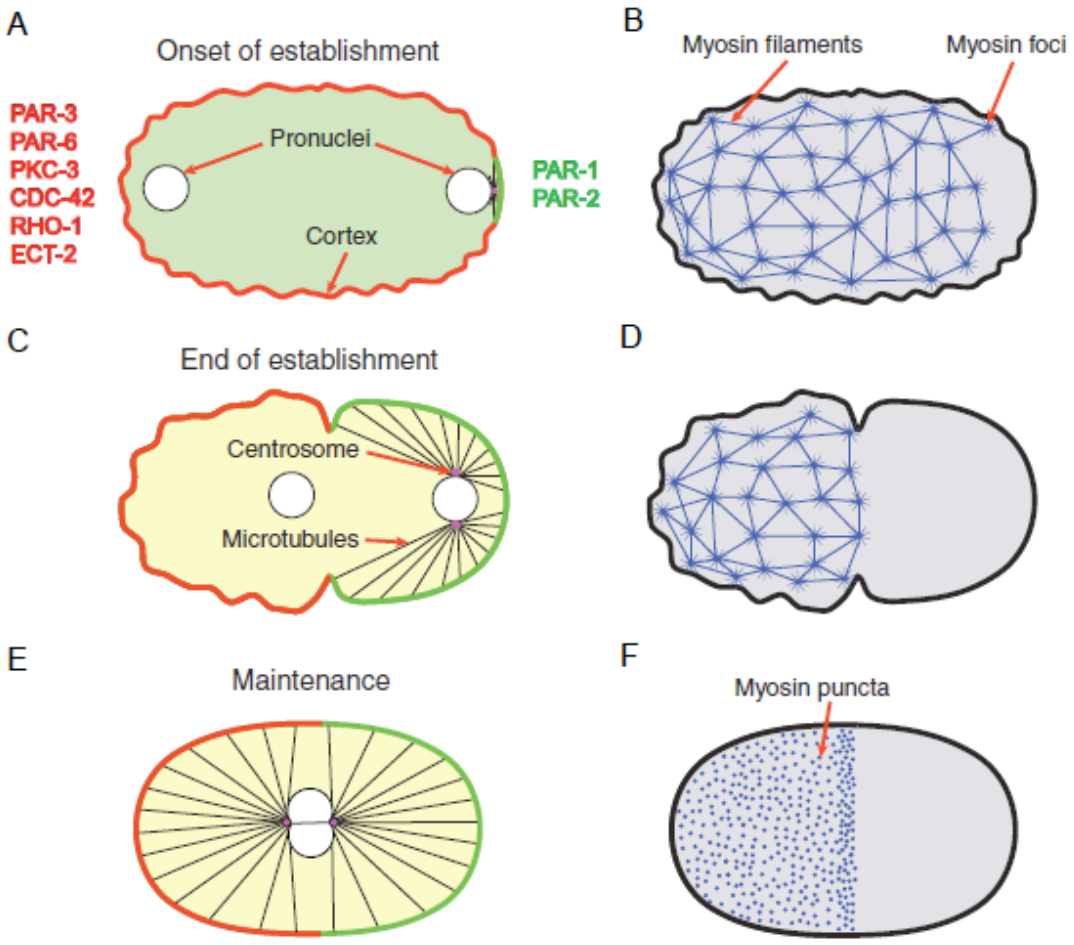

Fig. 1.1. Establishment and Maintenance of cortical asymmetries in the one-cell embryo. The anterior cortical domain and posterior cortical domain are shown in red and green, respectively. Adjacent panels depict similar time points. **(**Figure modified from Nance and Zallen, 2011).

GAPs, RGA-3/4 (Schonegg et al., 2007). The asymmetric distribution of the actomyosin cytoskeleton toward the anterior gives rise to a transient cortical invagination, called the pseudocleavage furrow, that marks the boundary between the contractile anterior cortex and the smooth posterior cortex (Munro et al., 2004). In addition, pseudocleavage also denotes a temporal boundary between the "establishment" and "maintenance" phases of polarity (Cuenca et al., 2003).

Although the primary mechanism of polarity establishment is mediated by RHO-1-regulated actomyosin contractility, Zonies and colleagues have recently uncovered a secondary mechanism that is dependent on the putative E3 ubiquitin ligase, PAR-2 (Zonies et al., 2010). When contractility is compromised by depleting MLC-4 or by a partial loss of function mutation in *ect-2*, PAR-2 is sufficient to partition cortical domains. In the hypomorphic *ect-2* mutant, PAR-2 appears to initiate cortical flow by antagonizing PAR-3-dependent cortical myosin. However, PAR-2 can also initiate PAR asymmetry in *mlc-4(RNAi),* suggesting that the PAR-2-dependent polarity pathway can function in the near absence of cortical contractility. While this secondary polarity establishment mechanism is not required, it likely enhances the robustness of polarity establishment.

1.2 Polarity Maintenance

Pseudocleavage marks a transitional period that separates polarity establishment and maintenance (Cuenca et al., 2003). During the transition, the pseudocleavage furrow recedes and the highly contractile anterior cortex begins to smooth as the actomyosin network is reorganized from large contractile foci into finer filaments (Fig 1.1F, (Munro et al., 2004)). Additionally, the pronuclei begin to

migrate and eventually meet toward the posterior of the embryo. After meeting, the joined pronuclei center and rotate, the nuclear envelope breaks down, and the first mitotic division proceeds. During these events, the cortical asymmetries generated by the cortical flows must be maintained (Fig 1.1E).

The maintenance of distinct cortical domains in the early embryo is mediated primarily by rho signaling and mutually antagonistic interactions between the anterior and posterior PAR proteins (Nance and Zallen, 2011). Unlike polarity establishment, which requires RHO-1, the rho-GTPase CDC-42 appears to be key Rho signaling protein during polarity maintenance (Kumfer et al., 2010; Motegi and Sugimoto, 2006; Schonegg and Hyman, 2006). During the maintenance phase, CDC-42 is enriched on the anterior cortex (Aceto et al., 2006; Motegi and Sugimoto, 2006; Schonegg and Hyman, 2006), and its active form interacts with the anterior PAR proteins via direct binding to PAR-6 (Aceto et al., 2006; Gotta et al., 2001). In *cdc-42(RNAi)* embryos, PAR-6 and PKC-3 become asymmetrically enriched on the anterior cortex at a reduced level during establishment, and are lost from the cortex around the time of nuclear envelope breakdown. PAR-3 remains cortical but often extends into the posterior and can overlap with PAR-2 (Gotta et al., 2001; Kay and Hunter, 2001). Embryos expressing a mutant PAR-6 defective for CDC-42 binding exhibit similar defects as *cdc-42(RNAi)* embryos suggesting that CDC-42 functions in polarity primarily via its physical interaction with PAR-6 (Aceto et al., 2006).

Reduction of CDC-42 function also results in defects in cortical myosin localization. In embryos depleted for CDC-42, NMY-2 dynamics are similar to wild type during establishment; however, cortical myosin is largely lost during the transition to the maintenance phase when myosin foci are normally reorganized and

replaced by finer filaments (Kumfer et al., 2010; Motegi and Sugimoto, 2006; Schonegg and Hyman, 2006). Because CDC-42 is required for the maintenance of cortical PAR-6/PKC-3 as well as cortical myosin, CDC-42 appears to provide a functional link between the anterior PAR proteins and the acto-myosin cytoskeleton during polarity maintenance.

The activity of CDC-42 in the early embryo is regulated, at least in part, by a putative CDC-42 GTPase activating protein, CHIN-1, and a guanidine exchange factor, CGEF-1 (Kumfer et al., 2010). These regulators were identified using a biosensor that specifically binds active GTP-bound CDC-42: *chin-1(RNAi)* one-cell embryos have increased cortical levels of active CDC-42 while *cgef-1(RNAi)* embryos have reduced cortical levels of active CDC-42. During polarity maintenance, CHIN-1 appears to inhibit NMY-2 accumulation on the posterior cortex, and CGEF-1 is required for robust recruitment of cortical NMY-2 in the anterior (Kumfer et al., 2010). Although *cgef-1(RNAi)* embryos display weak polarity phenotypes, the polarity perturbations in these embryos are not nearly as dramatic as in *cdc-42(RNAi)* embryos suggesting redundancy in CDC-42 regulation.

In addition to CDC-42-mediated Rho signaling, the anterior and posterior PAR proteins act in a mutually antagonistic manner to maintain the cortical asymmetries generated during establishment (Goldstein and Macara, 2007; Cheeks et al., 2004; Cuenca et al., 2003; Boyd et al., 1996; Etemad-Moghadam et al., 1995; Tabuse et al., 1998; Watts et al., 1996). The anterior PAR proteins exclude the posterior PAR proteins from the anterior cortex and vice versa. In *par-2* mutants, the anterior cortical domain extends into the posterior, suggesting PAR-2 is required to exclude the

anterior PAR proteins from the posterior (Cheeks et al., 2004; Munro et al., 2004). Munro and colleagues have proposed that PAR-2 may regulate cortical flows based on the observation that *par-2(RNAi)* embryos exhibit cortical flows directed toward the posterior during polarity maintenance (2004). The aberrant cortical flows are associated with appearance of ectopic NMY-2 fibers in the posterior as well as the redistribution of PAR-6::GFP to the posterior cortex. In addition, NMY-2 accumulates at uniformly low levels around the cortex in *par-3* embryos and uniformly high levels in *par-3; par-2(RNAi)* embryos. The uniformly high cortical levels of NMY-2 in *par-3; par-2(RNAi)* embryos indicate that the posterior cortical accumulation of NMY-2 in *par-2* is not an indirect consequence of a failure to restrict the anterior PAR proteins to the anterior cortical domain. These results suggest that PAR-2 could potentially act to maintain polarity by inhibiting NMY-2 accumulation on the posterior cortex, preventing cortical flows directed towards the posterior. However, the mechanism by which PAR-2 could exclude cortical myosin is unclear. On the anterior cortex, phosphorylation by PKC-3 antagonizes the cortical localization of PAR-2, and likely PAR-1, thus preventing the posterior cortical domain from extending into the anterior (Hao et al., 2006; Benton and St Johnston, 2003). Additionally, the 14-3-3 protein PAR-5 is also required for anterior and posterior protein to be mutually exclusive (Morton et al., 2002).

Although some of the details regarding the antagonistic interactions between the anterior and posterior PAR proteins have been determined, the exact molecular mechanisms by which polarity is maintained are not well understood. During the maintenance phase, the sizes of reciprocal PAR domains are stable, however, the individual PAR proteins exchange rapidly between the cortex and the cytoplasm

(Cheeks et al., 2004). Furthermore, cortical PAR proteins can diffuse freely across the anterior-posterior domain boundary. Free diffusion on the cortex combined with the rapid exchange of the PAR proteins between the cortex and the cytoplasm results in a flux on the interface between the anterior and posterior domain. The observation that the PAR proteins can diffuse freely on the cortex suggests the PAR proteins can maintain cortical domain polarity by a mechanism that does not rely on diffusion barriers, lateral sorting, or active transport (Goehring et al., 2011).

The mutual antagonism between anterior and posterior PAR proteins appears very sensitive to changes in protein levels (Hyenne et al., 2008; Watts et al., 1996; Zonies et al., 2010). For example, reducing the dose of PAR-6 is sufficient to partially rescue the maternal-effect embryonic lethality associated with a putative null *par-2* mutant (Watts et al., 1996). Similarly, decreasing CDC-42 levels suppresses PAR-2 depletion or mutation indicating PAR-2 and CDC-42 act antagonistically during polarity maintenance (Gotta et al., 2001; Kay and Hunter, 2001; Schonegg and Hyman, 2006). Although mechanistic details that underlie these genetic relationships are not clear, these observations suggest that there are additional PAR-2-independent pathways that antagonize the function of the anterior PAR proteins.

Although significant progress has been made toward understanding polarity maintenance, a number of key questions remain. What is the molecular mechanism by which PAR-2 acts to exclude the anterior PAR proteins from the posterior cortex and influence cortical flow? Are there additional, PAR-2-independent polarity maintenance pathways, and if so, what are the factors involved? Additionally, how do all of the polarity maintenance components cooperate and what is the level of interaction between them?

III. Lethal Giant Larvae

Members of the Lgl family of proteins function in cell polarity (Vasioukhin, 2006; Wirtz-Peitz and Knoblich, 2006). The first *lgl* alleles were isolated in *Drosophila* by Bridges and studied by Hadorn in the 1930's. The gene name was derived from the phenotype of the zygotic mutant; mutation of *lgl* results in marked hyperplasia of the brain and imaginal discs in larvae, ultimately leading to lethality (Bilder, 2004). Several decades after the initial studies, Lgl became the subject of further research when an additional, spontaneous *lgl* allele was isolated by Gateff and Schneiderman, and it was observed that the hyperplasic tissue in the *lgl* mutant resembled neoplastic tumors (Gateff, 1978). More specifically, the overgrown tissue in the *lgl* mutant exhibited a loss of polarity and failed to differentiate (Bilder, 2004). Because of the aforementioned phenotypes, *lgl* is one of only three *Drosophila* genes [along with *discs-large (dlg)* and *scribble (sribb)*] classified as a neoplastic tumor suppressor (Bilder, 2004).

The overall sequence and domain structure of Lgl is well conserved in metazoans. Lgl family members contain a characteristic C-terminal "Lgl domain" that is not predicted to have a catalytic function. The protein also includes a highly conserved series of aPKC phosphorylation consensus sequences (Vasioukhin, 2006). The N-terminal domain of Lgl homologs typically contains a series of WD-40 repeats that are predicted to form consecutive seven-bladed β-propeller structures. β-propeller structures are often involved in protein-protein interactions suggesting Lgl family members act as protein scaffolds (Vasioukhin, 2006).

Lgl is required for polarity in a number cell types (reviewed in Vasioukhin, 2006; Wirtz-Peitz and Knoblich, 2006). In *Drosophila*, Lgl is involved in the

maintenance of polarity in epithelial cells (Bilder et al., 2000; Hutterer et al., 2004). In *Drosophila* embryonic epithelial cells, Lgl is primarily localized to the basolateral membrane where it contributes to the maintenance of polarity by restricting apical proteins to the appropriate cortical domain (Hutterer et al., 2004). Lgl acts by antagonizing the activity of apical protein complexes consisting of Par6-Bazooka(Par-3)-aPKC and Crumbs-Stardust-Patj (Hutterer et al., 2004; Tanentzapf and Tepass, 2003). Similarly, the apical complexes act to inhibit Lgl function on the apical membrane (Hutterer et al., 2004). This antagonistic relationship results in the maintenance of distinct cortical domains, and is reminiscent of the mutual exclusion feedback loop that facilitates polarity maintenance in the *C. elegans* embryo.

Recent studies have shown that Lgl is involved in the polarization of the anterior-posterior axis in the *Drosophila* oocyte (Doerflinger et al., 2010; Fichelson et al., 2010; Li et al., 2008; Tian and Deng, 2008). In the early oocyte, Lgl is required for the proper posterior translocation of cell fate determinants as well as the centrosomes (Fichelson et al., 2010; Tian and Deng, 2008). At mid-oogenesis, phosphorylation by aPKC restricts Lgl to the posterior of the oocyte, along with Par-1 (Tian and Deng, 2008). After the oocyte has been polarized into distinct cortical domains, Lgl likely stabilizes the cortical localization of Par-1, and these proteins act to reciprocally inhibit the anterior Baz complex. As in other contexts, the mutual antagonism between proteins in opposing cortical domains serves to maintain polarity (Doerflinger et al., 2010).

Drosophila Lgl also plays a role in asymmetric cell division (Ohshiro et al., 2000; Peng et al., 2000; Wirtz-Peitz et al., 2008). In neuroblasts, Lgl is required for the basal targeting of fate determinants prior to mitotic division. In this context, Lgl

plays a role in the formation of polarity early in mitosis (Ohshiro et al., 2000; Peng et al., 2000; Wirtz-Peitz and Knoblich, 2006) and also appears to be involved in spindle positioning (Albertson and Doe, 2003). Lgl is also involved in the asymmetric cell divisions of sensory organ precursors (SOPs), where the protein is involved in the asymmetric localization of the cell-fate determinant Numb (Wirtz-Peitz et al., 2008).

Lgl also plays a key role in polarity in mammals, which have two Lgl orthologs, *Llgl1* and *Llgl2*. *Llgl1* knockout mice exhibit loss of polarity in neural progenitor cells of the developing brain. The loss of polarity and asymmetric cell division cause excessive neural proliferation without differentiation. As a result, *Llgl1*$^{-/-}$ mice die neonatally due to severe hydrocephalus (Klezovitch et al., 2004). Although *Llgl2* knock out mice exhibit placental branching defects, the protein is not required for proper development, possibly suggesting redundant function (Sripathy et al.). Loss of human Lgl (Hugl-1) function has been implicated in human cancers. Reduced expression of *Hugl-1* and over-expression of aPKCζ and aPKCι have both been linked to tumor progression in epithelial tissues (Schimanski et al., 2005; Grifoni et al., 2007).

Currently, the molecular mechanism by which Lgl participates in polarity is not well understood. Results from *Drosophila* and mammalian cells suggest three non-mutually exclusive hypotheses to explain how LGL-1 could function (Wirtz-Peitz et al., 2008; Vasioukhin, 2006; Wirtz-Peitz and Knoblich, 2006). One hypothesis, based initially on work on the LGL-1 homologues Sro7/77 in yeast (Hattendorf et al., 2007; Vasioukhin, 2006; Wirtz-Peitz and Knoblich, 2006) is that LGL could regulate polarized vesicular trafficking. Additional evidence from metazoans supports this role: Mlgl binds a component of the exocytic machinery, syntaxin-4, in mammalian

epithelial cells (Musch et al., 2002). The second proposes that Lgl could negatively regulate the activity of non-muscle myosin II. *Drosophila* and human Lgl proteins bind nonmuscle myosin II (Strand et al., 1994; Strand et al., 1995). Additionally, in *Drosophila* neuroblasts, reducing the dosage of the myosin II gene *zipper* suppresses the loss of basal protein targeting associated with the *lgl* mutation (Ohshiro et al., 2000; Peng et al., 2000). Furthermore, Lgl may function in neuroblasts to restrict myosin to the apical cortex (Barros et al., 2003), although this may be facilitated indirectly by inhibition of aPKC activity on the basal cortex (Atwood and Prehoda, 2009). Finally, in asymmetrically dividing cells in the *Drosophila* nervous system (Atwood and Prehoda, 2009; Betschinger et al., 2003; Wirtz-Peitz et al., 2008) Lgl appears to function by regulating the activity of aPKC, either by inhibiting its activity (Atwood and Prehoda, 2009) or by altering its target specificity (Wirtz-Peitz et al., 2008). It accomplishes this, at least in part, by exchanging with PAR-3 in the PAR-6/aPKC complex (Wirtz-Peitz et al., 2008). A similar exchange with PAR-3 also occurs in mammalian epithelial cells (Plant et al., 2003; Yamanaka et al., 2003).

Despite being a fundamental polarity component in a number of polarized cell types, Lgl is conspicuously absent from the model of polarity establishment and maintenance in the early *C. elegans* embryo. One *C. elegans* gene (F56F10.4, *lgl-1*) is predicted to encode a protein homologous to Lgl (Vasioukhin, 2006), but the role of this homolog had not yet been determined when I began my research. Although clearly a member of the Lgl family, the gene, *lgl-1*, is quite diverged at the primary sequence level relative to other family members (13.7% identical to *Drosophila* Lgl and 14.1% identical to mouse Lgl, Mgl-1).

Chapter two of this thesis details work demonstrating that LGL-1 functions redundantly with PAR-2 to maintain polarity in the early *C. elegans* embryo. Chapter three provides evidence for a third, independent pathway that contributes to polarity maintenance and appears to involve the CDC-42 regulators CHIN-1 and CGEF-1.

CHAPTER TWO*

THE *C. ELEGANS* HOMOLOG OF *DROSOPHILA* LETHAL GIANT LARVAE FUNCTIONS REDUNDANTLY WITH PAR-2 TO MAINTAIN POLARITY IN THE EARLY EMBRYO

INTRODUCTION

Polarity is critical for axis specification and generating cell diversity during development. In metazoans, cell polarity is mediated in part by a conserved set of regulatory proteins, known collectively as the PAR (*par*titioning-defective) proteins. The one-cell *C. elegans* embryo establishes an anterior-posterior axis shortly after fertilization and serves as a model for studying polarity (Goldstein and Macara, 2007; Schneider and Bowerman, 2003). The PAR proteins include the PDZ domain-containing proteins PAR-3 and PAR-6, an atypical protein kinase PKC-3, a serine/threonine kinase PAR-1, and in nematodes, a putative ubiquitin E3 ligase PAR-2.

Although most of the PAR proteins have been shown to be critical polarity components in a variety of animal systems (Goldstein and Macara, 2007), PAR-2 is puzzling because it appears to be nematode-specific. A possible answer to this puzzle is that PAR-2 has taken on a function in nematodes that is more commonly carried out by another protein or proteins in other polarity systems. In many systems, the PAR proteins interact with a number of other polarity modules, one of which includes the conserved tumor suppressor protein Lethal Giant Larvae (Lgl) (Betschinger et al., 2003; Plant et al., 2003; Vasioukhin, 2006; Wirtz-Peitz and Knoblich, 2006;

* This chapter has been published **Beatty, A., Morton, D. and Kemphues, K.** *Development* **137**, 3995-4004.. Fig. 2.1 was contributed by Diane Morton, who also carried out initial genetic mapping of the *it31* allele of *lgl-1*.

Yamanaka et al., 2003).

Despite being a fundamental polarity component in a number of polarized cell types, the role of an Lgl homolog in *C. elegans* has not yet been determined. Here, we show that a *C. elegans* homologue of Lgl, LGL-1, functions redundantly with PAR-2 to maintain polarity, and provide evidence that LGL-1 acts by preventing the cortical accumulation of NMY-2 in the posterior cortex of the early embryo.

MATERIALS AND METHODS

Nematode strains

Nematodes were cultured using standard conditions (Brenner, 1974). N2 (Bristol) was used as wild type. Mutations used in this analysis include *par-2(e2030)*, *par-2(it5)* (Kemphues et al., 1988), *par-2(lw32), par-2(it87)* (Cheng et al., 1995), *nmy-2(ne1490)*, *nmy-2(ne3401)* (Liu et al., 2010), *unc-119(ed4)* (Maduro and Pilgrim, 1995), *lgl-1(tm2616),* provided by the National Bioresource Project at Tokyo Women's Medical College, and *lgl-1(it31)* (this study). We confirmed that the *tm2616* allele of *lgl-1* is a 211bp deletion with a 9bp insertion that begins in the sixth intron and ends in the seventh intron. We determined the transcript produced by the *tm2616* mutant using RT-PCR (First-Strand cDNA Synthesis Kit, Amersham) followed by sequencing. *tm2616* was out-crossed to N2 six times.
We also used the transgene zuIs45[nmy-2::NMY-2::GFP] (Nance et al., 2003).

RNA interference

RNAi was performed by feeding (Timmons and Fire, 1998), with the exception of *lgl-1(RNAi)* in *par-2(it5)*, which was performed either by feeding or by injection (Fire et

al., 1998). All RNAi feeding experiments involving *par-2* mutants were performed at 16°C, and the worms were allowed to feed for 48-60hrs. All other RNAi experiments were done at 25°C, and worms were allowed to feed for 36hrs prior to imaging or immunostaining.

Imaging

Images of live embryos using either differential interference contrast (DIC) or wide-field fluorescence microscopy were captured using a Leica DM RA2 microscope with a 63X Leica HCX PL APO oil immersion lens, a Hamamatsu ORCA-ER digital camera, and Openlab software (Improvision). Blastomere cross-sectional areas were measured using Openlab. Fixed embryos were imaged using Leica TCS SP2 system with a Leica DMRE-7 microscope and an HCX PL APO 63X oil immersion lens. Images were processed using Leica Confocal Software and Adobe Photoshop CS4. The images in Fig. 2.8 were captured with a PerkinElmer UltraVIEW LCI confocal scanner with a Nikon Eclipse TE2000-U microscope using UltraVIEW Imaging Suite v5.5. The step size was 1μM with 10-14 sections per stack. The sections were stacked and processed using ImageJ and Adobe Photoshop CS4.

LGL-1 Polyclonal Antibody Production

A C-terminal fragment of LGL-1 (aa 490-941) fused to GST was used to generate a polyclonal antibody in guinea pigs. Antibody production was performed by Pocono Rabbit Farm & Laboratory, Inc. (Canadensis, PA). Crude serum was blot-affinity purified using GST-LGL-1(490-941) prior to use.

Immunohistochemistry

Immunostaining of PAR-2, GFP, LGL-1, and PKC-3 in embryos was performed using methanol fixation as described (Guo and Kemphues, 1995). Primary antibodies used include: anti-PAR-2 rabbit polyclonal (Boyd et al., 1996); anti-GFP goat polyclonal (Rockland Immunochemicals), anti-PKC-3 rat polyclonal, anti-LGL-1 guinea pig. Secondary antibodies used include: donkey anti-rat Cy3, donkey anti-rabbit Cy3, donkey anti-goat Cy3, goat anti-guinea pig Cy3 (Jackson Laboratories, West Grove, PA) and donkey anti-goat Alexa488 (Invitrogen). Samples were mounted using VectaSheild with DAPI (Vector Laboratories).

Transgenic Strains

lgl-1 transgenic constructs were generated by fosmid recombineering using a *galK* positive/counterselection cassette (Warming et al., 2005, also refer to http://recombineering.ncifcrf.gov/Protocol.asp, Recombineering protocol 3). To begin, the *galK* cassette (Warming et al., 2005) was amplified using primers that include 75bp arms on the 5' ends that are homologous to the regions flanking the region of genomic DNA to be modified. The purified PCR product was then transformed into SW102 cells containing a fosmid that included *lgl-1* (WRM065bB11). Homologous recombination was induced, and recombinants were selected as described previously (Warming, et al., 2005). Next, another cassette containing the region to be inserted flanked by the 75bp homology arms was generated either using PCR (as was the case for fluorophores) or by annealing two homologous single stranded primers (as was the case for mutations). The purified cassette was transformed, homologous recombination was induced, and recombinants were selected as described previously

(Warming et al., 2005). After making the desired modification to *lgl-1* in the fosmid, the gene as well as the upstream and downstream intergenic regions was recombineered into pJKL702 (unc-119 in pBSII-SK+), kindly provided by Kelly Liu, Cornell University. Approximately 500bp homology regions corresponding to the regions directly downstream of the gene upstream of *lgl-1* (X:872011-872531) and the region directly upstream of the gene downstream of *lgl-1* (X:863852-864392) were cloned into pJKL702 adjacent to one another in the same orientation. The vector was then linearized by cutting between the homology regions and used as a cassette for recombineering. Constructs were transformed using microparticle bombardment (Praitis et al., 2001). At least two independent integrated transgenic lines were examined for each construct. For the KK1080, we sequenced the transgene expressed in the line after bombardment to ensure the correct construct was transformed. One line for each construct was used to test for rescue.

RESULTS

Loss of *lgl-1* function enhances the maternal-effect embryonic lethality of weak *par-2* mutants

The *C. elegans* gene (F56F10.4) is predicted to encode a protein homologous to Lgl (Vasioukhin, 2006). Although clearly a member of the Lgl family, the gene, *lgl-1*, is quite diverged at the primary sequence level relative to other family members (13.7% identical to *Drosophila* Lgl and 14.1% identical to mouse Lgl, Mgl-1). To determine if *lgl-1* is required for polarity in the early embryo, we examined nematodes homozygous for a deletion/insertion allele of *lgl-1*, *tm2616*. *tm2616* is predicted to result in a frameshift after codon 342 and cause a premature stop codon after amino

acid 350 (Fig. 2.1). Embryos from *lgl-1(tm2616)* mutants are 99.2±0.4% embryonic viable (Fig. 2.2A, n=675) and do not exhibit observable early polarity defects (Fig. 2. 2C). In both wild type and *lgl-1(tm2616)* embryos the anterior blastomere, AB, accounts for similar proportions of the total area of the 2-cell zygote (56.8±2.2% in N2 and 56.5±2.1% in *lgl-1(tm2616)*, p=0.74, n=15). Furthermore, as in wild type, the second cleavages in *lgl-1(tm2616)* embryos are asynchronous, and the mitotic spindle is oriented transversely in the AB cell and longitudinally in the P1 cell (Fig. 2.2C, n=15). Thus, in contrast to its essential role in other polarity systems (Vasioukhin, 2006; Wirtz-Peitz and Knoblich, 2006), LGL-1 function is dispensable for polarity in the *C. elegans* embryo.

In *C. elegans*, the putative ubiquitin E3 ligase PAR-2 is required to maintain polarity in the early embryo by restricting the distribution of the anterior polarity proteins PAR-3, PAR-6 and PKC-3 (Cuenca et al., 2003; Hao et al., 2006; Kemphues et al., 1988). Of the PAR proteins, only PAR-2 is not conserved outside of nematodes (Goldstein and Macara, 2007). Because the role of Lgl proteins in polarity in other animals is analogous to that of PAR-2 in *C. elegans*, we hypothesized that LGL-1 of *C. elegans* functions redundantly with PAR-2. To test this hypothesis, we used RNAi to deplete LGL-1 in *par-2(it5)* at the permissive temperature of 16°C. We noted a dramatic enhancement of embryonic lethality. Embryos from homozygous *par-2(it5)* are predominantly viable at the permissive temperature, but the mutants exhibit strong temperature sensitivity (Cheng et al., 1995). At permissive temperature, RNAi control *par-2(it5)* worms exhibited 15.4±4% embryonic lethality (n=878). In contrast, the embryonic lethality of *par-2(it5ts)* treated with *lgl-1(RNAi)* was 97.0±0.5% (Fig. 2.2A, n=1252). Furthermore, *par-2(it5); lgl-1(tm2616)* double mutants were 100%

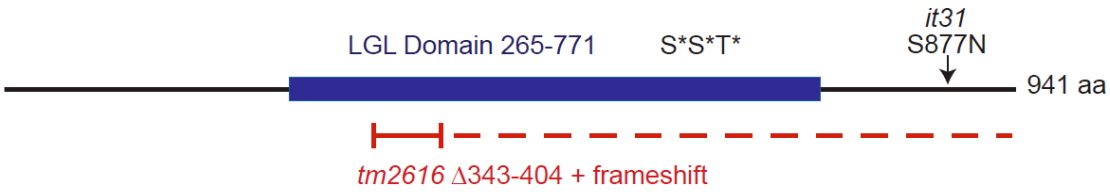

Fig. 2.1. Schematic representation of *C. elegans* LGL protein. Conserved LGL domain [Pfam LLGL2 (Katoh, 2004)] spans amino acids 273-368. Conserved serines 661, 665 and threonine 669, marked with asterisks, are sites of LGL 3A and 3E mutations. The tm2616 deletion/insertion mutation removes codons for amino acids 343 to 404 and results in a frameshift (dashed red line) and early stop to produce a 350 amino acid truncated protein.

Fig. 2.2. Loss of *lgl-1* function enhances weak *par-2* mutants. (**A**) The percentage of embryos that failed to complete embryogenesis in the labeled genotypes. Error bars represent standard deviation in all bar graphs unless otherwise specified. (**B**) Percentage embryonic lethality of weak *par-2* alleles compared to the respective *par-2; lgl-1* double mutant. The *lgl-1* mutation used is *tm2616*. (**C**) DIC images of two-cell embryos during interphase (left column), and prior to the second mitotic division (right column). The black lines mark the orientation of the mitotic spindles. Anterior is to the left in all figures.

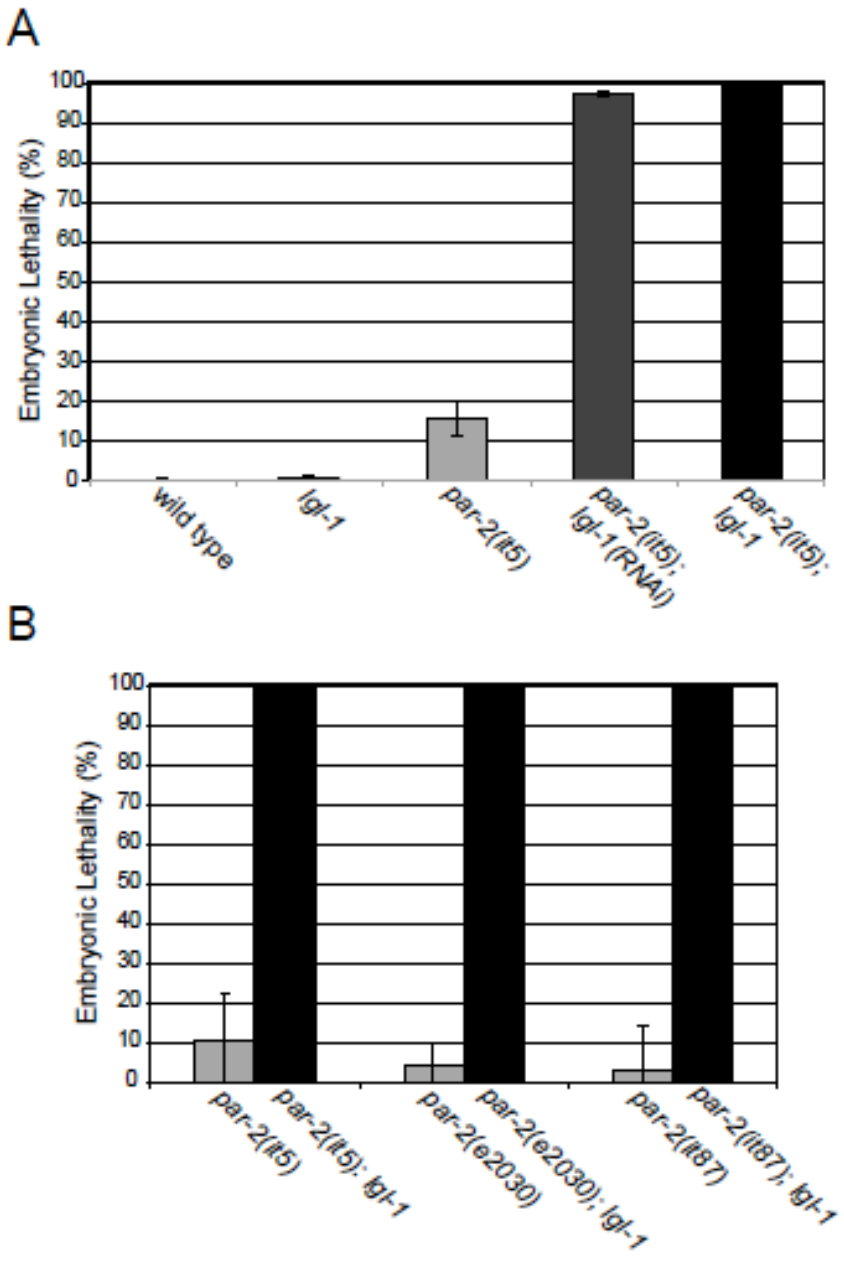
A
Embryonic Lethality (%)
100
90
80
70
60
50
40
30
20
10
0
wild type
lgl-1
par-2(lt5)
par-2(lt5); lgl-1(RNAi)
par-2(lt5); lgl-1
B
Embryonic Lethality (%)
100
90
80
70
60
50
40
30
20
10
0
par-2(lt5)
par-2(lt5); lgl-1
par-2(e2030)
par-2(e2030); lgl-1
par-2(lt87)
par-2(lt87); lgl-1

C

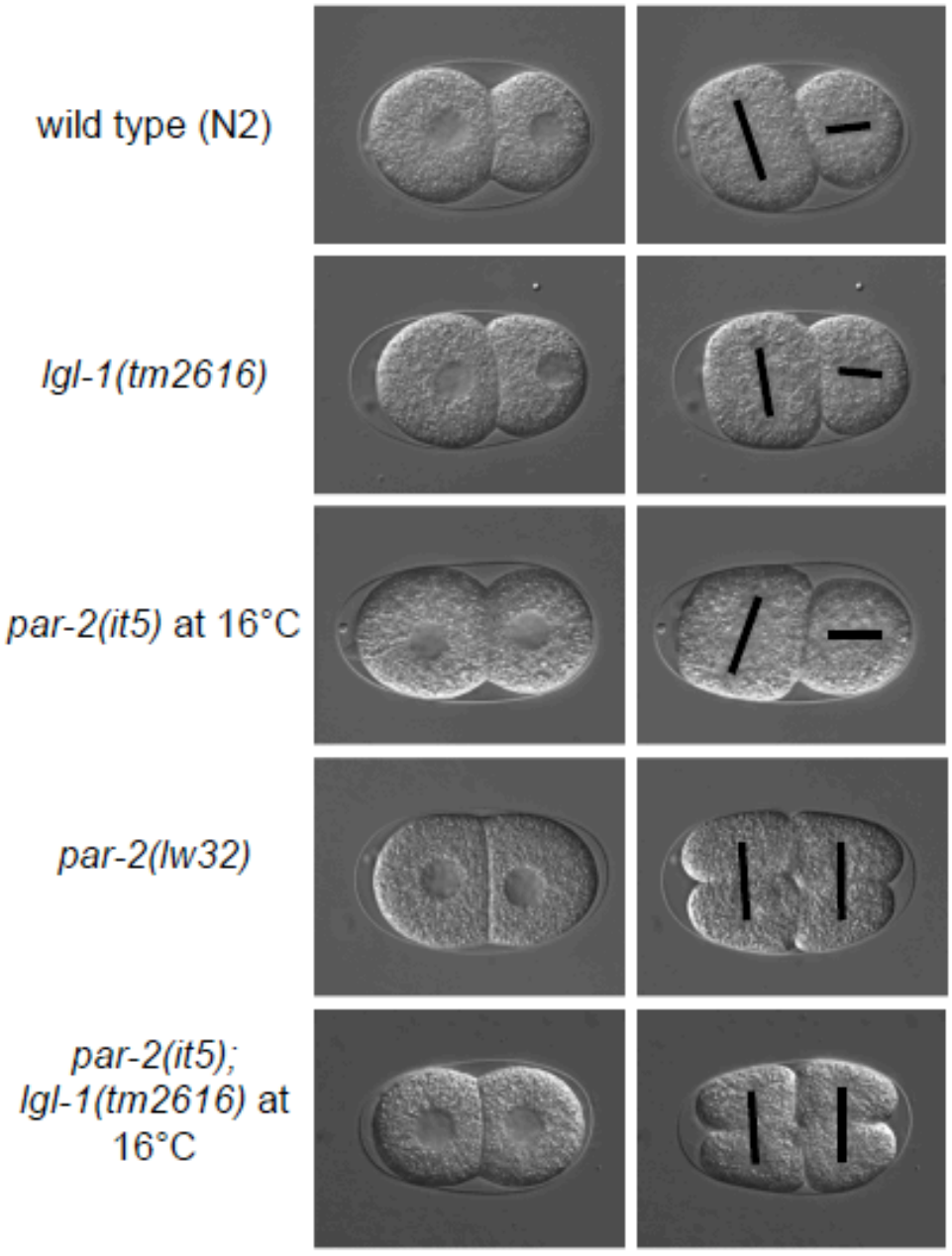
wild type (N2)
lgl-1(tm2616)
par-2(it5) at 16°C
par-2(lw32)
par-2(it5); lgl-1(tm2616) at 16°C

maternal-effect embryonic lethal at the permissive temperature (Fig. 2.2A, n=1000). This enhancement was not allele specific; *lgl-1(tm2616)* in double mutant combination with maternal effect sterile *par-2* alleles *e2030* or *it87* (Cheng et al., 1995; Kemphues et al., 1988), gave >99% maternal-effect embryonic lethality (Fig. 2.2B, n=765 and 857, respectively).

Furthermore, *lgl-1(RNAi)* did not enhance *par-3(e2074); sup-7(st5)*. The amber suppressor *sup-7(st5)* partially rescues the maternal-effect embryonic lethality of *par-3(e2074)* (Kirby, 1992). When fed empty vector *par-3(e2074); sup-7(st5)* was 54.1%±10.5% embryonic lethal while *par-3(e2074); sup-7(st5)*; *lgl-1(RNAi)* displayed 33.6%±6.5% embryonic lethal (Fig. 2.3, n>4000). These data indicate that *lgl-1* is not a non-specific enhancer of weak par mutants and may even subtly suppress partial loss of *par-3* function (p=0.03).

In addition, we determined that depleting another *C. elegans* homolog of Lgl, *tom-1,* (Vasioukhin, 2006) could not enhance *par-2(it5)*. RNAi control *par-2(it5)* worms gave 10.3±12% embryonic lethality (n=715) while *par-2(it5)* worms treated with *tom-1(RNAi)* showed 14.9±10.3% lethality (p=0.50, n=839).

Mutation of LGL-1 enhances *par-2* polarity defects in the early embryo

Although loss of *lgl-1* function enhanced the maternal-effect embryonic lethality of hypomorphic *par-2* mutants, it was unclear whether the embryonic lethality was a result of enhanced early embryonic polarity defects or whether it revealed a cryptic role for the proteins in later embryogenesis. Therefore, we used DIC microscopy to examine the first two mitotic divisions of embryos from *par-2(it5);lgl-1(tm2616)* mutants at permissive temperature. At this temperature, most

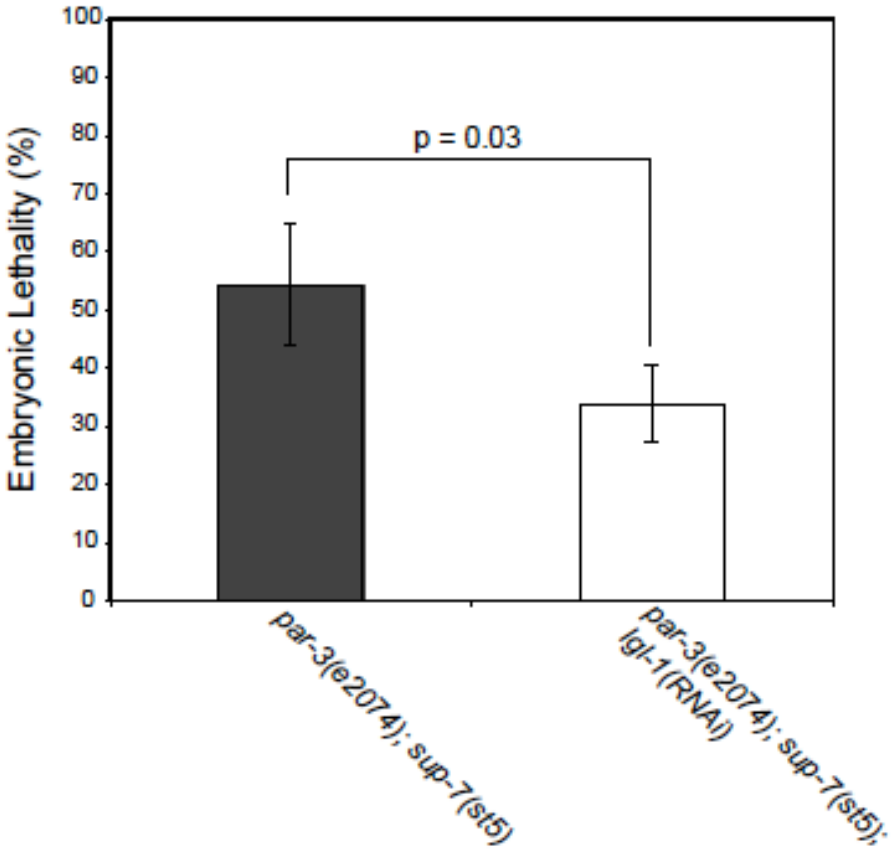

Fig. 2.3 Loss of *lgl-1* function does not enhance a weak *par-3* mutant.) Percentage embryonic lethality for *par-3(e2030); sup-7(st5)* and *par-3(e2030); sup-7(st5); lgl-1(RNAi)*. The error bars represent the standard error of the mean.

embryos from *par-2(it5)* mothers divided asymmetrically (n=18/19) and exhibited an asynchronous second mitotic division with spindles oriented transversely in AB and longitudinally in P1 (Fig. 2.2C, n=10/13). In contrast, all embryos from *par-2(it5); lgl-1(tm2616)* exhibited a strong *par-2* mutant phenotype (Fig. 2.3C, Cheng et al., 1995; Hao et al., 2006; Kemphues et al., 1988); the double mutant embryos exhibited a symmetrical first cleavage (the AB blastomere accounted for 49.9±1.9% of the total area of the two-cell embryo) and a synchronous second cleavage (Fig. 2.2C, n=12/12). Additionally, the mitotic spindles in both the AB and P1 cells had a transverse orientation with respect to the longitudinal axis of the embryo (Fig. 2.2C, n=12/12). Therefore, compromising *lgl-1* function enhances the polarity defects associated with *par-2* in the early embryo.

LGL-1 is asymmetrically localized to the posterior of the one-cell embryo and to the basolateral cortex in epithelial cells

To determine the subcellular localization of LGL-1 in the early embryo, we generated transgenic lines that express *gfp and mCherry*-tagged *lgl-1* under the control of its endogenous promoter (see Materials and Methods). Similar to PAR-2 (Boyd et al., 1996), LGL-1::GFP and LGL-1:mCherry localized asymmetrically to the posterior cortex of the one-cell embryo (Fig. 2.4A). Unlike PAR-2, however, LGL-1::GFP were present throughout the cortex at a low level just prior to polarization, and the anterior localization the protein persists even as it was becoming enriched in the posterior.

The fluorescently tagged transgenes rescued the enhanced maternal-effect

Fig. 2.4. LGL-1 localizes to the posterior cortex of the early embryo. (**A**) Confocal mid-sections of fixed embryos immunostained for LGL-1::GFP (green) and PAR-2 (red). Establishment refers to the time following pronuclear decondensation but prior to pronuclear meeting. The embryos were dissected from mothers of the genotype *lgl-1::gfp; lgl-1(tm2616)*. Transgenes in this study were crossed or transformed into the *lgl-1(tm2616)* mutant background because the cortical signal of the transgene was stronger in the absence of functional endogenous protein. (**B**) Percentage embryonic lethality for *par-2(it5); lgl-1(tm2616)* and *par-2(it5); lgl-1(tm2616); lgl-1::gfp*.

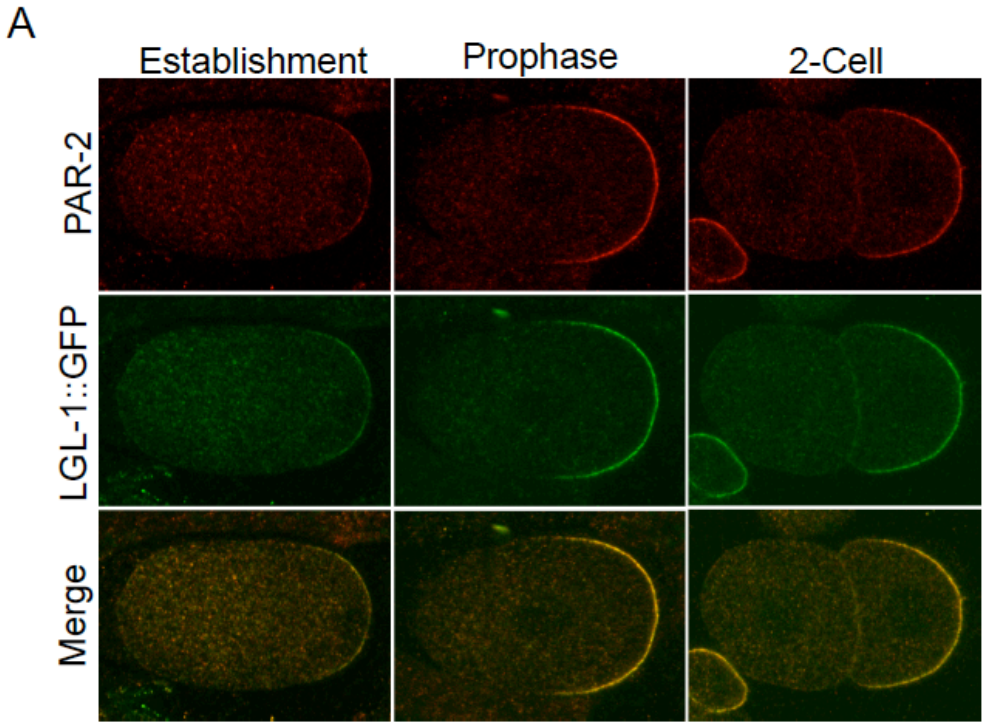
A
Establishment
Prophase
2-Cell
PAR-2
LGL-1::GFP
Merge

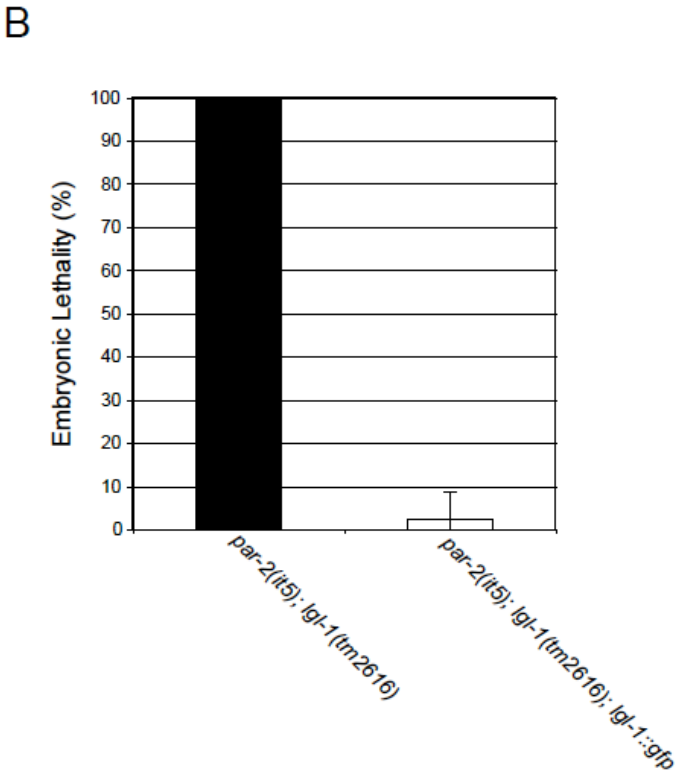
B
Embryonic Lethality (%)
100
90
80
70
60
50
40
30
20
10
0
par-2(it5); lgl-1(tm2616)
par-2(it5); lgl-1(tm2616); lgl-1::gfp

embryonic lethality of *par-2(it5)* by *lgl-1(tm2616)* at the permissive temperature. For example, expression of LGL-1::GFP in *par-2(it5); lgl-1(tm2616)* mutants resulted in 98% viable embryos (Fig. 2.4B, n=927). Immunostaining fixed embryos with a polyclonal antibody raised against the N-terminus of LGL-1 confirmed the localization pattern of LGL-1 (Fig. 2.5). The subcellular localization of LGL-1 to the posterior cortex in the early embryo is consistent with the hypothesis that LGL-1 acts redundantly with PAR-2 to maintain polarity.

We also observed that LGL-1::GFP localized asymmetrically in differentiated epithelial cells. In the elongating embryo, LGL-1::GFP localized to basolateral cortex of gut and epidermal cells (Fig. 2.6). This subcellular distribution suggests that LGL-1 has a role in polarity in differentiated epithelial cells in addition to its role in the early embryo. Because the embryos from *lgl-1*(*tm2616)* are viable, the role of *lgl-1* in these epithelial tissues, if any, is likely to be a redundant function.

PKC-3 is required for the asymmetric cortical localization of LGL-1

In asymmetrically dividing *Drosophila* neuroblasts, migrating fibroblasts, and polarized mammalian epithelial cells, Lgl is a substrate for aPKC (Betschinger et al., 2003; Plant et al., 2003; Yamanaka et al., 2003). In *Drosophila,* phosphorylation of Lgl on a series of conserved aPKC consensus sites likely results an intramolecular association between the N-terminal and C-terminal domains of the protein, resulting in cortical disassociation and presumably inactivation (Betschinger et al., 2005). *C. elegans* LGL-1 includes a highly conserved motif that contains three putative aPKC phosphorylation sites (S661, S665, and T669) suggesting LGL-1 may be similarly regulated by the aPKC homolog, PKC-3, in the early embryo (Fig. 2.1, Vasioukhin,

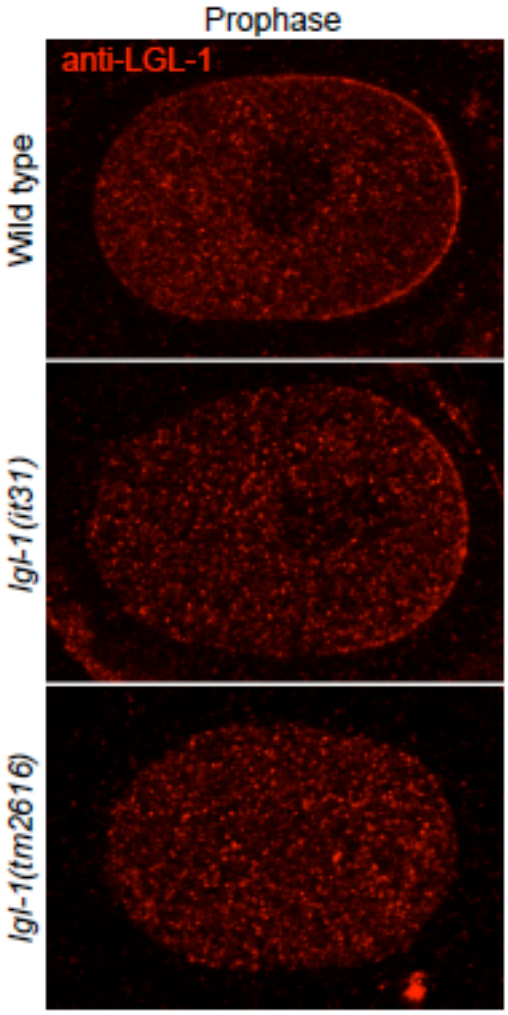

Fig. 2.5. Endogenous LGL-1 is localized asymmetrically in one-cell embryos. Confocal mid-sections of prophase one-cell embryos from N2, *lgl-1(it31),* and *lgl-1(tm2616)* immunostained for LGL-1.

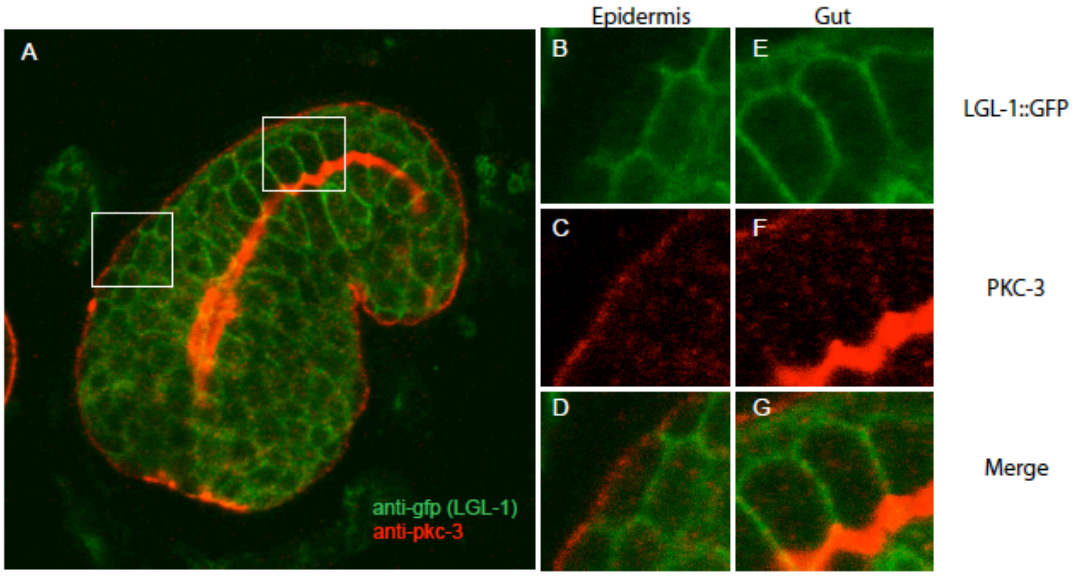

Fig. 2.6. LGL-1 is asymmetrically localized to the basolateral cortex of differentiated epithelial cells. (A) Confocal immunofluorescence image of an elongating embryo stained for GFP (LGL-1::GFP) in green and PAR-2 in red. The white box to the left indicates the region of the embryo magnified in (B-D) and the white box toward the right denotes the region of the embryo magnified (E-G) (**B-D**) Confocal image of an epidermal cell stained for LGL::GFP (green, B), PKC-3 (red, C) and a merge of panels B and C (D). (**E-G**) Confocal image of a gut cell stained as in panels B-D.

2006). To test this hypothesis, we used RNAi to deplete PKC-3, and monitored the localization of LGL-1::GFP. After depleting PKC-3, LGL-1::GFP was no longer restricted to the posterior cortex following polarity establishment (Fig. 2.7A). Thus, PKC-3 is required for the asymmetric localization of LGL-1::GFP.

To determine if the putative PKC-3 phosphorylation sites were required for LGL-1 asymmetry, we generated transgenic lines expressing a mutant form of LGL-1::mCherry in which the three putative PKC-3 phosphorylation sites were mutated to alanine. Consistent with the expected role of these conserved serines, LGL-1^{3A}::mCherry was strongly cortical prior to establishment and failed to become asymmetric during polarity establishment. Instead, the mutant protein remained symmetrically distributed around the cortex (Fig. 2.7B). Additionally, the cortical signal of LGL-1^{3A}::mCherry appeared more intense relative to the cytoplasmic signal compared to wild type (Fig. 2.7B). LGL-1^{3A}::mCherry failed to rescue the enhancement of *par-2(it5)* by *lgl-1(tm2616)* at the permissive temperature; both *par-2(it5); lgl-1(tm2616)* and *par-2(it5); lgl-1(tm2616)* expressing LGL-1^{3A}::mCherry were 100% maternal-effect embryonic lethal (n=1000 for each genotype). Furthermore, worms of genotype *par-2(it5)/ sC1 [dpy-1(s2171)]; lgl-1(tm2616)* expressing LGL-1^{3A}::Cherry were 91±4.0% viable at the permissive temperature suggesting that ectopic localization of LGL-1^{3A}::Cherry in the anterior of the one-cell embryo did not substantially affect embryonic viability in a dominant-negative manner (n=587).

We also generated a phosphomimetic mutant by mutating the potential PKC-3 phosphorylation sites to glutamic acid. We expected this mutant to be cytoplasmic. However, although cytoplasmic levels were clearly higher than wild type LGL-

Fig. 2.7. PKC-3 is required for the asymmetric localization of LGL-1.

(**A**) Confocal mid-sections of fixed embryos at the indicated stage of development immunostained for LGL-1::GFP. The top row shows control embryos from *lgl-1::gfp*; *lgl-1(tm2616)* worms treated with the L4440 vector alone, and the bottom row shows embryos from *lgl-1::gfp*; *lgl-1(tm2616); pkc-3(RNAi)* (**B**) Wide-field fluorescence images from time-lapse movie of embryos progressing through the first mitotic cell cycle. The top panel shows an embryo expressing LGL-1::mCherry prior to establishment (between meiosis II and pronuclear decondensation), at pseudocleavage, nuclear envelope breakdown (NEB), and after the first mitotic division. The middle and bottom panel shows embryos at similar stages expressing LGL-1^{3A}::mCherry and LGL-1^{3E}::mCherry, respectively.

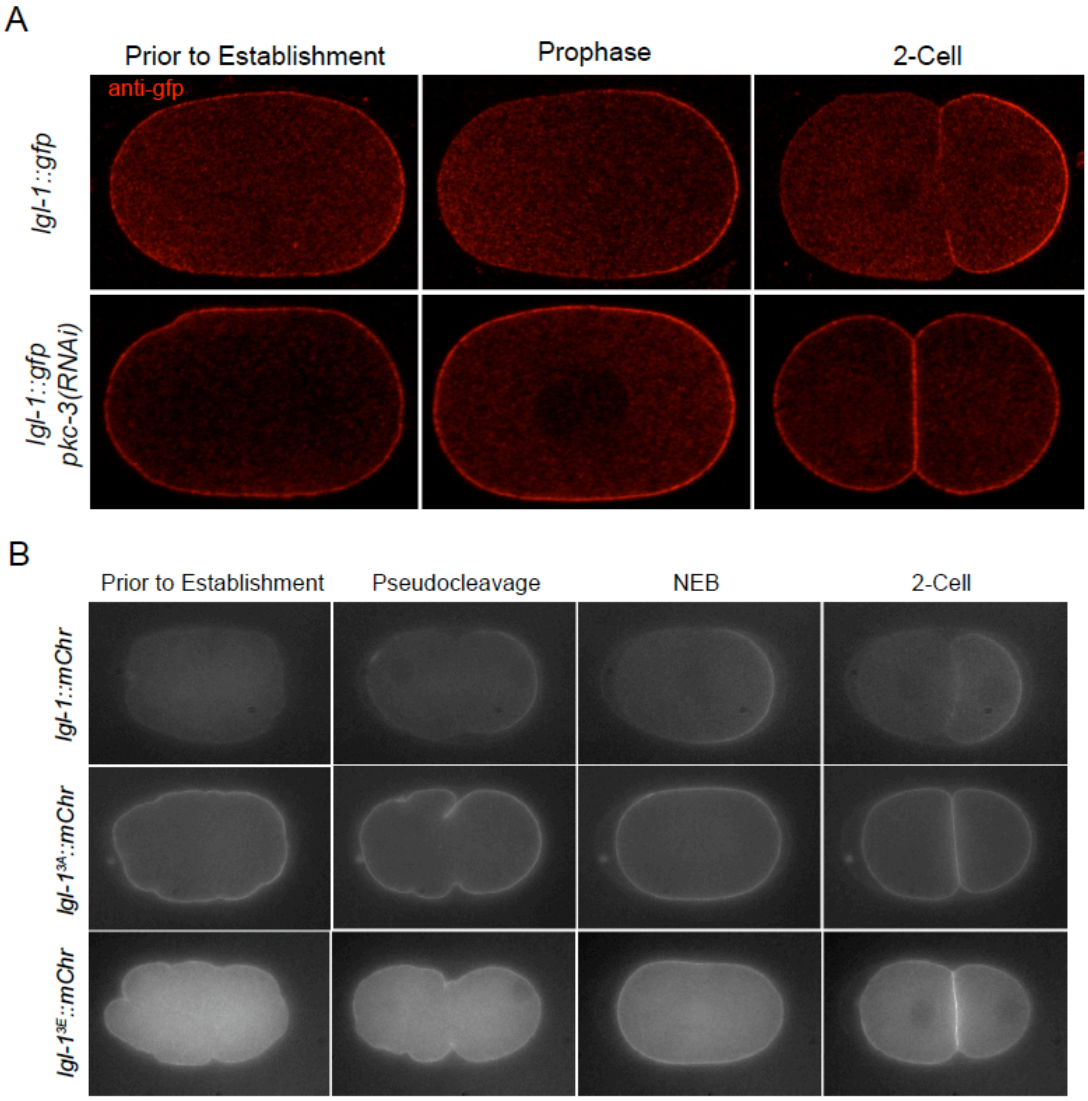
A
Prior to Establishment
Prophase
2-Cell
anti-gfp
lgl-1::gfp
lgl-1::gfp
pkc-3(RNAi)
B
Prior to Establishment
Pseudocleavage
NEB
2-Cell
lgl-1::mChr
lgl-1^3A::mChr
lgl-1^3E::mChr

1::mCherry, LGL-1$^{S661E;S665E;T669E}$::mCherry was still detectable at the cortex (Fig. 2.7B). Expression of LGL-1^{3E}::mCherry failed to rescue the enhancement of *par-2(it5)* by *lgl-1(tm2616)*. Embryos from *par-2(it5); lgl-1(tm2616); lgl-1^{3E}::mcherry* were 100% lethal (n=1000).

We conclude that one or more of the three putative PKC-3 phosphorylation sites are required for LGL-1 asymmetry, consistent with the hypothesis that phosphorylation of LGL by PKC-3 negatively regulates the cortical accumulation of LGL-1 in the anterior.

Over-expression of LGL-1 is sufficient to rescue PAR-2 loss-of-function

par-2(lw32) is a strong *par-2* allele that produces a truncated protein predicted to be 233aa (Levitan et al., 1994) and lacks the domain required for cortical localization (Hao et al., 2006). If LGL-1 and PAR-2 function redundantly, we hypothesized that over-expression of LGL-1 might be sufficient to rescue the lethality of *par-2(lw32)*. To test this hypothesis, we crossed the *lgl-1::gfp* transgene into *par-2(lw32)* and quantified embryonic lethality of *par-2(lw32)* expressing LGL-1::GFP. Embryos from *par-2(lw32)* were 98.0±0.4% lethal (n=2216). In contrast, the embryonic lethality of *par-2(lw32); lgl-1::gfp* was 5.7±0.6%, suggesting that over-expression of LGL-1 robustly rescued *par-2* loss-of-function (Fig. 2.8A, n=1128).

par-2(lw32) produces a truncated protein and might not be a true functional null. To be confident that expression of the *lgl-1::gfp* transgene was bypassing the need for PAR-2 rather than acting through residual PAR-2, we treated *par-2(lw32); lgl-1::gfp* worms with *par-2(RNAi)*. As expected if *par-2(lw32)* is a functional null, *par-2(RNAi)* did not enhance the embryonic lethality of *par-2(lw32)* (Fig. 6A,

Fig. 2.8. Over-expression of LGL-1 rescues *par-2* loss of function. (**A**) The percentage embryonic lethality in *par-2(lw32)* and *par-2(lw32); lgl-1::gfp* when fed either L4440 vector alone (left), *par-2(RNAi)* (middle) or *lgl-1(RNAi)* (right) (**B**) Confocal mid-sections of anaphase one-cell embryos immunostained for PKC-3. The centrosomal staining is non-specific (**C**) Confocal mid-sections of two-cell embryos immunostained for PKC-3

A

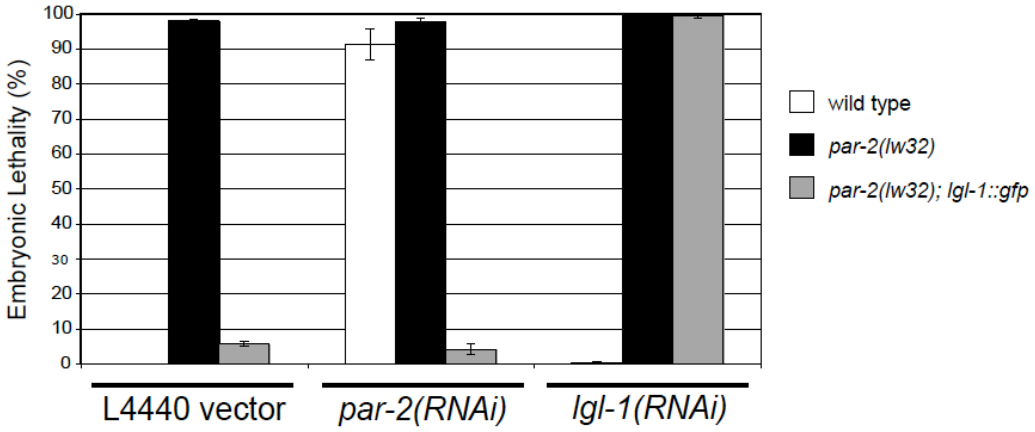
Embryonic Lethality (%)
100
90
80
70
60
50
40
30
20
10
0
L4440 vector
par-2(RNAi)
lgl-1(RNAi)
wild type
par-2(lw32)
par-2(lw32); lgl-1::gfp

B

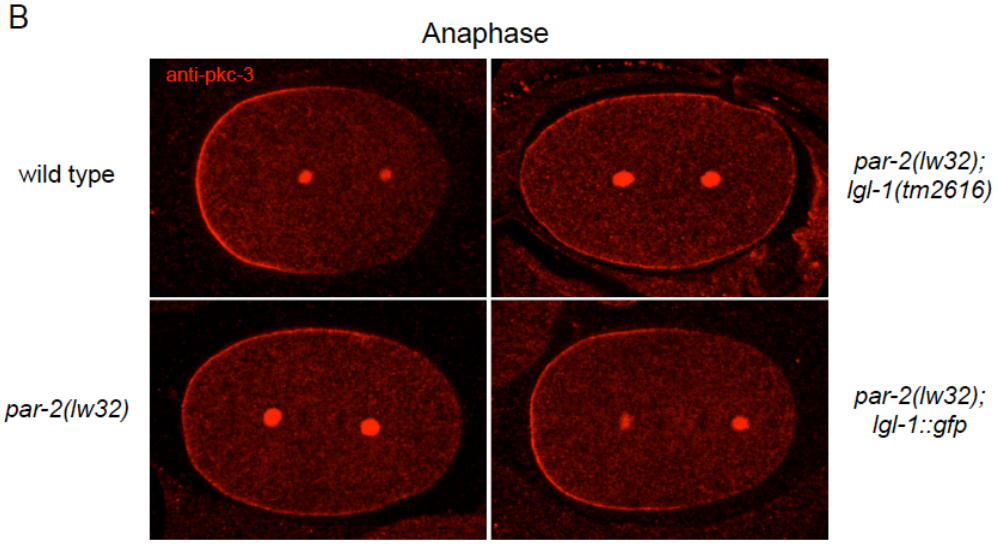
Anaphase
anti-pkc-3
wild type
par-2(lw32)
par-2(lw32); lgl-1(tm2616)
par-2(lw32); lgl-1::gfp

C

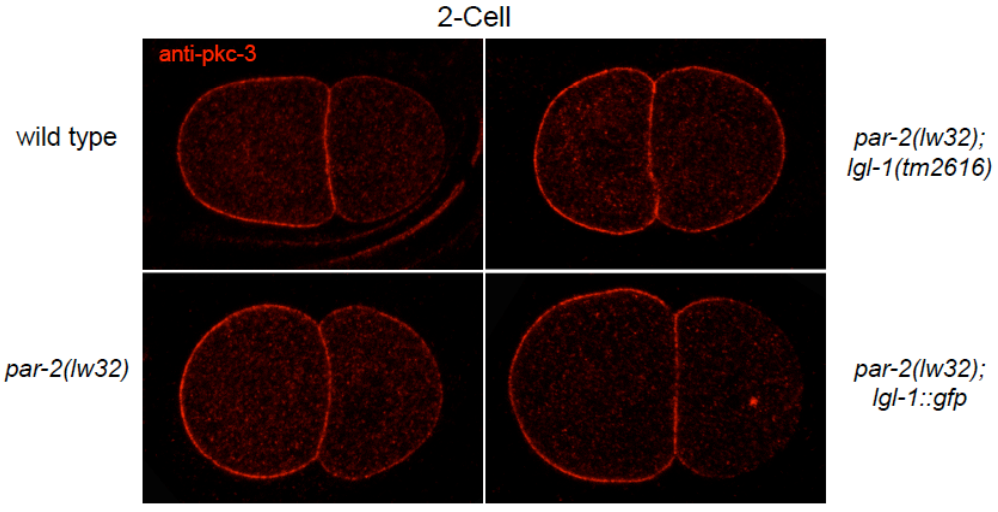
2-Cell
anti-pkc-3
wild type
par-2(lw32)
par-2(lw32); lgl-1(tm2616)
par-2(lw32); lgl-1::gfp

n=2473). Furthermore, *par-2(lw32); lgl-1::gfp* treated with *par-2(RNAi)* had similar levels of embryonic lethality as those fed bacteria containing empty vector (Fig. 2.8A, n=2091). Assuming that *par-2* RNAi removes any residual active PAR-2 in the *lw32* background, we conclude that expression of the *lgl-1::gfp* transgene can bypass the need for PAR-2.

Finally, to confirm that viability of *par-2(lw32); lgl-1::gfp* resulted from LGL-1 over-expression, we depleted LGL-1 in *par-2(lw32); lgl-1::gfp* using RNAi and scored embryonic lethality. Embryos from *par-2(lw32); lgl-1::gfp; lgl-1(RNAi)* worms were 99.4±0.8% lethal indicating the rescue of *par-2(lw32)* was a result of LGL-1 over-expression (Fig. 2.8A, n=696). Embryos from *par-2(lw32)* worms treated with *lgl-1(RNAi)* were 100% lethal suggesting that the small percentage of viable embryos produced by the *par-2(lw32)* mutant can be attributed to LGL-1 function (Fig. 2.8A, n=917).

We also compared the cortical polarization of early embryos from *par-2(lw32), par-2(lw32); lgl-1(tm2616)*, and *par-2(lw32); lgl-1::gfp* by immunostaining endogenous PKC-3. In one-cell wild type embryos during anaphase, PKC-3 occupies 63.3±3.8% of the cortex (Fig. 6B, n=10). In *par-2(lw32),* PKC-3 extends significantly further into the posterior (84.2±9.8%, Fig. 2.8B, $p=1.7x10^{-4}$, n=10). Furthermore, PKC-3 is found throughout the entire cortex in *par-2(lw32); lgl-1(tm21616)* embryos (Fig. 2.8B, $p=6.7x10^{-4}$, n=8), consistent with the hypothesis that both PAR-2 and LGL-1 contribute to polarity maintenance. In contrast, the amount of the cortex occupied by PKC-3 in *par-2(lw32); lgl-1::gfp* embryos is not significantly different than wild-type (65.5±7.0%, Fig. 2.8B, p=0.40, n=10) indicating over-expression of LGL-1 can rescue loss of *par-2* function.

In wild-type two-cell embryos, PKC-3 is enriched on the anterior cortex of the AB blastomere and the most anterior portion of P1 (Fig. 2.8C, Tabuse et al., 1998). In contrast, PKC-3 is cortically localized in both AB and P1 in *par-2(lw32)* although the intensity of the PKC-3 signal is notably weaker in the posterior than in the anterior (Fig. 2.8C). Furthermore, in embryos from *par-2(lw32); lgl-1(tm2616)*, PKC-3 is also localized to the cortex of both the anterior and posterior blastomeres during the 2-cell stage, but the discrepancy in the signal intensity was less substantial (Fig. 2.8C). We quantified the difference by measuring the signal on the posterior cortex and the anterior cortex, and then determining the ratio of the signals. In *par-2(lw32)* two-cell embryos, the posterior to anterior signal ratio was 0.65±0.22 (n=8) while the ratio in *par-2(lw32); lgl-1(tm2616)* embryos was 0.97±0.32 (n=8), indicating PKC-3 is significantly more symmetrical in *par-2(lw32); lgl-1(tm2616)* compared to *par-2(lw32)* (p=0.03). These data are consistent with idea that PAR-2 and LGL-1 function redundantly to maintain polarity. Finally, in embryos from *par-2(lw32); lgl-1::gfp,* the asymmetrical cortical localization of PKC-3 was restored and PKC-3 was again enriched in the AB blastomere and the most anterior portion of P1 (Fig. 2.8C). Embryos from *par-2(lw32); lgl-1::gfp* worms exhibited asymmetric first cell divisions (n=17/19), and the mitotic spindles of the second cell division were oriented in transverse to the A-P axis in the AB cell and along the A-P axis in the P1 cell (n=16/18). LGL-1::GFP was also asymmetrically localized in these embryos.

We conclude that over-expression of LGL-1 is sufficient to restore viability in the absence of functional PAR-2 by rescuing the early embryonic failure in polarity maintenance of *par-2* mutants.

Depletion of germline-enriched RING-finger proteins or cullin family members does not enhance *par-2(lw32); lgl-1::gfp*

In showing that LGL-1 over-expression rescues *par-2* mutants, we generated a line in which LGL-1 is required for polarity maintenance, *par-2(lw32); lgl-1::gfp*. We used this genetic background to perform several small scale RNAi screens in an attempt to identify proteins that interact genetically with LGL-1. Because over-expression of LGL-1 is sufficient to rescue *par-2* loss-of-function and PAR-2 is a putative RING-type E3 ubiquitin ligase, it is plausible that LGL-1 functions by localizing or regulating the activity of a redundant E3 ligase. In the absence of PAR-2 activity, the redundant ligase would likely be required. In an attempt to identify a redundant RING-type E3 ligase, we screened through a set of 24 RING-finger genes identified as being enriched in the germline (Moore and Boyd, 2004). However, none of these genes caused increased lethality after RNAi depletion in *par-2(lw32); lgl-1::gfp* compared to the wild type control.

We also screened through genes encoding cullin family members to determine if depletion of any of the cullins (*cul-1* through *cul-6*) caused embryo lethality in *par-2(lw32); lgl-1::gfp.* If LGL-1 functions redundantly with PAR-2 by acting as a substrate adaptor for a cullin complex, knockdown of the cullin might produce lethality in a situation where LGL-1 is functioning in place of PAR-2. We saw no increase in lethality for any of the cullins in *par-2(lw32); lgl-1::gfp* compared to the wild type control. In the case of *cul-1*, which displayed a late embryonic lethal phenotype in wild type, we examined early embryos from *par-2(lw32); lgl-1::gfp; cul-1(RNAi)* mothers and failed to observe polarity defects. Treatment with *cul-2(RNAi)* resulted in an early embryonic lethal phenotype in wild type. In order to test for

enhancement, we performed a weak RNAi such that the lethality in wild type was considerably reduced, but failed to observe a significant difference in embryonic lethality in *par-2(lw32); lgl-1::gfp* treated similarly.

Depletion of conserved Rab GTPases does not enhance lethality of *par-2(lw32); lgl-1::gfp*

Asymmetric endocytosis contributes to polarity maintenance in the early embryo (Nakayama et al., 2009). LGL-1 might function in polarity maintenance by regulating polarized endocytosis in the early embryo or, as suggested by work in mammalian polarized epithelial cells (Musch et al., 2002), in membrane trafficking. Because Rab GTPases play roles at multiple steps in membrane trafficking (Stenmark, 2009), we chose to target Rab family members for RNAi depletion in *par-2(lw32); lgl-1::gfp*. We depleted each of the 22 Rab family members that were identified as having a vertebrate homolog (Pereira-Leal and Seabra, 2001) in *par-2(lw32); lgl-1::gfp*. We observed no increase in embryonic lethality for any of the Rab GTPases in *par-2(lw32); lgl-1::gfp* compared to the N2 control.

it31* is a hypomorphic allele of *lgl-1

par-2(e2030) was initially isolated in a strain with a maternal-effect embryonic lethal phenotype; however, the embryonic lethality of the strain was dependent on an additional locus linked to the X chromosome (K. K., unpublished data). When separated from the X-linked locus, *par-2(e2030)* exhibited a maternal-effect sterile phenotype (Kemphues et al., 1988). The X-linked mutation, *it31*, also enhanced the maternal-effect embryonic lethality of *par-2(it5)*. At the permissive temperature, *par-*

2(it5) single mutants and *par-2(it5); (it31)* double mutants displayed 4.9±2.8% (n=509) and 61.6±14.9% (n=1077) maternal-effect embryonic lethality, respectively (Fig. 2.9A). As a single mutant, *it31* is viable (2.5±1.9% embryonic lethality, Fig. 2.9A, n=440) and does not display any detectable phenotypes. Genetic mapping placed *it31* on the left end of Linkage Group X at approximately -20cM very near *lgl-1*, at -19.5cM, raising the possibility that *it31* was a mutation in *lgl-1*. Sequencing revealed a missense mutation, S877N. Furthermore, *it31* fails to complement *lgl-1(tm2616)* for the ability to enhance *par-2(it5)*. An average of 99.8±0.3% of embryos from six *par-2(it5); lgl-1(tm2616)/ it31* mothers failed to hatch (n=636). Thus, *it31* is an allele of *lgl-1*.

To determine the affect of the *it31* S877N mutation on the subcellular localization of LGL-1, we generated transgenic lines expressing LGL-1^{S877N}::GFP. In early embryos, LGL-1^{S877N}::GFP localized very weakly to the posterior cortex compared to LGL-1::GFP (Fig 2.9B). Additionally, we stained endogenous LGL-1 in *it31* embryos and observed that the cortical signal of LGL-1 was notably weaker with respect to wild type (Fig. 2.5). Taken together, these data suggest that the serine at position 877 is required for normal cortical localization of LGL-1 or for stability of the protein. As expected for a hypomorphic mutation, LGL-1^{S877N}::GFP was only weakly able to rescue the enhancement of *par-2(it5)* by *lgl-1(tm2616)* (Fig 2.9A, n=970).

Fig. 2.9. The *it31* S877N mutation compromises the ability of LGL-1 to accumulate on the posterior cortex (**A**) The percentage of embryos that failed to complete embryogenesis in the labeled genotypes (**B**) Confocal mid-sections of fixed two-cell embryos immunostained for GFP

A

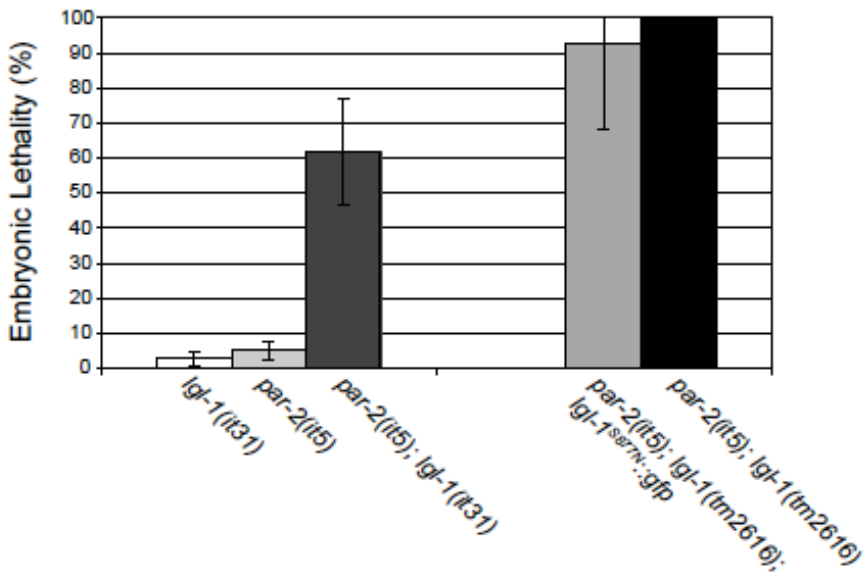
Embryonic Lethality (%)
100
90
80
70
60
50
40
30
20
10
0
lgl-1(tl31)
par-2(tl5)
par-2(tl5); lgl-1(tl31)
par-2(tl5); lgl-1Ser7N::gfp
par-2(tl5); lgl-1(tm2616);
par-2(tl5); lgl-1(tm2616)

B

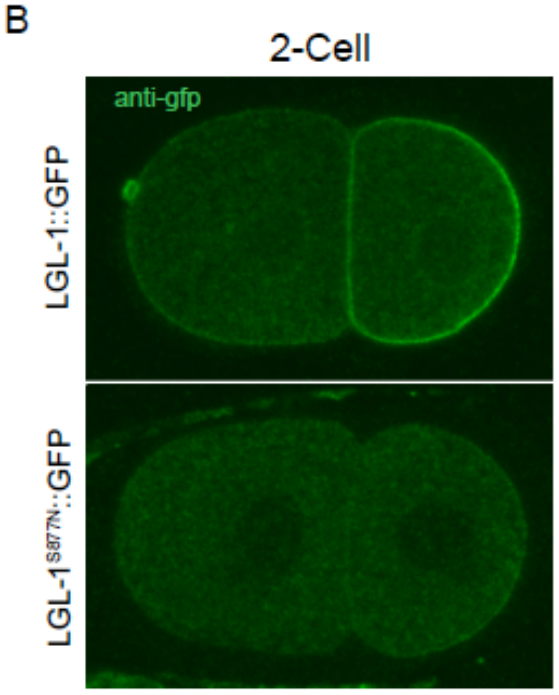
2-Cell
anti-gfp
LGL-1::GFP
LGL-1Ser7N::GFP

Mutation of LGL-1 affects the cortical accumulation of NMY-2 during polarity maintenance

During the maintenance phase of polarity, PAR-2 is required to prevent the recruitment of NMY-2 to the posterior cortex (Cuenca et al., 2003; Munro et al., 2004). Because LGL-1 functions redundantly with PAR-2 during polarity maintenance, we hypothesized that LGL-1 may also affect the posterior cortical accumulation of NMY-2. To test this hypothesis, we compared the localization of NMY-2::GFP in *par-2(RNAi)* and *par-2(RNAi); lgl-1(tm2616)* mutant embryos during the first mitotic division. In wild-type embryos, NMY-2::GFP foci become asymmetrically distributed to the anterior half of the embryo during the establishment phase (Fig. 2.10A). Around the time of pronuclear meeting, the NMY-2 foci are reorganized into finer filaments, which remain enriched in the anterior of the embryo (Fig. 2.10B, (Munro et al., 2004)). During metaphase, NMY-2::GFP is mostly restricted to the anterior half of the embryo although there is a patch of NMY-2::GFP that appears at the posterior pole (Fig. 2.10C). In *lgl-1(tm2616)*, the dynamics of NMY-2::GFP are similar to wild-type (Fig. 2.10E-F). In *par-2(RNAi)* embryos, establishment of NMY-2 asymmetry occurs relatively normally although the cap of NMY-2::GFP foci extends further into the posterior than in wild-type (Fig. 2.10 Munro et al., 2004). The asymmetry fails to be maintained, and shortly after pseudocleavage, NMY-2::GFP asymmetry is lost (Fig. 2.10H, Munro et al., 2004). Around the time of nuclear envelope breakdown, however, NMY-2::GFP partially

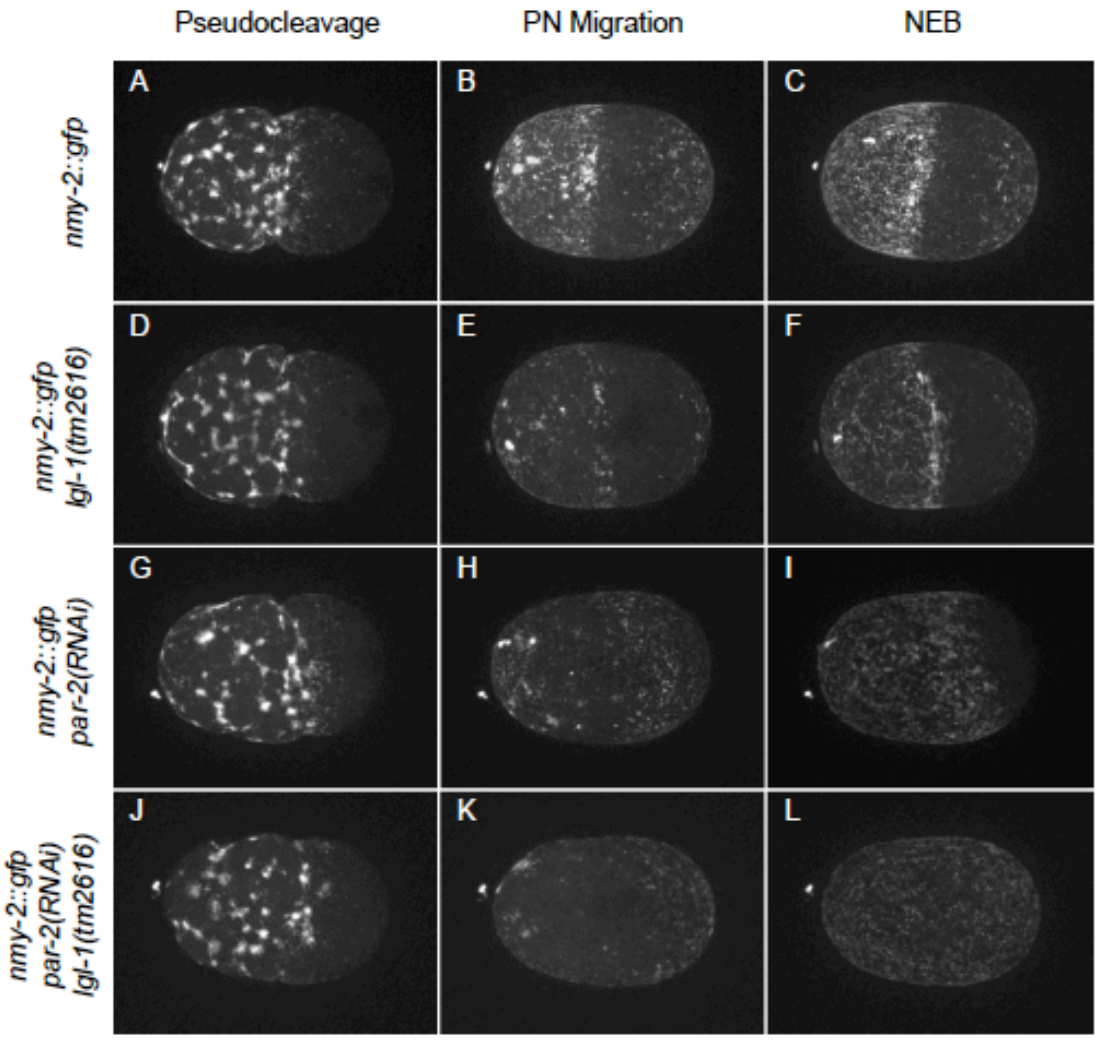

Fig. 2.10. LGL-1 negatively regulates the accumulation of NMY-2 in the posterior in the absence of PAR-2. Confocal projections of cortical NMY-2::GFP in single embryos at pseudocleavage, during pronuclear migration, and at nuclear envelope breakdown. The genotypes of the embryos are (**A-C**) *nmy-2::gfp*, (**D-F**) *nmy-2::gfp; lgl-1(tm2616)*, (**G-I**) *nmy-2::gfp; par-2(RNAi)*, (**J-L**) *nmy-2::gfp; par-2(RNAi); lgl-1(tm2616).*

clears from the posterior (Fig. 2.10I, n=10/12). NMY-2::GFP filaments extend into the posterior, but little NMY-2::GFP is observable on the posterior pole. In *par-2(RNAi); lgl-1(tm2616)* embryos, the dynamics of NMY-2::GFP are similar to that of *par-2(RNAi)* embryos until nuclear envelope breakdown (Fig. 2.10J,K). After that, in contrast to *par-2(RNAi)* embryos, the NMY-2::GFP filaments remain nearly uniformly distributed around the cortex in *par-2(RNAi) lgl-1(tm2616)* embryos, and in most cases, fail to clear from the posterior (Fig. 2.10L, n=11/12). We quantified the extent of NMY-2::GFP clearing based on total embryo length in both *par-2(RNAi)* and *par-2(RNAi); lgl-1(tm2616)*. Although NMY-2 failed to clear in most *par-2(RNAi); lgl-1(tm2616)*, if we include the few embryos that showed some clearing, the average clearing was 5.3±7.1% compared to 21.8±11.1% in *par-2(RNAi)* (n=10, p=0.001). These data suggest that LGL-1 functions redundantly with PAR-2 to negatively regulate the accumulation of NMY-2 in the posterior of the one-cell embryo.

Because LGL-1 inhibits the accumulation of NMY-2::GFP in the posterior in *par-2(RNAi)* embryos, we hypothesized that decreasing the dose of NMY-2 in the early embryo may be sufficient to partially rescue *par-2(it5); lgl-1(tm2616).* To test this hypothesis, we used partial RNAi to reduce NMY-2 levels in the *par-2(it5); lgl-1(tm2616)*. NMY-2 was depleted such that a low level of lethality was observed in N2 (15.1±13.1%). Similar to *par-2(it5); lgl-1(tm2616)* controls, *par-2(it5); lgl-1(tm2616); nmy-2(RNAi)* was 100% embryonic lethal. Results were similar when we compromised NMY-2 function using either of two conditional *nmy-2* alleles (Liu et al., 2010) at semi-restrictive temperature, suggesting reduced NMY-2 function is not sufficient to partially rescue *par-2(it5); lgl-1(tm2616)*.

After determining LGL-1 influences the cortical accumulation of NMY-2, we

screened genes identified in a previous study as affecting the cortical dynamics of the early embryo (Sonnichsen et al., 2005) to determine if RNAi depletion of any of the genes blocked the ability of LGL-1::GFP to rescue *par-2(lw32)* mutants. We found several that caused higher levels of embryonic lethality in *par-2(lw32); lgl-1::gfp* relative to wild type. One of these genes, *let-502*, a homolog of Rho-associated kinase, ROCK (Piekny and Mains, 2002; Wissmann et al., 1997) also compromised early embryonic polarity in *par-2(lw32); lgl-1::gfp* (Fig. 2.11). Specifically, five out of 12 *par-2(lw32); lgl-1::gfp; let-502(RNAi)* embryos had symmetrical first cleavages, and the mitotic spindles of the second cell division were oriented transversely to the A-P axis in both the AB and P1 cells (Fig. 2.11, n=13/13). When LET-502 was depleted in N2, we failed to observe similar polarity defects (Fig. 2.11, n=15/15, also see Sonnichsen et al., 2005).

After identifying a requirement for *let-502* for *lgl-1* over-expression rescue of *par-2(lw32)* we also tested the possible requirement for *m*yotonic dystrophy-*r*elated *C*dc42 binding *k*inase homolog (MRCK-1). MRCK-1 is a potential downstream effector of CDC-42, and both LET-502 and MRCK-1 are involved in the cortical recruitment of NMY-2 in the one-cell embryo (Kumfer et al., 2010). In embryos from *par-2(lw32); lgl-1::gfp; mrck-1(RNAi)* we observed an increased frequency of symmetrical first cleavages (n=6/12) and the mitotic spindles of the second cell division were oriented in transverse to the A-P axis in both the AB and P1 cell (n=12/12), but we did not observe similar defects in *mrck-1(RNAi)* embryos (Fig. 2.11, n=15/15, also see Sonnichsen et al., 2005).

Fig. 2.11. Depletion of LET-502 or MRCK-1 block the ability of LGL-1::GFP to rescue *par-2(lw32)*. (**A**) The percentage of embryos that failed to complete embryogenesis in the labeled genotypes. (**B**) DIC images of two-cell embryos during interphase (left column), and prior to the second mitotic division (right column). The black lines mark the orientation of the mitotic spindles.

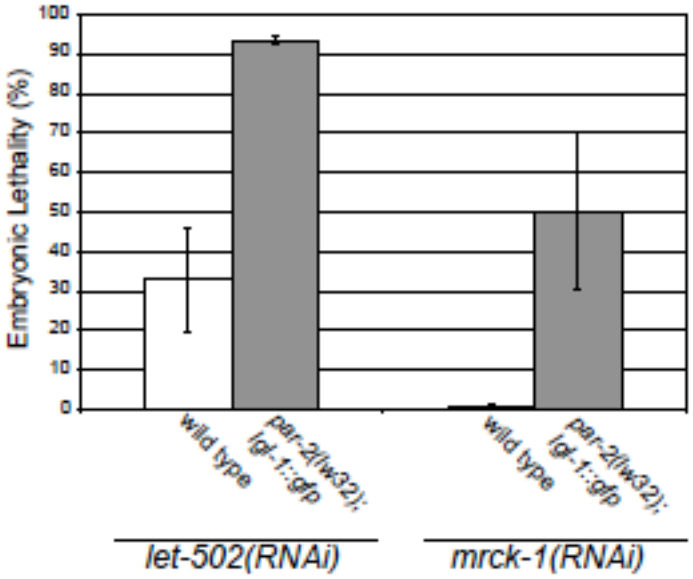
Embryonic Lethality (%)
100
90
80
70
60
50
40
30
20
10
0
wild type
par-2(lw32); lgl-1::gfp
wild type
par-2(lw32); lgl-1::gfp
let-502(RNAi)
mrck-1(RNAi)


let-502(RNAi)
par-2(lw32); lgl-1::gfp let-502(RNAi)
mrck-1(RNAi)
par-2(lw32); lgl-1::gfp mrck-1(RNAi)

DISCUSSION

PAR-2 and LGL-1 function redundantly

We have shown that LGL-1, the *C. elegans* homolog of Lgl, functions redundantly with PAR-2 to maintain polarity in the early embryo. Loss of LGL-1 function robustly enhances both the embryonic lethality and early polarity phenotypes of hypomorphic *par-2* mutants. We also found that LGL-1 and PAR-2 colocalize in the early embryo, and over-expressing LGL-1 in a putative *par-2* null was sufficient to restore embryonic viability and rescue the early polarity defects associated with *par-2* loss of function. These results indicate that LGL-1 and PAR-2 function redundantly and suggest that the respective pathways to which the proteins belong must ultimately converge on a common target or set of targets.

We noted that LGL-1, in addition to posterior cortical localization in the early embryo, is strongly expressed in *C. elegans* epithelial cells and localized basolaterally. However, *lgl-1(tm2616)* worms are viable and fertile with no obvious defects in epithelial function. Because we do not detect PAR-2 in epithelial cells and *lgl-1(tm2616); par-2(lw32)* worms exhibit only maternal effect lethality, we speculate that a polarity protein other than *par-2* functions redundantly with LGL-1 in epithelial cells or that LGL-1 has no function in these cells.

The cortical asymmetry of LGL-1 is regulated by PKC-3

Lgl proteins in flies and mammals are regulated via phosphorylation by aPKC (Betschinger et al., 2003; Plant et al., 2003; Tian and Deng, 2008; Yamanaka et al., 2003). Our results are consistent with conservation of this regulation in *C. elegans*. The asymmetric localization of LGL-1 depends on the aPKC homologue, PKC-3, and

mutating three conserved putative PKC-3 target sites to alanines blocks asymmetry. However, mutating the three conserved putative PKC-3 phosphorylation sites to glutamic acid yielded unexpected results. We hypothesized that the phosphomimetic mutant would fail to localize to the cortex. Instead LGL-1^{3E}::mCherry localized cortically and symmetrically, in addition to being distributed to the cytoplasm. Several explanations for this unexpected result are possible. Perhaps glutamic acid does not closely enough mimic a phosphate group to completely block the cortical localization of LGL-1. Another possibility is that residual cortical LGL-1 is the result of over-expression of the transgene relative to wild type. Alternatively, the regulation of the cortical localization of LGL-1 may depend on additional sites in the protein. Finally, it is possible that the mutated sites may not serve as phosphorylation sites in *C. elegans*.

Two potential modes of LGL-1 action in *C. elegans*

Currently, the molecular mechanism by which Lgl participates in polarity is not well understood. Results from *Drosophila* and mammalian cells suggest three non-mutually exclusive hypotheses to explain how LGL-1 could function (Vasioukhin, 2006; Wirtz-Peitz and Knoblich, 2006). One hypothesis, based initially on work on the LGL-1 homologues Sro7/77 in yeast (Hattendorf et al., 2007; Vasioukhin, 2006; Wirtz-Peitz and Knoblich, 2006) is that LGL could regulate polarized vesicular trafficking. Additional evidence from metazoans supports this role: Mlgl binds a component of the exocytic machinery, syntaxin-4, in mammalian epithelial cells (Musch et al., 2002). The second proposes that Lgl could negatively regulate the activity of non-muscle myosin II. *Drosophila* and human Lgl proteins

bind nonmuscle myosin II (Strand et al., 1994; Strand et al., 1995). Additionally, in *Drosophila* neuroblasts, reducing the dosage of the myosin II gene *zipper* suppresses the loss of basal protein targeting associated with the *lgl* mutation (Ohshiro et al., 2000; Peng et al., 2000). Furthermore, Lgl may function in neuroblasts to restrict myosin to the apical cortex (Barros et al., 2003), although this may be facilitated indirectly by inhibition of aPKC activity on the basal cortex (Atwood and Prehoda, 2009). Finally, in asymmetrically dividing cells in the *Drosophila* nervous system (Atwood and Prehoda, 2009; Betschinger et al., 2003; Wirtz-Peitz et al., 2008) Lgl appears to function by regulating the activity of aPKC, either by inhibiting its activity (Atwood and Prehoda, 2009) or by altering its target specificity (Wirtz-Peitz et al., 2008). It accomplishes this, at least in part, by exchanging with PAR-3 in the PAR-6/aPKC complex (Wirtz-Peitz et al., 2008). A similar exchange with PAR-3 also occurs in mammalian epithelial cells (Plant et al., 2003; Yamanaka et al., 2003). The mode of action of LGL-1 in the early *C. elegans* embryo is not clear. Our evidence argues strongly that the major role of LGL-1 in the early embryo is in maintenance rather than establishment of polarity. Thus, at the time that LGL-1 acts, it is not in a complex with PKC-3 and PAR-6 but acts to exclude these proteins from the posterior cortex. It is possible that LGL-1 prevents binding of PAR-6 and PKC-3 at the cortex by forming PAR-6/LGL-1/PKC-3 complexes that, in contrast to the situation in Drosophila and mammalian cells, can no longer bind cortically. In this model the observed accumulation of myosin in the posterior in the *lgl-1(tm2616); par-2(RNAi)* embryos is a consequence of the abnormal presence of the PAR-6/PKC-3/PAR-3 complex rather than a cause. However, if LGL-1 acted by promoting dissociation of PAR complexes from the cortex, we would expect to see dominant

effects of mislocalizing LGL-1 to the anterior and we do not.

Alternatively, LGL-1 may have an activity that is independent of its complex formation with PAR-6 and PKC-3, such as regulating membrane trafficking or myosin activity. Of these, regulating recruitment of myosin or its activity at the cortex is most consistent with our data. Lgl inhbition of myosin was previously proposed in Drosophila embryonic neuroblasts (Peng et al., 2000). In *Drosophila* neuroblasts, Lgl mutations can be suppressed by compromising myosin activity (Peng et al., 2000). We carried out similar experiments in *C. elegans* to no effect, however; reducing myosin activity using either temperature sensitive *nmy-2* mutations or weak *nmy-2(RNAi)* failed to suppress the enhancing effects of loss of LGL-1 on *par-2* mutants. Evidence that LGL-1 does act at least indirectly through myosin comes from our discovery that rescue of *par-2* mutants via LGL-1 over-expression is dependent upon the activities of Rho kinase (*let-502*) and *mrck-1*, a downstream effector of CDC-42. However, in contrast to the proposed role as an inhibitor of myosin contractility, the requirement for LET-502 and MRCK-1 argues that LGL-1 promotes myosin contractility. Perhaps by blocking myosin accumulation in the posterior, LGL-1 indirectly promotes increased myosin accumulation and hence contractility in the anterior.

The discovery of a role for Lgl in polarity in *C. elegans* underscores the degree to which cell polarity mechanisms are conserved. The creation of a *C. elegans* strain that is completely dependent upon LGL-1 provides a new opportunity to explore the precise mode of action of this interesting protein.

Acknowledgements

We would like to thank Wendy Hoose and Mona Hassab for technical support, and Sylvia Lee for helpful comments on the manuscript. We would also like to thank the National Bioresource Project for the Experimental Animal *C. elegans*, for *lgl-1(tm2716)*, the Biological Resources Branch at NCI for recombineering reagents, the Caenorhabditis Genetics Center for providing worm strains, and Jun Kelly Liu for providing pJKL702.

CHAPTER THREE

THREE DISTINCT PATHWAYS FUNCTION TO MAINTAIN POLARITY IN THE *C. ELEGANS* EARLY EMBRYO

INTRODUCTION

Cell polarity in the one-cell *C. elegans* embryo occurs in two phases: establishment and maintenance (Cuenca et al., 2003). Polarity maintenance is necessary to perpetuate the cortical asymmetries generated during establishment. The maintenance of distinct cortical domains in the *C. elegans* early embryo appears to be mediated primarily by Rho signaling and mutually antagonistic interactions between the anterior and posterior PAR proteins (Nance and Zallen, 2011). While a number of the key proteins involved in polarity maintenance have been identified, the molecular mechanisms by which the proteins contribute to polarity maintenance, as well as the level of interaction between the components are not well understood.

The Rho GTPase CDC-42 appears to be a key regulator during polarity maintenance (Aceto et al., 2006; Kumfer et al., 2010; Motegi and Sugimoto, 2006; Schonegg and Hyman, 2006). During the maintenance phase, CDC-42 is enriched on the anterior cortex (Aceto et al., 2006; Motegi and Sugimoto, 2006; Schonegg and Hyman, 2006), and its active form interacts with the anterior PAR proteins via direct binding to PAR-6 (Aceto et al., 2006; Gotta et al., 2001). In *cdc-42(RNAi)* embryos, PAR-6 and PKC-3 become asymmetrically enriched on the anterior cortex at a reduced level during establishment, and are lost from the cortex around the time of nuclear envelope breakdown. PAR-3 remains cortical but often extends into the posterior and can overlap with PAR-2 (Gotta et al., 2001; Kay and Hunter, 2001).

Embryos expressing a PAR-6 mutant defective for CDC-42 binding exhibit similar defects as *cdc-42(RNAi)* embryos suggesting that CDC-42 functions in polarity primarily via its physical interaction with PAR-6 (Aceto et al., 2006).

Reduction of CDC-42 function also results in defects in cortical myosin localization. In embryos depleted for CDC-42, NMY-2 dynamics are similar to wild type during establishment. However, cortical myosin is largely lost during the transition to the maintenance phase when myosin foci are normally reorganized and replaced by finer filaments (Kumfer et al., 2010; Motegi and Sugimoto, 2006; Schonegg and Hyman, 2006). Because CDC-42 is required for the maintenance of cortical PAR-6/PKC-3 as well as cortical myosin, CDC-42 appears to provide a functional link between the anterior PAR proteins and the acto-myosin cytoskeleton during polarity maintenance

The activity of CDC-42 in the early embryo is regulated, at least in part, by a putative CDC-42 GTPase activating protein, CHIN-1, and a guanidine exchange factor, CGEF-1 (Kumfer et al., 2010). These regulators were identified using a biosensor that specifically binds active GTP-bound CDC-42: *chin-1(RNAi)* one-cell embryos have increased cortical levels of active CDC-42 while *cgef-1(RNAi)* embryos have reduced cortical levels of active CDC-42. During polarity maintenance, CHIN-1 appears to inhibit NMY-2 accumulation on the posterior cortex and CGEF-1 is required for robust recruitment of cortical NMY-2 in the anterior (Kumfer et al., 2010). Although *cgef-1(RNAi)* embryos display weak polarity phenotypes, the polarity perturbations in these embryos are not nearly as dramatic as in *cdc-42(RNAi)* embryos suggesting redundancy in CDC-42 regulation.

In addition to Rho signaling, polarity maintenance is also mediated by mutual exclusion between the PAR proteins. On the posterior cortex of the one-cell embryo, the putative E3 ubiquitin ligase PAR-2 is required to prevent the anterior cortical domain from expanding into the posterior during the first mitotic division (Boyd et al., 1996; Cuenca et al., 2003; Hao et al., 2006). Recently, LGL-1, the homolog of the *Drosophila* tumor suppressor protein Lethal Giant Larvae, was found to localize asymmetrically to the posterior cortex and function redundantly with PAR-2 to maintain polarity (Beatty et al., 2010; Hoege et al., 2010). LGL-1 is not required for polarity maintenance; however, *lgl-1;par-2* double mutants have a stronger phenotype than par-2 alone and over-expression of LGL-1 is sufficient to rescue loss of *par-2* function suggesting the proteins function redundantly.

Although it is clear that both PAR-2 and LGL-1 act in polarity maintenance, the molecular mechanisms by which the proteins function are not well understood. Munro and colleagues have proposed that PAR-2 may regulate cortical flows based on the observation that *par-2(RNAi)* embryos exhibited cortical flows directed toward the posterior during polarity maintenance (2004). The aberrant cortical flows were associated with appearance of ectopic NMY-2 fibers in the posterior as well as the redistribution of PAR-6::GFP to the posterior cortex. In addition, NMY-2 accumulated at uniformly low levels around the cortex in *par-3* embryos and uniformly high levels in *par-3; par-2(RNAi)* embryos. The uniformly high cortical levels of NMY-2 in *par-3; par-2(RNAi)* embryos indicates that the posterior cortical accumulation of NMY-2 in *par-2* is not an indirect consequence of a failure to restrict the anterior PAR proteins to the anterior cortical domain. These results suggest that

PAR-2 could potentially act to maintain polarity by inhibiting NMY-2 accumulation on the posterior cortex, preventing cortical flows directed towards the posterior. Furthermore, when cortical flows during polarity establishment are greatly reduced using a temperature sensitive *ect-2* mutant, PAR-2 is required to promote polarizing cortical flows (Zonies et al.,2010), providing additional evidence that PAR-2 may regulate cortical flows. However, PAR-2 can also promote domain partitioning when contractility is nearly abolished by depleting MLC-4 suggesting that the ability of PAR-2 to generate cortical flows is not absolutely necessary for its polarity establishment role (Zonies et al., 2010).

Because over-expression of LGL-1 can completely rescue loss of PAR-2 function, the genetic pathways of the two proteins must ultimately converge on the same target or set of targets. PAR-2 and LGL-1 inhibit the cortical accumulation of NMY-2 on the posterior cortex (Beatty et al., 2010; Munro et al., 2004) consistent with the hypothesis that the respective genetic pathways of the proteins converge on NMY-2. An alternative hypothesis is that the affects of LGL-1 on NMY-2 are indirect and are mediated by direct regulation of the anterior PAR proteins. Heoge and coworkers have suggested that LGL-1 contributes to polarity maintenance by acting on the anterior PAR proteins via a mutual destruction mechanism (2010). This model proposes that PAR-6 and PKC-3 physically interact with LGL-1, likely near the interface of the anterior and posterior cortical domains. The interaction leads to phosphorylation of LGL-1 by PKC-3, which results in the cortical removal of the entire complex. In this way, LGL-1 could facilitate the cortical removal of PAR-6 and PKC-3 that diffuses into the posterior cortical domain and thus contribute to polarity maintenance. Paradoxically however, the mutual destruction suggests that

phosphorylated LGL-1 promotes the cortical removal of PAR-6/PKC-3 despite having a drastically reduced affinity for the proteins (Hoege et al., 2010; Prehoda and Bowerman, 2010). Further studies are necessary to clarify the mechanisms of polarity maintenance and determine how the components of polarity maintenance cooperate to contribute to the partitioning of distinct cortical domains.

METHODS

Nematode strains

Nematodes were grown using standard conditions (Brenner, 1974), and N2 (Bristol) was used as wild type. Mutations used in this analysis include *par-2(it5)* (Kemphues et al., 1988), *par-2(lw32)* (Cheng et al., 1995), *unc-119(ed4)* (Maduro and Pilgrim, 1995), *lgl-1(tm2616)*, *lgl-1(it31)* (Beatty et al., 2010), and *cgef-1(gk261)* (Kumfer et al., 2010). We also used the transgene zuIs45[nmy-2::NMY-2::GFP+unc-119(+)] (Nance et al., 2003), ojIs40 [pie-1::mGFP::wsp-1(G-protein binding domain) + unc-119(+)], ojIs69 [pie-1::mGFP::chin-1 + unc-119(+)] (Kumfer et al., 2010), and itIs167 [Ppie-01::GFP::PAR-06 unc-119(+)] (Li et al., 2010).

RNA interference

RNAi was performed by feeding (Timmons and Fire, 1998). Egg lays were done on RNAi feeding plates and the progeny were allowed to grow to adulthood prior to dissecting and imaging their embryos. All RNAi feedings were done at 25°C with the exception of experiments using *par-2(lw32)*, which were done at 22°C, and where otherwise noted.

Imaging

Confocal images were captured with a PerkinElmer UltraVIEW LCI confocal scanner with a Nikon Eclipse TE2000-U microscope using UltraVIEW Imaging Suite v5.5. The sections were stacked and processed using ImageJ and Adobe Photoshop CS4.

Measuring cortical NMY-2 levels

The fraction of the cortex with NMY-2::GFP signal was measured using ImageJ. Twelve confocal sections starting at the top of the cortex to near the midsection were stacked. The spacing between sections was 1.0μm. Using the *par-6(RNAi)* data set, threshold levels were selected such that most of the NMY-2::GFP filaments in each of the stacks were recognized as particles. Then the area of the particles relative to the total area of the embryo was calculated, and the ratio was referred to as the "fraction of the embryo with signal". The same threshold was applied to the *par-2(lw32); par-6(RNAi)* and *par-2(lw32); lgl-1(tm2616); par-6(RNAi)* data sets, and the means were compared using Student's t test.

Measuring PAR-6 levels

The cortical and cytoplasmic PAR-6 levels were measured using ImageJ. For each embryo, three confocal sections centered on the midsection were stacked. The spacing between sections was 0.5μm. The average cortical PAR-6 signal was determined by drawing nine lines of roughly equal length on the cortical domain (three near the pole and six laterally) and measuring the average signal intensity for each of the lines. The average signal intensities were then averaged and the background signal was

subtracted to yield an average cortical signal for the embryo. The average cytoplasmic signal was determined similarly using three lines per embryo in the anterior or posterior cytoplasm as appropriate. The cortical signal was calculated by measuring the relative area of the embryo associated with the cortical domain and then multiplying that value by the average cortical signal. The cytoplasmic signal was determined by multiplying the total area of the embryo minus the area of the anterior cortical domain by the average cytoplasmic signal and correcting for background signal. Means were compared using Student's t test.

Measuring cortical enrichment of GFP::GBDwsp-1

Cortical enrichment of GFP::GBDwsp-1 was measured using Image J. For each embryo, three confocal sections centered on the midsection were stacked. The spacing between sections was 0.5μm. The anterior and posterior signals were determined by drawing three lines on the anterior or posterior cortex, respectively, and measuring the average signal intensity for each of the lines. The average signal intensities were averaged to yield the cortical signal. The cytoplasmic signal was determined similarly. The cortical enrichment value was calculated by subtracting the cytoplasmic signal from the cortical signal.

RESULTS

LGL-1 activity is mediated through the anterior PAR proteins

In *par-2(RNAi)* embryos, LGL-1 negatively regulates the posterior cortical accumulation of myosin during polarity maintenance, and over-expression of LGL-1 is sufficient to maintain cortical asymmetry (Beatty et al., 2010). However, it is unclear

whether LGL-1 effects cortical NMY-2 independently of the anterior PAR proteins, or whether the observed asymmetry in cortical NMY-2 is a secondary consequence of the removal of the anterior PAR proteins from the posterior cortex by mutual elimination (Hoege et al., 2010). To distinguish between these two potential mechanisms, we compared cortical NMY-2::GFP levels in *par-6(RNAi)*, *par-6(RNAi); par-2(lw32)*, and *par-6(RNAi); par-2(lw32); lgl-1(tm2616)* embryos during polarity maintenance. Consistent with the previously published results (Munro et al., 2004), the cortical levels of NMY-2 in *par-6(RNAi); par-2(lw32)* embryos were substantially higher than in *par-6(RNAi)* embryos. In *par-6(RNAi)* embryos, we determined that the fraction of the cortex occupied by NMY-2::GFP (at a given threshold, see Methods) was 0.21±0.08 at the time of nuclear envelope breakdown (Fig 3.1A, D, n=15). Using identical imaging conditions and threshold values, we observed that the fraction of the cortex occupied by NMY-2::GFP was approximately two-fold higher in *par-2(lw32); par-6(RNAi)* embryos (0.49±0.11, $p=2.8x10^{-5}$, Fig 3.1B, D, n=8). If the effect of LGL-1 on NMY-2 is independent of the protein's interaction with PAR-6 and PKC-3, NMY-2::GFP levels would be higher in *par-2; lgl-1; par-6(RNAi)* embryos than in *par-2; par-6(RNAi)*. However, if LGL-1 functions through the anterior PAR proteins, *lgl-1* would be epistatic to *par-6(RNAi)*, and the levels of cortical NMY-2::GFP would be similar in *par-2; lgl-1; par-6(RNAi)* compared to *par-2; par-6(RNAi)*. Consistent with the latter scenario, we found that cortical NMY-2 levels in *par-2; lgl-1; par-6(RNAi)* embryos (0.43±0.14, Fig 3.1C, D, n=8) were higher than in *par-6(RNAi)* (p=0.001) but similar to *par-2; par-6(RNAi)* (p=0.42).

Taken together, these data suggest that PAR-2 negatively regulates the cortical

Fig 3.1. LGL-1 acts through the anterior PAR proteins to regulated cortical myosin levels in the absence of PAR-2. Confocal projections of cortical NMY-2::GFP at nuclear envelope breakdown in (**A**) *par-6(RNAi)*, (**B**) *par-2(lw32); par-6(RNAi)*, (**C**) *par-2(lw32); lgl-1(tm2616); par-6(RNAi)* (left column). The right column shows micrographs left column overlaid with the threshold mask used to calculate the fraction of the embryo with cortical signal. (**D**) The mean fraction of the embryo with cortical signal for the designated genotypes. Error bars represent standard deviation in all bar graphs unless otherwise specified.

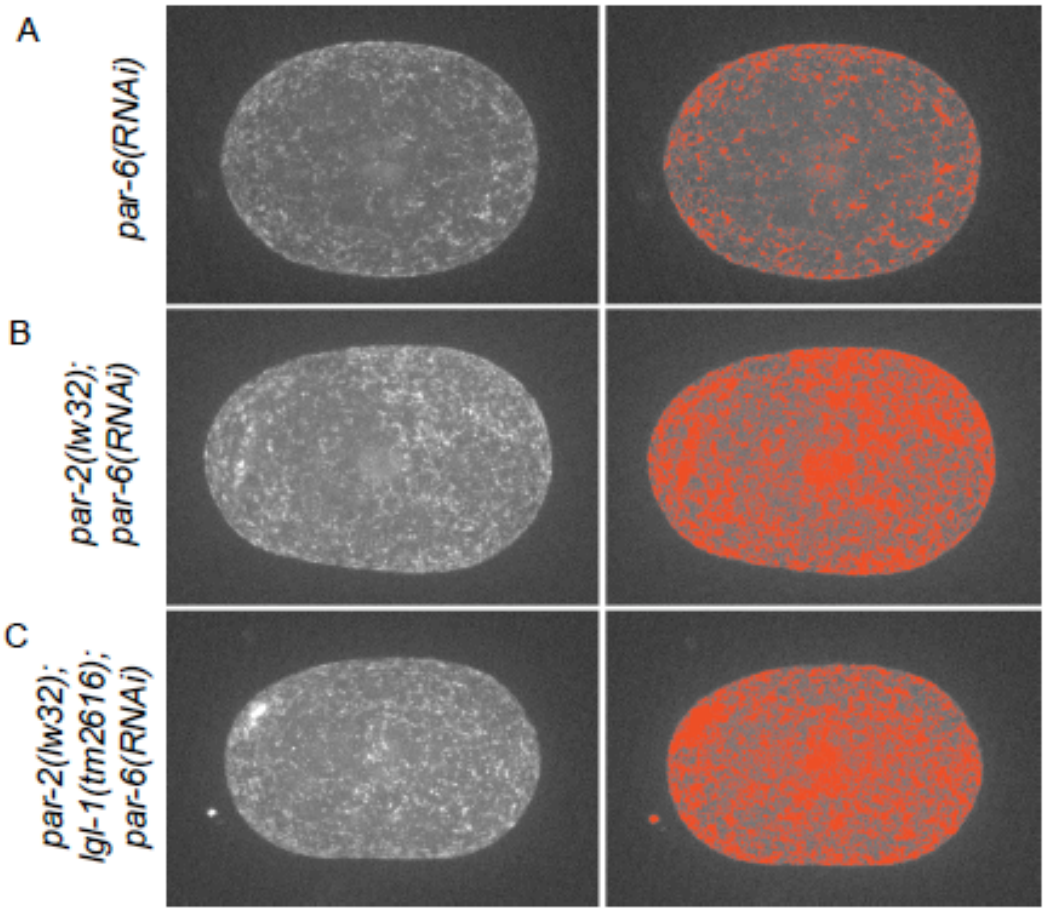
A
par-6(RNAi)
B
par-2(lw32);
par-6(RNAi)
C
par-2(lw32);
lgl-1(tm2616);
par-6(RNAi)

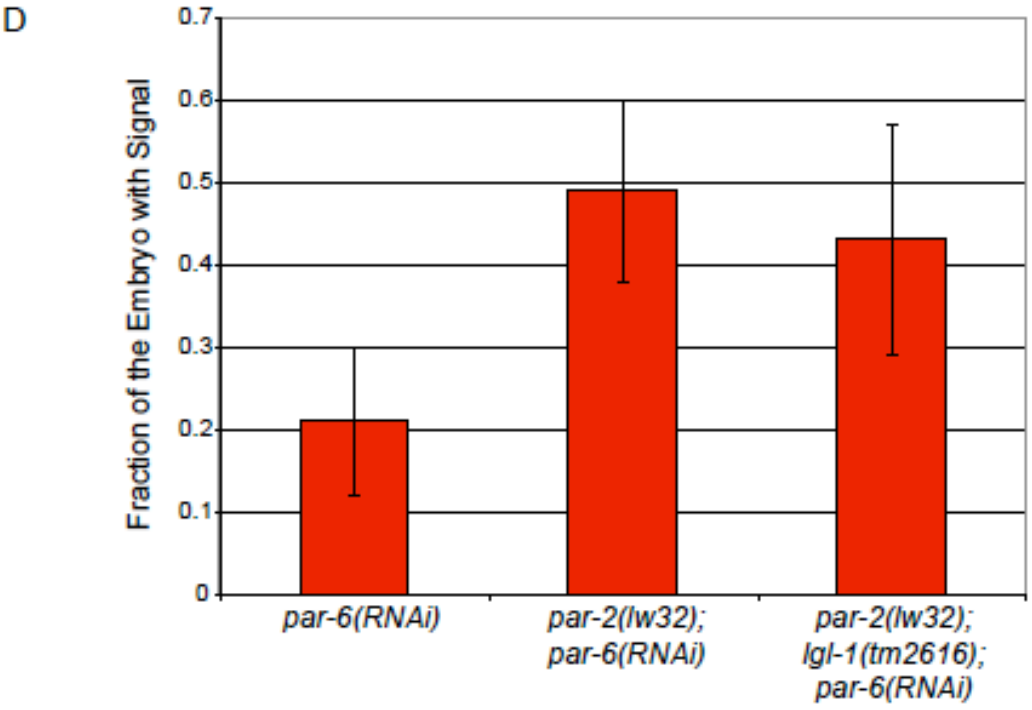
D
Fraction of the Embryo with Signal
0.7
0.6
0.5
0.4
0.3
0.2
0.1
0
par-6(RNAi)
par-2(lw32);
par-6(RNAi)
par-2(lw32);
lgl-1(tm2616);
par-6(RNAi)

accumulation of NMY-2 on the posterior cortex in a manner that is independent of the anterior PAR proteins while LGL-1 acts through the anterior PAR proteins.

PAR-6 levels in the early embryo are increased following LGL-1 depletion

If LGL-1 mediates the removal of PAR-6 from the cortex, we hypothesized that cortical levels of PAR-6 in the one-cell embryo should be increased after depleting LGL-1. To test this hypothesis, we compared the cortical and cytoplasmic of PAR-6 in control and *lgl-1(RNAi)* during polarity maintenance (see methods). In three independent trials, we found the cytoplasmic levels of PAR-6::GFP were higher after depleting LGL-1 compared to the controls (cytoplasmic levels: p=0.05, 0.002, 0.006, n=8 for each trial, Fig 3.2A,B). The cortical levels of PAR-6 were only significantly higher than the control in one out of three trials (p=0.08, 0.26, 0.01, Fig 3.2A,B). Additionally, the area of the PAR-6 cortical domain with respect to the total area of the embryo cross-section was similar in *lgl-1(RNAi)* embryos and control embryos (p=0.47, 0.22, 0.25, Fig 3.2A,B).

We performed a similar experiment comparing PAR-6 levels after depleting PAR-2. In *par-2(RNAi)* embryos, the area of the cortical PAR-6::GFP domain was expanded (p=0.0001, Fig. 3.7A); however, the cortical and cytoplasmic PAR-6 levels were similar to the control (p=0.24, 0.47, respectively, n=10, Fig. 3.7B).

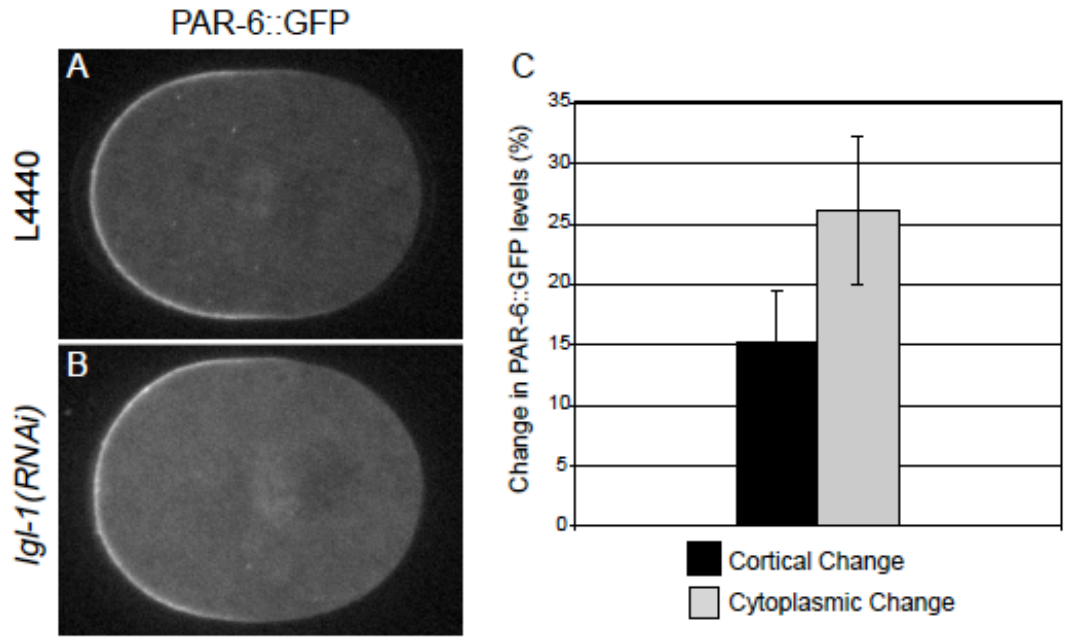

Fig 3.2. PAR-6::GFP levels are increased in *lgl-1(RNAi)* embryos. Confocal midsections of PAR-6::GFP in a **A)** control and an **B)** *lgl-1(RNAi)* embryo. (**C)** The percentage change in cortical and cytoplasmic PAR-6::GFP levels in *lgl-1(RNAi)* embryos with respect to the controls.

Consistent with the previously described role for PAR-2 in polarity maintenance (Cuenca et al., 2003; Hao et al., 2006), we conclude that PAR-2 negatively regulates the size of the cortical PAR-6 domain, but not the levels of PAR-6. In contrast, LGL-1 appears to have no effect on anterior domain size, but instead appears to regulate the overall levels of PAR-6.

Depletion of PAR-6 partially rescues *par-2(lw32); lgl-1(tm2616)*

Reducing the dose of PAR-6 is sufficient to partially suppress *par-2(lw32)* (Watts et al., 1996), suggesting there is at least one additional, PAR-2-independent mechanism that antagonizes the anterior PAR proteins during polarity maintenance. A pathway that includes LGL-1 has been identified (Beatty et al., 2010; Hoege et al., 2010). In *par-2(lw32); lgl-1(tm2616)* mutant embryos, the anterior PAR proteins occupy the entire cortex by anaphase (Beatty et al., 2010). However, the proteins exhibit a graded distribution from anterior to posterior, indicating that there may be an additional polarity maintenance pathway in the early embryo. To determine if there could potentially be another pathway that contributes to polarity maintenance, we tested whether reducing the dose of PAR-6 could partially suppress *par-2(lw32); lgl-1(tm2616)*. Embryos from *par-2(lw32); lgl-1(tm2616)* are 100% maternal effect embryonic lethal (n=815) and both *lw32* and *tm2616* are likely null alleles (Beatty et al., 2010). To reduce PAR-6 function, we fed *par-2(lw32); lgl-1(tm2616)* a 1:1 mixture of *par-6(RNAi)* bacteria and bacteria containing the empty RNAi vector. Wild type worms fed the diluted *par-6(RNAi)* laid 97.3±2.0% dead embryos (n=1326). When the same culture was fed to *par-2(lw32); lgl-1(tm2616)* gave a low level of

viable progeny (97.6±2.8% lethal, n=508) indicating the reducing the dose of PAR-6 is sufficient to modestly suppress the double mutant. These data suggest that there is an additionally mechanism that is independent of PAR-2 and LGL-1 that antagonizes the anterior PAR proteins.

Depletion of CHIN-1 blocks the ability of LGL-1::GFP to rescue *par-2(lw32)*

The putative CDC-42 GAP CHIN-1 has been shown to inhibit the accumulation of NMY-2 on the posterior cortex during polarity maintenance (Kumfer et al., 2010). We wanted to determine whether CHIN-1 was in a genetic pathway with PAR-2, LGL-1, or a component of an independent pathway. To test whether CHIN-1 activity was required for over-expression of *lgl-1* to rescue *par-2(lw32),* we used RNAi to deplete CHIN-1 in *lgl-1::gfp; par-2(lw32)*. Embryos from *chin-1(RNAi)* were mostly viable (0.6±0.9% lethality, n=872); embryos from *lgl-1::gfp; par-2(lw32)* were also mostly viable (Beatty et al., 2010). However, *lgl-1::gfp; par-2(lw32)*; *chin-1(RNAi)* produced 81.5±18.6% dead embryos (n=1286), suggesting that depletion of CHIN-1 blocks the ability of *lgl-1* over-expression to robustly rescue *par-2(lw32)*. One possible explanation for these data is that *chin-1* and *lgl-1* are components of a common genetic pathway. An alternative explanation is that *chin-1* and *lgl-1* are components of parallel genetic pathways, both of which contribute to polarity maintenance. Furthermore, these data suggest that *chin-1* and *par-2* are likely not components of a common genetic pathway.

If *lgl-1* and *chin-1* are components of the same pathway or both contribute independently to polarity maintenance, we expected that depletion of CHIN-1 would

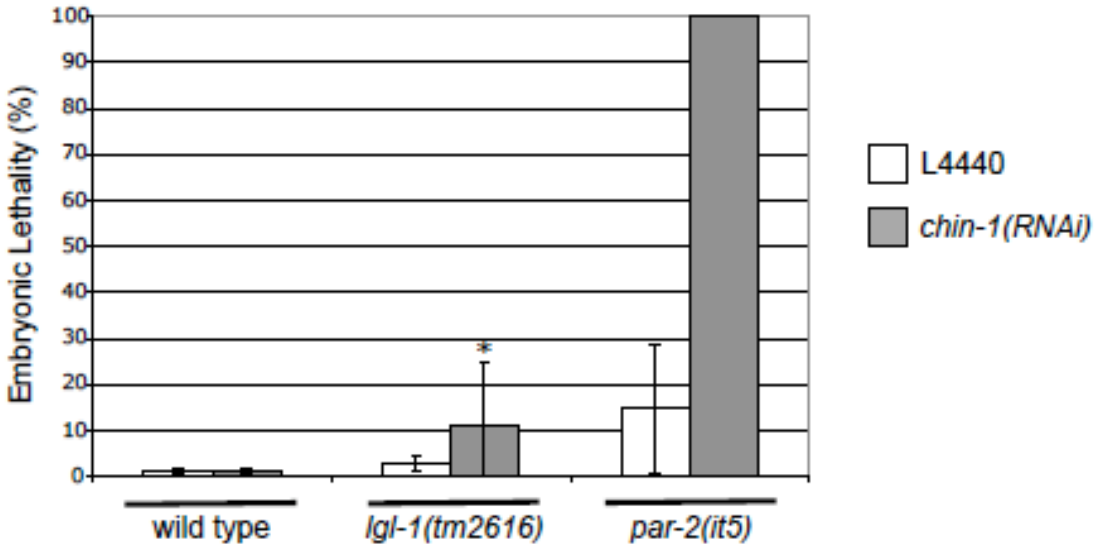

Fig. 3.3. *chin-1(RNAi)* interacts synthetically with *lgl-1(tm2616)* and enhances weak *par-2(it5)* mutants. The percentage of embryos that failed to complete embryogenesis in the labeled genotypes. The asterisk denotes that *lgl-1(tm2616); chin-1(RNAi)* lay more dead embryos than would be expected assuming an additive effect ($p<0.0001$, χ^2 test).

enhance *par-2(it5ts)* at the permissive temperature of 16°C similar to *lgl-1* (Beatty et al., 2010). Indeed, embryos from *par-2(it5); chin-1(RNAi)* worms were 100% embryonic lethal (n=355) compared to *chin-1(RNAi)* and *par-2(it5)* at 16°C, which gave 1.6±1.2% and 14.5±14.2% embryonic lethality, respectively.

Additionally, *lgl-1(tm2616); chin-1(RNAi)* exhibited low levels of synthetic lethality. The embryonic lethality for *lgl-1(tm2616)* and *chin-1(RNAi)* were 2.8±1.5% (n=1123) and 1.2±0.6% (n=1451) respectively while the lethality of *lgl-1(tm2616); chin-1(RNAi)* was 10.66±13.8% (n=844, $p<0.0001$, χ^2 test assuming 4.0% lethality was expected for *lgl-1(tm2616); chin-1(RNAi)* if there was no synthetic interaction, Fig. 3.3). These data are consistent with the hypothesis that *chin-1* and *lgl-1* are components of distinct genetic pathways.

Loss of CGEF-1 function rescues *par-2(lw32)*

In addition to CHIN-1, Kumfer and colleagues also identified a putative CDC-42 GEF, CGEF-1, which appeared to antagonize CHIN-1 (2010). Because CHIN-1 depletion enhanced *par-2*, we hypothesized that depletion or mutation of CGEF-1 may be sufficient to suppress *par-2*. Consistent with this hypothesis, embryos from *par-2(lw32); cgef-1(RNAi)* were 65±20% viable (n=618) while *par-2(lw32)* fed bacteria containing empty vector did not yield any viable progeny (n=653, Fig. 3.4). Similar results were observed using *par-2(it5)* at the restrictive temperature; embryos from *par-2(it5)* and *par-2(it5);cgef-1(RNAi)* were 11.2±2.2% (n=1049) and 42.9±29.0% (n=462) viable, respectively. Furthermore, embryos from *cgef-1(gk261); par-2(lw32)* were 76.4±4.5% viable (n=505, Fig. 3.4). The gk261 allele of *cgef-1* is a deletion that

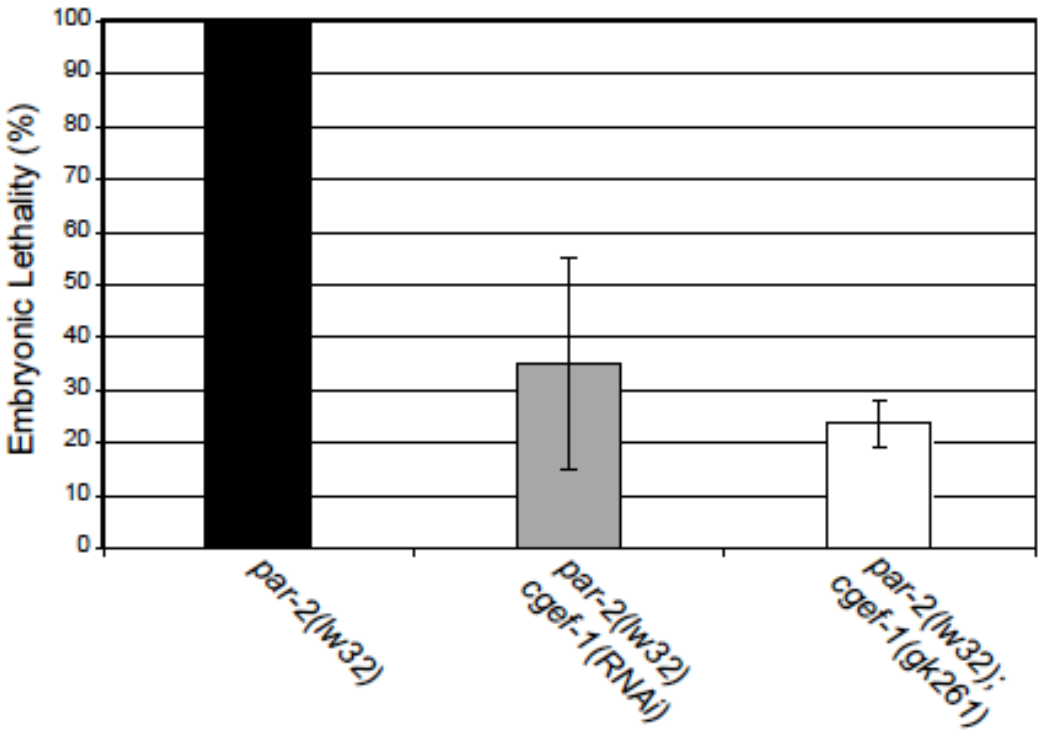

Fig. 3.4. Loss of *cgef-1* function rescues *par-2(lw32).* The percentage embryonic lethality in *par-2(lw32)* and *par-2(lw32); cgef-1(RNAi)* and *par-2(lw32); cgef-1(gk261)*.

Genotype		Embryonic Lethality		
***par-2* allele**	***lgl-1* allele**	**L4440**	***cgef-1(RNAi)***	**p-value**
lw32	*tm2616*	100% (n=563)	99.9±0.4% (n=765)	0.17
lw32	*It31*	100% (n=788)	68.3±8.3% (n=687)	7.4×10^{-6}
it5	*tm2616*	100% (n=628)	100% (n=556)	1
it5	*It31*	97.2±3.4% (n=714)	83.0±15.3% (n=1731)	0.001

Table 3.1. *cgef-1(RNAi)* is sufficient to rescue *par-2; lgl-1* when the *lgl-1* allele is hypomorphic. The mean embryonic lethality values were compared using Student's t test and the corresponding p-values are given in the column on the right.

disrupts the RhoGEF domain and results in a frameshift upstream of the C-terminal PH domain (Kumfer et al., 2010). We conclude that loss of *cgef-1* function suppresses the embryonic lethality associated with *par-2*.

We also tested whether CGEF-1 depletion could suppress *par-2; lgl-1*. To do this, we made a series of *par-2; lgl-1* double mutants by generating all possible pairwise combinations of two putative null alleles (*lw32* and *tm2616*) and two hypomorphic alleles (*it5* and *it31*) of *par-2* and *lgl-1* (Table 3.1). Then, we treated each of the *par-2; lgl-1* double mutants with *cgef-1(RNAi)* and quantified embryonic lethality. When *lgl-1(it31)* was paired with either *par-2(it5)* or *par-2(lw32)*, CGEF-1 depletion resulted in significantly more embryonic viability compared to the respective double mutant fed control RNAi. In contrast, when *lgl-1(tm2616)* was paired with either *par-2(it5)* or *par-2(lw32), cgef-1(RNAi)* was not sufficient to suppress the embryonic lethality associated with the double mutant. These data suggest that *cgef-1(RNAi)* can only suppress *par-2; lgl-1* when a hypomorphic allele of *lgl-1* is coupled with a null allele of *par-2,* but not when a hypomorphic allele of *par-2* is coupled with a null allele of *lgl-1*. Additionally, loss of LGL-1 function abolishes the viability of *cgef-1(gk261); par-2(lw32)*. Taken together, these data indicate that *lgl-1* function is required for loss of *cgef-1* function to rescue *par-2*.

CHIN-1 and CGEF-1 can regulate CDC-42 in *par-2(lw32); lgl-1(tm2616)*

In order to determine the functional relationship between CHIN-1/CGEF-1, PAR-2, and LGL-1, with respect to CDC-42 regulation, we used a transgenic line that expresses the G-protein binding domain of the *C. elegans* homolog of WSP-1 tagged with GFP (GFP::GBDwsp-1). The GBD of WSP-1 selectively binds active, GTP-

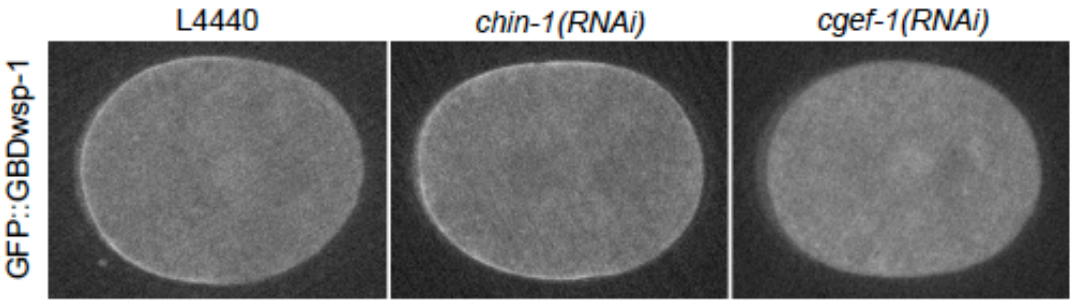

Fig. 3.5. CHIN-1 and CGEF-1 regulate the cortical levels of active CDC-42. Confocal midsections of embryos expressing GFP::GBDwsp-1 at nuclear envelope breakdown. The panel on the left shows a control embryo, the middle panel depicts a *chin-1(RNAi)*, the right panel shows a cgef-1(RNAi) embryo.

bound CDC-42, and thus acts as a biosensor that reports the localization of active CDC-42 (Kumfer et al., 2010). During polarity maintenance, at the time of nuclear envelope breakdown, GFP::GBDwsp-1 is asymmetrically enriched on the anterior cortex of the embryo. To quantify the cortical enrichment and asymmetry, we measure the cortical enrichment of signal at the cortex relative to the cytoplasm in both the anterior and the posterior of the embryo (Table 3.2). We observed an enrichment of signal relative to the cytoplasm of 21.5±1.1 and 1.9±0.4 (arbitrary units) at the anterior and posterior pole respectively (n=10). Consistent with published results, both *chin-1(RNAi)* and *cgef-1(RNAi)* altered localization of the probe during polarity maintenance (Fig. 3.5). In *chin-1(RNAi)*, the cortical enrichment of GFP::GBDwsp-1 in the anterior was similar to the control (20.3±2), but there was increased cortical enrichment in the posterior (10.2±1.7, n=5, Fig. 3.5). In contrast, *cgef-1(RNAi)* resulted in a marked reduction of cortical GFP::GBDwsp-1 (2.7±2.7 on the anterior cortex, 2.0±6.1 on the posterior cortex, n=5, Fig. 3.5). These data are consistent with the hypothesis that CHIN-1 functions as a CDC-42 GAP and CGEF-1 functions as a CDC-42 GEF (Kumfer et al., 2010).

We also tested whether LGL-1 influenced the level or distribution of active CDC-42 in the one-cell embryo by examining the localization of GFP::GBDwsp-1 in *lgl-1(tm2616)* embryos. In *lg1-1(tm2616)* embryos, GFP::GBDwsp-1 was enriched on the anterior cortex, but the cortical enrichment was reduced relative to the control ($p=0.002$).

	GFP::GBDwsp1 signal (arbitrary units)	
Genotype	**Anterior Cortical Enrichment**	**Posterior Cortical Enrichment**
L4440	21.5±1.1	1.9±0.4
chin-1(RNAi)	20.3±3.2	10.2±1.7
cgef-1(RNAi)	2.7±2.7	-2.0±6.1
*lgl-1(tm2616)*_L4440	12.6±3.8	-1.3±3.4
par-2(lw32); lgl-1(tm2616) _L4440	14.7±2.8	1.0±4.2
par-2(lw32); lgl-1(tm2616); chin-1(RNAi)	13.8±5.2	10.8±6.7
par-2(lw32); lgl-1(tm2616); cgef-1(RNAi)	5.1±2.6	-1.0±3.1
par-6(RNAi)	15.6±2.4	6.2±3.3

Table. 3.2. Cortical Enrichment and asymmetry of GFP::GBDwsp1.

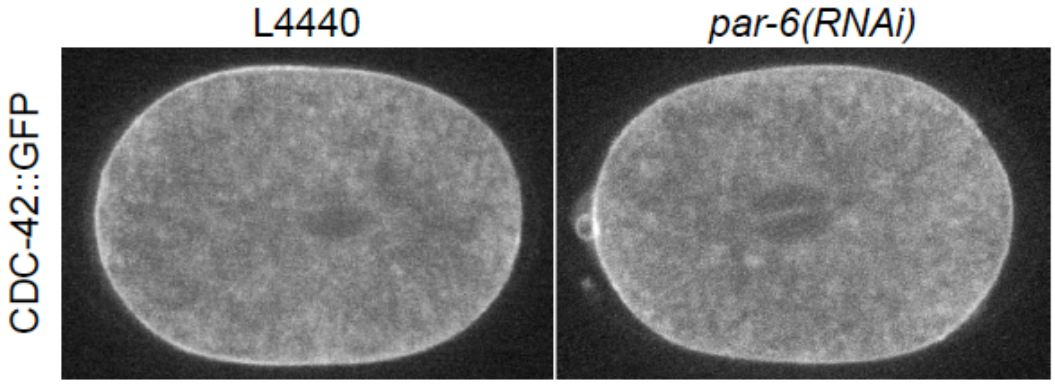

Fig 3.6. CDC-42::GFP remains cortical after depleting PAR-6. Confocal midsections of a control embryo (left) and a *par-6(RNAi)* embryo (right) expressing CDC-42::GFP at nuclear envelope breakdown.

To determine if PAR-2 and LGL-1 are required for CHIN-1 and/or CGEF-1 function, we examined and quantified the localization of GFP::GBDwsp-1 in *par-2(lw32); lgl-1(tm2616), par-2(lw32); lgl-1(tm2616); chin-1(RNAi)* and *par-2(lw32); lgl-1(tm2616); cgef-1(RNAi).* Surprisingly, GFP::GBDwsp-1 was distributed asymmetrically in *par-2(lw32); lgl-1(tm2616).* Furthermore, the cortical levels of the biosensor were increased in *par-2(lw32); lgl-1(tm2616); chin-1(RNAi)* and reduced in *par-2(lw32); lgl-1(tm2616); cgef-1(RNAi).* Based on these data, we conclude that active CDC-42 asymmetry is maintained, at least in part, by a mechanism that is independent of both PAR-2 and LGL-1. In addition, CHIN-1 and CGEF-1 can function in the absence PAR-2 and LGL-1 suggesting that these proteins are likely components of a genetic pathway that does not include PAR-2 or LGL-1.

We also examined the localization of CDC-42 and active CDC-42 after depleting PAR-6. Consistent with previously published data, we observed that CDC-42 was enriched two-fold on the anterior cortex compared to the posterior cortex (2.0±0.7 fold enrichment, n=6, Fig. 3.6, Aceto et al., 2006; Motegi and Sugimoto, 2006; Schonegg and Hyman, 2006). PAR-6 binding to CDC-42 is required for PAR-6 to be maintained at the cortex (Aceto et al., 2006). To test whether the cortical CDC-42 is reduced in the absence of PAR-6, we measured the cortical enrichment of CDC-42::GFP relative to the cytoplasm in both control and *par-6(RNAi)* embryos shortly after nuclear envelope breakdown. In control embryos, CDC-42::GFP was enriched on the anterior cortex two-fold compared to the posterior cortex (2.0±0.7, n=6). We found that PAR-6 was not required for CDC-42 to localize to the cortex, but the

anterior to posterior signal ratio was significantly reduced relative to the controls (1.2±0.4, n=6, p=0.02). After confirming that PAR-6 is not required for CDC-42 to localize to the cortex, we examined GFP::GBDwsp-1 localization after depleting PAR-6. In *par-6(RNAi)* embryos, GFP::GBDwsp-1 was still enriched in the anterior, but the levels of the biosensor on the posterior were modestly increased relative to the control. The enrichment on the anterior cortex was 15.6±2.4 and the enrichment on the posterior cortex was 6.2±3.3 (n=5).

Cortical PAR-6 levels are increased in *chin-1(RNAi)* embryos and reduced in *cgef-1(RNAi)* embryos

We compared the cortical and cytoplasmic levels of PAR-6::GFP in control, *chin-1(RNAi)*, and *cgef-1(RNAi)* embryos at the time of nuclear envelope breakdown. After depleting CHIN-1, PAR-6 extended further into the posterior than in controls (Fig. 3.7A). The area of PAR-6 cortical domain relative to the area of the entire embryo cross section was 0.041±0.002 for *chin-1(RNAi)* (n=5) compared to 0.030±0.002 for the control ($p=2.9x10^{-6}$, n=6). Consistent with these data, the cortical signal in embryos in which CHIN-1 was depleted was also increased ($p=3.6x10^{-6}$). In addition, the cytoplasmic PAR-6 levels were increased in *chin-1(RNAi)* embryos (p=0.01, Fig. 3.7B).

In *cgef-1*(RNAi) embryos, the area of the PAR-6 domain was smaller than in the controls (p=0.003, n=10) and was sometimes positioned laterally (n=3/10, Fig 3.7A). The cortical PAR-6 levels were reduced (p=0.01) while the cytoplasmic levels were increased with respect to the controls (p=0.05, Fig. 3.7B).

Fig. 3.7. Depletion of CHIN-1 and CGEF-1 affect PAR-6::GFP levels. (**A**) Confocal midsections of PAR-6::GFP at nuclear envelope breakdown in control, *par-2(RNAi), chin-1(RNAi)*, and *cgef-1(RNAi)*. (**B**) The percentage change in cortical and cytoplasmic PAR-6::GFP levels in *par-2(RNAi), chin-1(RNAi)*, and *cgef-1(RNAi)* embryos with respect to the controls. The asterisks denote statistically significant changes.

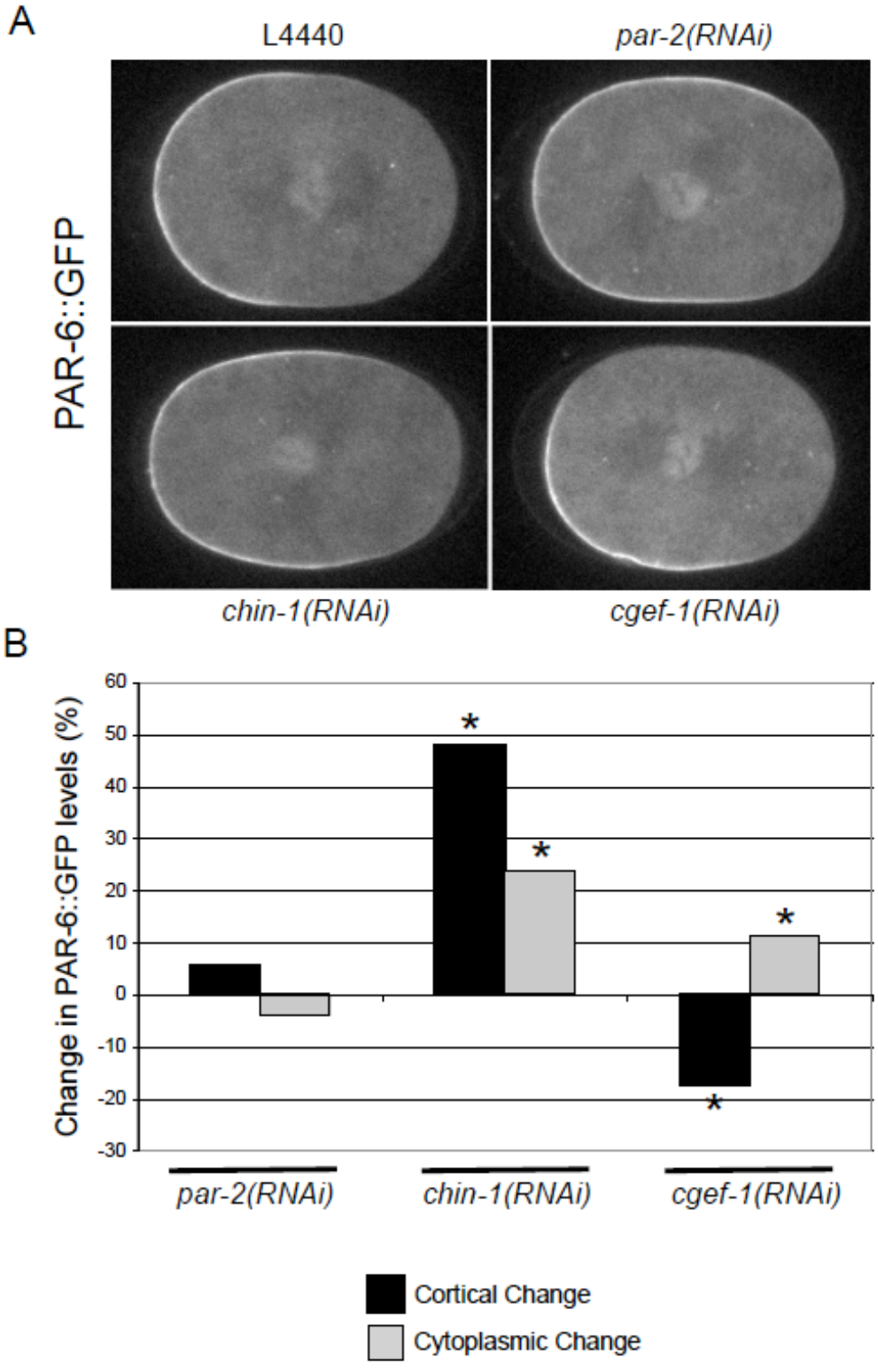
A
L4440
par-2(RNAi)
PAR-6::GFP
chin-1(RNAi)
cgef-1(RNAi)
B
Change in PAR-6::GFP levels (%)
60
50
40
30
20
10
0
-10
-20
-30
*
*
*
*
par-2(RNAi)
chin-1(RNAi)
cgef-1(RNAi)
Cortical Change
Cytoplasmic Change

DISCUSSION AND FUTURE DIRECTIONS

We plan to publish the research described in chapter in the future; however, the story is not complete at this time. My previous work described in Chapter 2, showed the existence of two redundant pathways for polarity maintenance. In this Chapter, I presented two kinds of evidence for the existence of yet a third redundant pathway. First is the observation that *par-2(lw32); lgl-1(tm2616)* can be suppressed by decreasing PAR-6 levels suggesting that there is an additional polarity maintenance pathway that antagonizes the anterior PAR proteins. Second, active CDC-42, as reported by GFP::GBDwsp-1, is asymmetric in *par-2(lw32); lgl-1(tm2616)*, and the levels of cortical, active CDC-42 are regulated by CHIN-1 and CGEF-1 in the double mutant background, suggesting these proteins are functional in the absence of PAR-2 and LGL-1.

Based on these data, I hypothesize that CHIN-1 and CGEF-1 are components of a novel maintenance pathway. To test this hypothesis, I would like to deplete CHIN-1 in strain that lacks function LGL-1 and PAR-2, and has a reduced dose of PAR-6. To this end, I plan to construct the following strain: *par-6(zu222)/hIN1; par-2(lw32); lgl-1(tm2616)*. In the absence of functional PAR-2 and LGL-1, I suspect that reducing the dose of PAR-6 will restore a low level of viability. If this proves to be true, I plan to deplete CHIN-1 in *par-6(zu222)/hIN1; par-2(lw32); lgl-1(tm2616).* If *chin-1(RNAi)* abolishes the embryonic viability associated with the line, I will conclude that CHIN-1 is a component of a third polarity pathway that is independent of PAR-2 and LGL-1.

Polarity maintenance components appear to influence overall PAR-6 levels

An underlying mechanism in polarity maintenance appears to be the balance of antagonistic polarity components. Unlike PAR-2, which seems to primarily regulate the size of the anterior domain, LGL-1 appears to regulate PAR-6 levels, especially the cytoplasmic levels. Our observations are consistent with the "mutual destruction" model proposed by Hoege and colleagues (2010). This proposed mechanism for LGL-1 action predicts that cortical PAR-6::GFP levels should be higher after depleting LGL-1, perhaps at the expense of cytoplasmic levels; however, our data suggest that LGL-1 may influence the degradation of the protein in addition to regulating the level of cortical PAR-6,.

The CDC-42 regulators CHIN-1 and CGEF-1 are also likely regulate PAR-6 levels in the early embryo. While *cgef-1(RNAi)* embryos exhibit reduced levels of cortical PAR-6, *chin-1(RNAi)* embryos have increased amounts of PAR-6 on the cortex and in the cytoplasm suggesting both proteins to influence polarity via the anterior PAR proteins, although the two proteins may not be completely antagonistic. These data are consistent with previously published results demonstrating that reducing CDC-42 levels are sufficient to suppress *par-2*. Because PAR-6 must bind CDC-42 to be maintained at the cortex (Aceto et al., 2006), CHIN-1 and CGEF-1 presumably influence PAR-6 cortical levels by modulating the amounts of active CDC-42 at the cortex.

Redundant roles for PAR-2 and LGL-1 during polarity establishment

Our results highlight the robustness of the polarity system in the early embryo. Both polarity establishment and maintenance appear to involve redundant mechanisms. Recently, Zonies and colleagues have reported that two redundant pathways function to polarize the one-cell embryo: one pathway dependent on actomyosin driven cortical flows, and another parallel pathway dependent on PAR-2 (Zonies et al., 2010). In the absence of the ECT-2-dependent cortical flows, PAR-2 is able to occupy the cortex asymmetrically. These results raise the question as to whether LGL-1 also functions redundantly with PAR-2 during establishment, or whether the overlap in function is limited to the maintenance phase. We can test these alternative hypotheses by determining if LGL-1 is required for the PAR-2-mediated domain partitioning and if over-expression of LGL-1 is sufficient to drive polarity establishment in the absence of both PAR-2 and ECT-2-dependent cortical flows.

APPENDIX 1

A.1. Directed RNAi screens using *lgl-1(tm2616)* did not yield any robust synthetic interactors

After identifying *lgl-1* as a strong enhancer of *par-2(it5)*, we were interested in finding additional factors that function in polarity maintenance with PAR-2 and LGL-1. To this end, we performed two small-scale RNAi screens using the *lgl-1* deletion allele, *tm2616*.

A.1.1. Directed RNAi screen using the "top 100" enhancers of par-1/par-4

In an attempt to identify other proteins that may be involved in genetic pathways that act in parallel to LGL-1, we used a directed RNAi screen to find proteins that, when depleted by RNAi, resulted in early embryonic phenotypes in an *lgl(tm2616)* mutant background but not in a wild-type (N2) background. The set of RNAi clones screened were the "top 100" genes identified in a genome-wide screen for enhancers of the *par-1* and *par-4* temperature sensitive mutants (D. Morton, W. Hoose, and K Kemphues, unpublished data). Using this set enabled us to limit our screen to a group of genes that have already been implicated in polarity in the early embryo.

From the screen, we identified eight genes that, when depleted, caused *lgl-1(tm2616)* to grow slower and often appear sicker than the wild-type control (Table A.1.1). However, none of the genes resulted in obvious early embryonic phenotypes when depleted in *lgl-1(tm2616)*; therefore, none of the genes were pursued in the context of studying the role of *lgl-1* in polarity.

Gene	Protein Description
math-33	ubiquitin carboxyl-terminal hydrolase
F42C5.10	Unknown
uba-2	ubiquitin-activating enzyme
aos-1	activator of SUMO
gei-17	protein containing a MIZ domain
kin-10	casein kinase II
mdt-6	LET-425 transcriptional mediator
C26E6.3	cell differentiation family, like Rcd1

Table A.1.1. Genes and corresponding proteins that, when depleted by RNAi, caused *lgl-1(tm2616)* to grow more slowly than the wild type control.

A.1.2. Directed RNAi screen using genes involved in cortical dynamics in the early embryo

We also performed a similar screen using the list of genes identified by Sonnichsen and colleagues as affecting cortical dynamics in the early embryo (2005). For this screen, we compared the dynamics of NMY-2::GFP in *lgl-1(tm2616)* and control embryos after depleting each of the candidate genes. While a number of the RNAi treatments resulted in altered the dynamics of NMY-2::GFP in the early embryo, the respective phenotypes were indistinguishable in *nmy-2::gfp; lgl-1(tm2616)* compared to *nmy-2::gfp*. It should be noted that we screened the same candidate list in *par-2(lw32); lgl-1::gfp* and identified a several genes that blocked the ability of LGL-1::GFP to rescue *par-2(lw32)* (Please refer to Chapter Two, pgs 49-50).

APPENDIX 2

A.2. S478 and S479 of LGL-1 are not required for asymmetry.

The cortical asymmetries of the one-cell embryo result in the asymmetric distribution of the cytoplasmic cell fate determinants MEX-5 and MEX-6 (Cheeks et al., 2004; Cuenca et al., 2003; Schubert et al., 2000). These nearly identical zinc finger proteins, in turn, direct the partitioning of other cytoplasmic cell fate determinants such as PIE-1 (Cuenca et al., 2003; Schubert et al., 2000; Tenlen et al., 2008). Recently, Tenlen and colleagues identified a likely PAR-1/PAR-4 phosphorylation sequence in MEX-5 (Tenlen et al., 2008). The sequence includes an RXXL motif four residues upstream of two adjacent residues that each contain a free hydroxyl group. Mutating either both or the most downstream of the phosphorylatable residues to alanine or glutamic acid was sufficient to markedly reduce the asymmetry of the protein. Furthermore, the mutant proteins failed to rescue *mex-5; mex-6* indicating the residues are required for MEX-5 function.

A.2.1. LGL-1 contains a putative PAR-1/PAR-4 phosphorylation site

Similar to MEX-5, LGL-1 contains a putative PAR-1/PAR-4 phosphorylation sequence. More specifically, LGL-1 contains an RTSL motif at positions 469-472 followed by two serine residues at positions 478 and 479. The presence of a potential PAR-1/PAR-4 phosphorylation sequence suggests that these kinases could play a role in regulating LGL-1.

If LGL-1 is in some way regulated by PAR-1/PAR-4, we hypothesized that *par-2(lw32), lgl-1::gfp* might be more sensitive to PAR-1 or PAR-4 depletion than wild type. To test this hypothesis, we fed "aged" *par-1(RNAi)* bacteria to *par-2(lw32),*

lgl-1::gfp and quantified embryonic lethality. Storing induced RNAi bacterial cultures for extended periods at 4°C (1-2 months) often reduces the effectiveness of the culture in depleting the targeted mRNA. Consistent with this notion, wild type worms fed "aged" *par-1(RNAi)* were mostly viable (3.3±6.8% embryonic lethality, n=635) compared to fresh *par-1(RNAi)* bacteria which typically results in >95% embryonic lethality. In contrast, feeding "aged" *par-1(RNAi)* to *par-2(lw32), lgl-1::gfp* yielded 98.9±1.4% lethality (n=267). Furthermore, *par-4(RNAi)* caused much high levels of lethality in *par-2(lw32); lgl-1::gfp* than in wild type (Diane Morton, unpublished data). These data suggest that even weak depletion of PAR-1 or PAR-4 blocks the ability of LGL-1 over-expression to rescue *par-2(lw32)*.

A.2.2. LGL-1^{S478A,S479A}::GFP and LGL-1^{S478E,S479E}::GFP localize asymmetrically

To determine if the potential *par-1/par-4* phosphorylation sites in LGL-1 are involved in the protein's localization or function, we generated transgenic lines expressing LGL-1::GFP in which the phosphorylatable residues were mutated to either alanine or glutamic acid (*lgl-1^{S478A,S479A}::gfp* and *lgl-1^{S478E,S479E}::gfp*, respectively). Both LGL-1^{S478A,S479A}::GFP and LGL-1^{S478E,S479E}::GFP localized asymmetrically to the posterior cortex of the one-cell embryo; however, the cortical signal intensity of both mutants was reduced compared to LGL-1::GFP. The reduction was most notable for LGL-1^{S478E,S479E}::GFP. The difference in intensity could have been a result of lower expression of the transgene, but the trend was similar for all of the lines examined (2 independent lines for each).

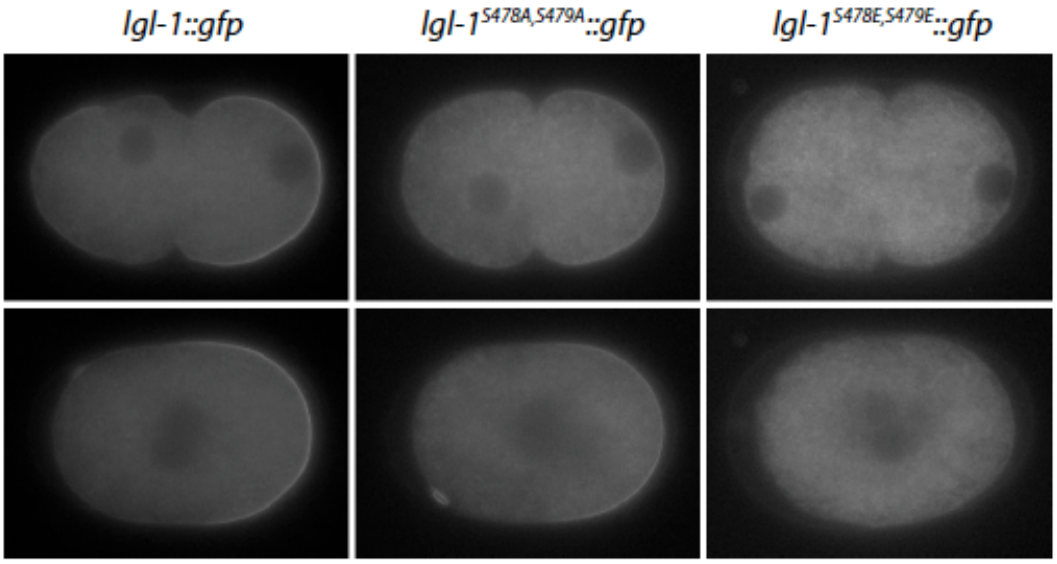

Fig A.2.1. LGL-1^{S478A,S479A}::GFP and LGL-1^{S478E,S479E}::GFP localize asymmetrically, but at a reduced level compared to LGL-1::GFP. Wide-field fluorescence micrographs depicting embryos expressing LGL-1::GFP at pseudocleavage (top row) and slightly before nuclear envelope breakdown (bottom row).

Additionally, expression of LGL-1^{S478A,S479A}::GFP rescued the enhancement of *par-2(it5)* by *lgl-1(tm2616)*, suggesting the mutant protein was functional. *par-2(it5); lgl-1(tm2616)* is 100% maternal-effect embryonic lethal; however, expression of LGL-1^{S478A,S479A}::GFP in *par-2(it5); lgl-1(tm2616)* restores viability. We have not yet tested if LGL-1^{S478E,S479E}::GFP is similarly capable of rescuing *par-2(it5); lgl-1(tm2616)*. Taken together, these data suggest S478 and S479 are not required for LGL-1 asymmetry and function.

APPENDIX 3

A.3. NUM-1 does not appear to be a downstream effector of LGL-1 in the early *C. elegans* embryo

A.3.1. num-1(RNAi) modestly enhanced par-2(it5ts) at the permissive temperature

In *Drosophila* sensory organ precursor cells, Lgl modulates the substrate specificity of aPKC, which enables Numb to be released from the cortex on only one side of the cell prior to asymmetric cell division (Wirtz-Peitz et al., 2008). We hypothesized LGL-1 may act similarly in *C. elegans*, and thus be genetically upstream of the Numb homolog, NUM-1, in the early embryo. NUM-1 is expressed in the early embryo (as well as other tissues), and plays a nonessential role in negatively regulating endocytic recycling (Nilsson et al., 2008). If NUM-1 is genetically downstream of LGL-1, we predicted that loss of NUM-1 function would enhance weak *par-2* alleles. However, depletion of NUM-1 by RNAi only marginally enhanced the embryonic lethality of *par-2(it5)*. At the permissive temperature, *par-2(it5)* fed bacteria containing empty RNAi vector were 3.5±2.7% embryonic lethal (n=2331) compared to *par-2(it5); num-1(RNAi)* which were 11.2± 10.1% lethal (n=1972, p=0.03). The positive control, *lgl-1(RNAi)*, robustly enhanced *par-2(it5)* ($p=9.5x10^{-7}$).

A.3.2. num-1(bc365) did not enhance *par-2(it5)* or *par-2(it5); lgl-1(it31) at the permissive temperature*

In an attempt to verify the modest enhancement observed using *num-1(RNAi)*, we constructed a *par-2(it5); num-1(bc365)* double mutant. We measured the embryonic lethality of *par-2(it5); num-1(bc365)* and found no significant difference in embryonic lethality from the double mutant compared to *par-2(it5)* isolated from the same cross used to generate the *par-2(it5); num-1(bc365)*. And finally, we made a

par-2(it5); lgl-1(it31); num-1(bc365), and compared the viability of the triple mutant to *par-2(it5); lgl-1(it31)*. Again, there was no significant difference in viability. In conclusion, we were unable to find convincing genetic evidence that NUM-1 is a downstream effector of LGL-1 in the *C. elegans* early embryo; however, it should be noted that while the deletion associated with *bc365* removes most of the sequence coding for the phosphotyrosine interaction domain (PTB/PID) in the a,c,d and e isoforms of *num-1*, the deletion does not disrupt the coding region of the b isoform (Nilsson et al., 2008). Consequently, it is still a formal possibility that the b isoform plays a role downstream of LGL-1 in the early embryo.

APPENDIX 4

A.4. The conserved putative AIR-1 phosphorylation site in PAR-6 is not required for the asymmetry or function of the protein in the early embryo

In *Drosophila* sensory organ precursor cells, PAR-6/aPKC bind Lgl to the exclusion of Baz(PAR-3). At the onset of mitosis, PAR-6 is phosphorylated by AruraA kinase which results in the activation of aPKC and sets off a regulatory cascade that results in the partitioning of distinct cortical domains (Wirtz-Peitz et al., 2008). The potential AruraA phosphorylation site on PAR-6 is conserved in *C. elegans* (S29) (Wirtz-Peitz et al., 2008), but the role of AruraA kinase in cell polarity is not clear in this system.

A.4.1 Depletion of AIR-1 alters the localization of LGL-1::GFP in the one-cell embryo

AIR-1 is involved in centrosome maturation (Hannak et al., 2001) and has been proposed to be a regulator of cortical domain size in the early embryo (Schumacher et al., 1998). To examine the role of AIR-1 in polarity in the early embryo, we examined LGL-1::GFP localization throughout the first mitotic division in *air-1(RNAi)* embryos. In addition to cytokinesis and furrow positioning defects, LGL-1 was mislocalized in most embryos (n=17/18). In some cases, the LGL-1 domain was weak or reduced in size (Fig. A.4.1B,C, n=9/17). In other instances, polarity was reversed (Fig. A.4.1E, n=7/19), and there was an LGL-1 domain in both the anterior and posterior in one embryo (Fig. A.4.1D).

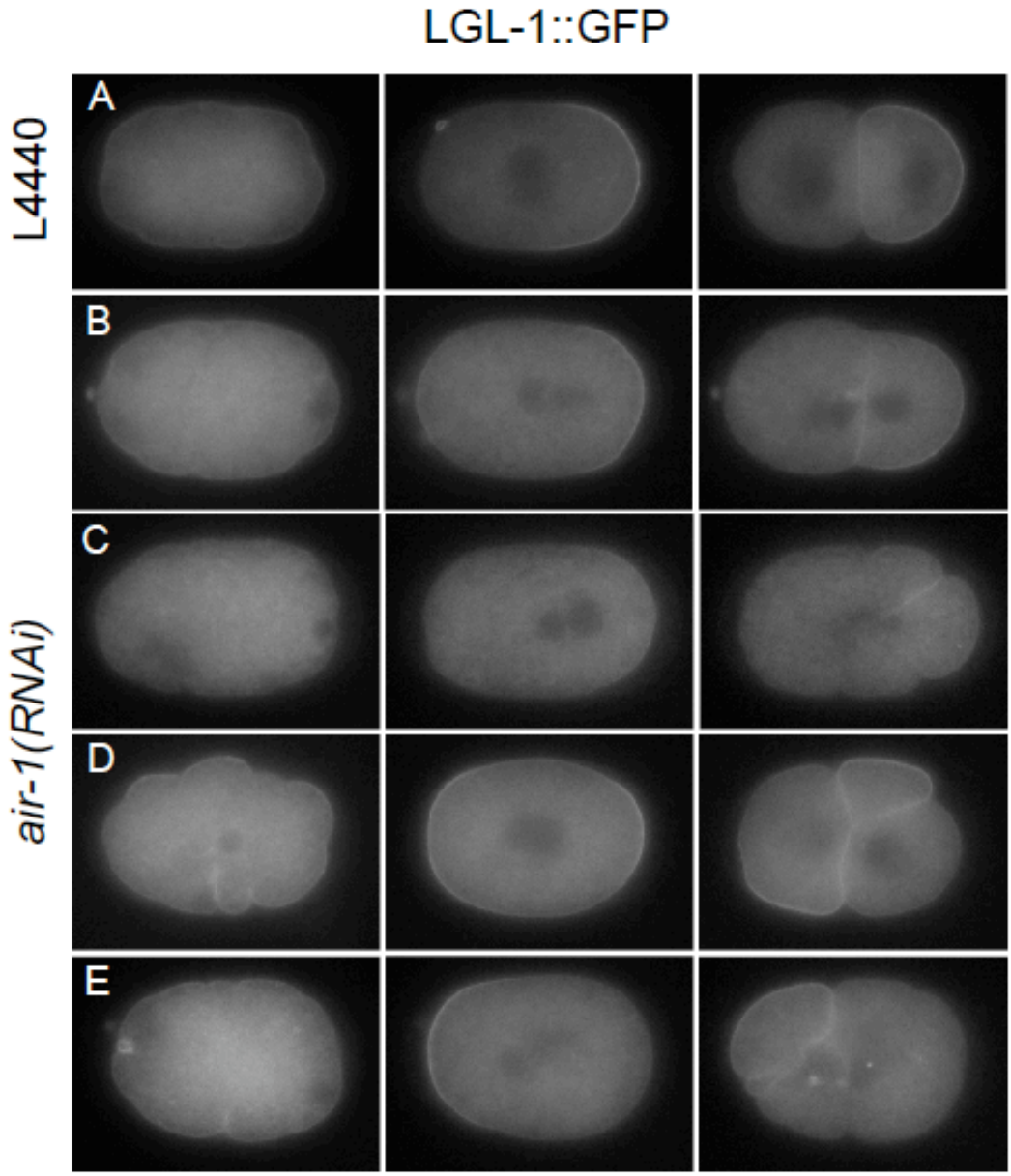

Fig. A.4.1. LGL-1::GFP is mislocalized in *air-1(RNAi)* embryos. Wide field fluorescence images of LGL::GFP in (**A**) control and (**B-E**) *air-1(RNAi)* embryos. Each row shows a single embryo prior to polarity establishment (left column), at pronuclear migration (middle column), and near the time of the first cytokinesis (right column.

A.4.2 Serine 29 in PAR-6 is not required for function

Although *air-1(RNAi)* resulted in a range of polarity defects, we could not determine whether the defects were because AIR-1 directly regulates polarity components, or whether the observed polarity phenotypes were an indirect consequence of a centrosome maturation defect. If AIR-1 regulated polarity by phosphorylation PAR-6, we hypothesized mutating the conserved potential AIR-1 phosphorylation site on PAR-6 would result in a polarity defect. To test this hypothesis, we generated a transgenic line expressing PAR-6::mCherry in which the conserved residue (Ser29) is mutated to alanine. To determine if PAR-6^{S29A}::mCherry was functional, we expressed the mutant protein in *par-6(zu222)*. In *par-6(zu222)* embryos, PAR-6^{S29A}::mCherry localized asymmetrical to the anterior cortex as in wild type. Furthermore, *par-6(zu222); par-6^{S29A}::mcherry* lines could be maintained. These data suggest that the polarity defects in *air-1(RNAi)* embryos are likely a result of a centrosome maturation defects although we cannot rule out the possibility that there are additional AIR-1 phosphorylation sites on PAR-6 that are redundant with S29 or that S29 is not an AIR-1 phosphorylation site in *C. elegans*.

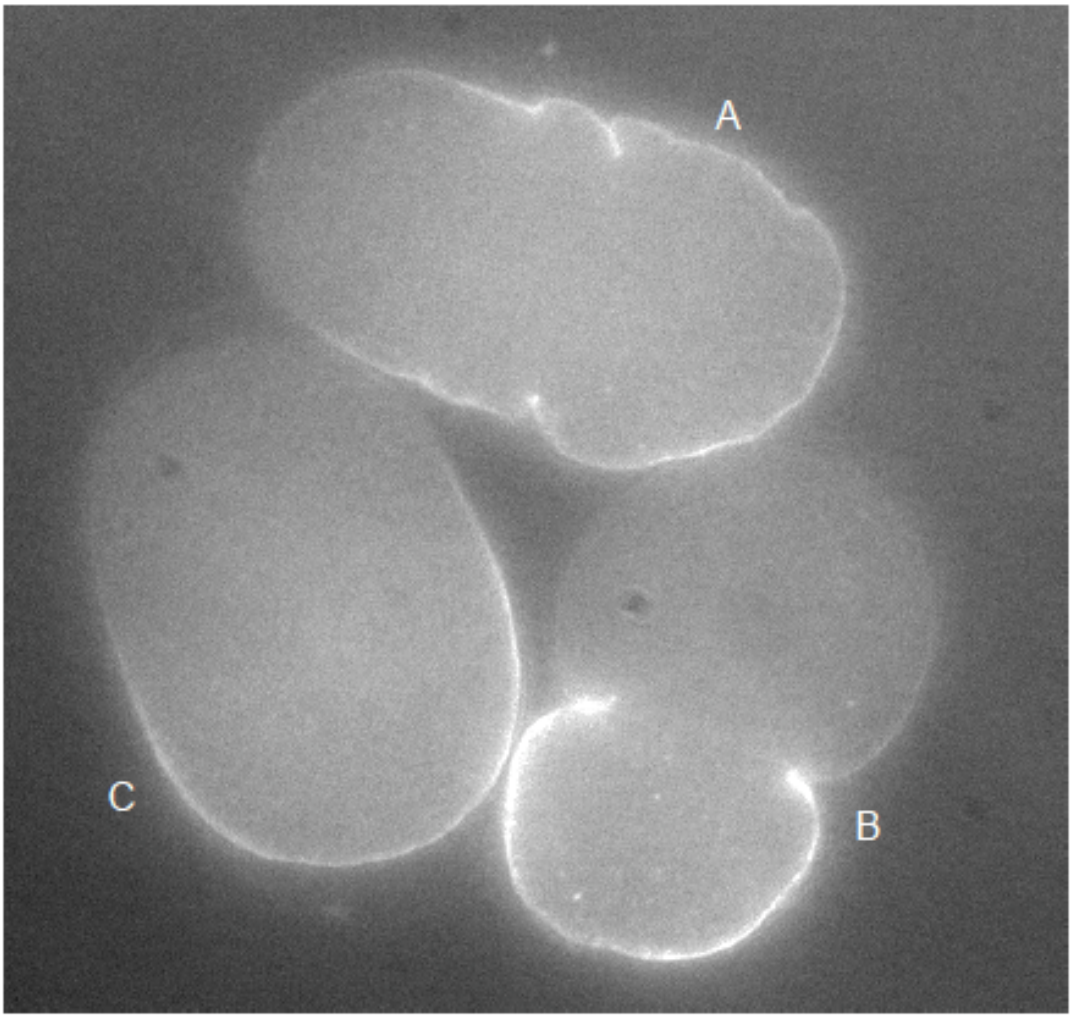

Fig. A.4.2. PAR-6^{S29A}::mCherry localizes asymmetrically in the early embryo. A wide field fluorescence micrograph showing embryos expressing PAR-6^{S29A}::mCherry (**A**) during polarity establishment, (**B**) at pseudocleavage, and (**C**) during mitosis.

APPENDIX 5

A.5. *C. elegans rcd-1* appears to be synthetic lethal with *par-2*

A.5.1. C. elegans rcd-1 was identified as an enhancer of par-1 and par-4

One of the strongest enhancers of *par-1* and *par-4* identified in a genome-wide RNAi screen was a highly conserved gene designated C26E6.3 (D. Morton, W. Hoose, and K. Kemphues, manuscript in preparation). Despite the high degree of conservation (Garces et al., 2007), relatively little is known about the role of the gene in higher eukaryotes. The protein was initially identified in *Schizosaccharomyces pombe* as being required for sexual differentiation in response to nitrogen starvation (Okazaki et al., 1998). Later structural and biochemical studies revealed that mammalian RCD-1 is armadillo-like-repeat protein capable of binding either single or double stranded nucleic acids (Garces et al., 2007), and associates with components of the CCR4-NOT transcriptional mediator complex (Chen et al., 2001; Garapaty et al., 2008; Haas et al., 2004). While these studies suggest RCD-1 family members are involved in transcriptional regulation, they do not preclude a role for the protein outside of the nucleus. In fact, members for the CCR4/POP2/NOT complex have been reported to be involved in asymmetrically localizing mRNA in the *Drosophila* embryo by mediating localized mRNA degradation (Semotok et al., 2005). Because of the sequence similarity between C26E6.3 and *S. pombe* RCD1, I will refer to C26E6.3 as *rcd-1*.

A.5.2. GFP::RCD-1 localizes to the cytoplasm of the one-cell embryo

To determine the subcellular localization of RCD-1, we generated transgenic lines expressing *gfp::rcd-1* under the control of the *pie-1* promoter and 3' UTR. In the

one-cell embryo, GFP::RCD-1 was diffusely cytoplasmic although some brighter puncta were observable in the vicinity of the mitotic spindle after centration (Fig. A.5.1).

A.5.3 C. elegans rcd-1 appears to be synthetic lethal with par-2

In addition to enhancing weak *par-1* and *par-4* mutants, RNAi depletion of *rcd-1* also enhances *par-2(it5ts)* at the permissive temperature (D. Morton, W. Hoose, and K. Kemphues, manuscript in preparation). To further study the phenotype of *par-2; rcd-1*, we made a line of the genotype *par-2(it5)/sC1[dpy-1(s2171)]; rcd-1(ok1728)*. The *ok1723* allele is a 790bp deletion plus a 31bp insertion that completely deletes exons 3 and 4. The allele likely to be a loss of function because, although *rcd-1(ok1728)* are mostly viable (5.4% embryonic lethality, n=332), the mutant is sensitive to *par-4(RNAi)*. In wild type, *par-4(RNAi)* resulted in 26.4% embryonic lethality (n=1176) while *rcd-1(ok1728); par-4(RNAi)* were 93.5% lethal (n=216, Fig. A.5.2). Similarly, the positive control, *par-1(zu310),* was only 4.5% lethal when treated with empty L4440 vector at the permissive temperature (n=920); however, *par-1(zu310); par-4(RNAi)* were 99.5% lethal (n=920, Fig. A.5.2).

Surprisingly, *par-2(it5); rcd-1(ok1728)* embryos appeared to be zygotic lethal. When the non-dpy progeny from *par-2(it5)/sC1; rcd-1* mothers were singled, we expected 1/3 of them to be homozygous for *par-2(it5)* and thus give no dpy progeny in the F1 generation (or possibly be maternal-effect lethal). However, all the F1 progeny segregated dpy progeny in the F2 generation indicating all the parental worms were of the genotype *par-2/sC1; rcd-1*. This segregation pattern suggested that *par-2; rcd-1*

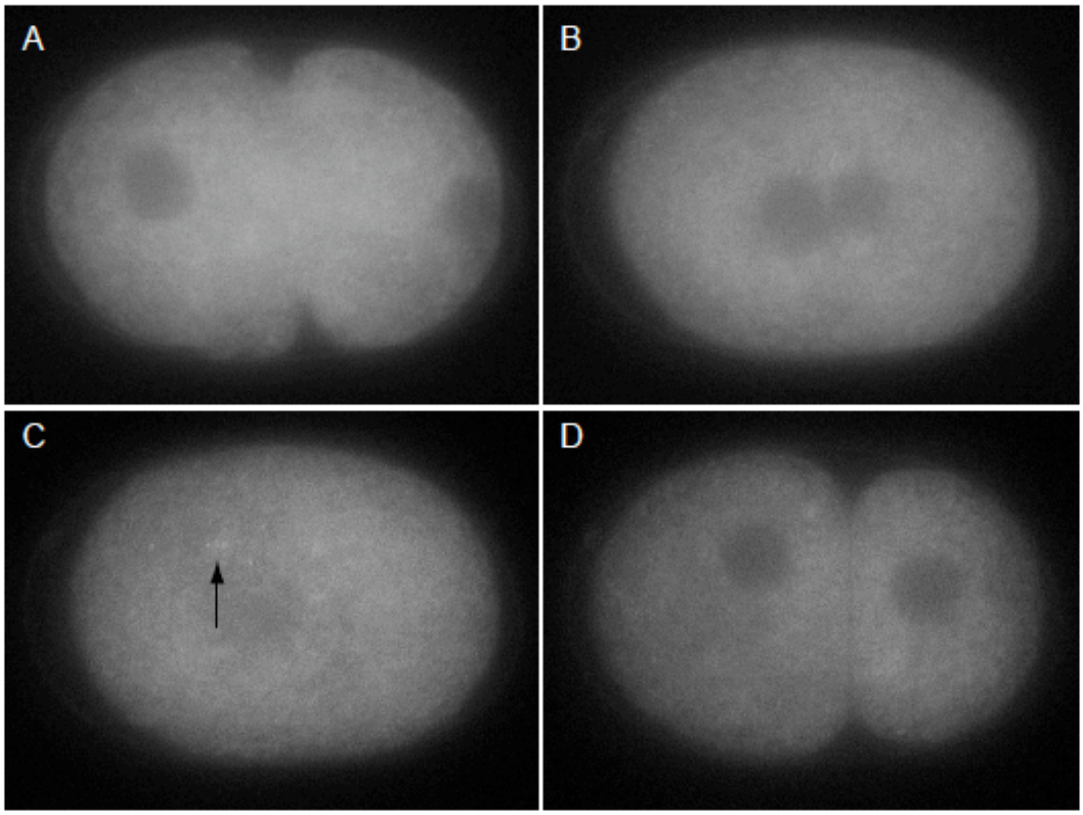

Fig. A.5.1. GFP::RCD-1 is localizes to the cytoplasm in the early embryo. Wide-field fluorescence images from time-lapse movie of an embryo expressing *gfp::rcd-1* at pseudocleavage (**A**), slightly before nuclear envelope breakdown (NEB) (**B**), slightly after NEB (**C**) and after the first mitotic division (**D**). The black arrow points to small puncta in the vicinity of the spindle asters.

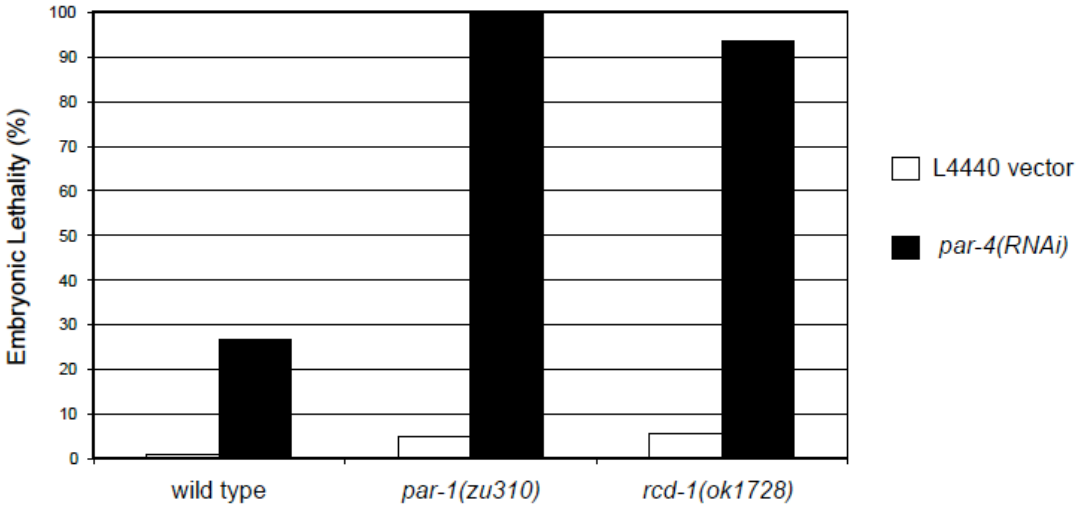

Fig. A.5.2. *rcd-1(ok1728)* are sensitive to *par-4(RNAi)*. Percentage embryonic lethality for wild type, *par-1(zu310),* and *rcd-1(ok1728)* when treated with either L4440 vector alone (white bars) or *par-4(RNAi)* (black bars).

may be zygotic lethal. Furthermore, embryos from *par-2/sC1; rcd-1* were 22.5±6.3% lethal (n=641), consistent with the expected 1/4 lethality expected if *par-2* homozygotes were zygotic lethal. To determine the terminal phenotype of the dead embryos, we dissected 2- and 4-cell embryos, mounted them, and allowed them to develop on an agar pad. After about 20hrs at 16°C, we examined the embryos using DIC microscopy and observed that 3/10 embryos had arrested prior to elongation but had some morphology (Fig. A.5.3).

Taken together, these data suggest that *par-2* may play a role zygotically, although currently we cannot rule out the possibility that there is another mutant gene in background of *par-2(it5)* that is synthetic lethal with *rcd-1*. We could exclude the latter possibility by coupling *rcd-1(ok1728)* with another *par-2* allele besides *it5*. If the second *par-2; rcd-1* double mutant is zygotic lethal, the phenotype is likely a result of a synthetic interaction between *par-2* and *rcd-1*.

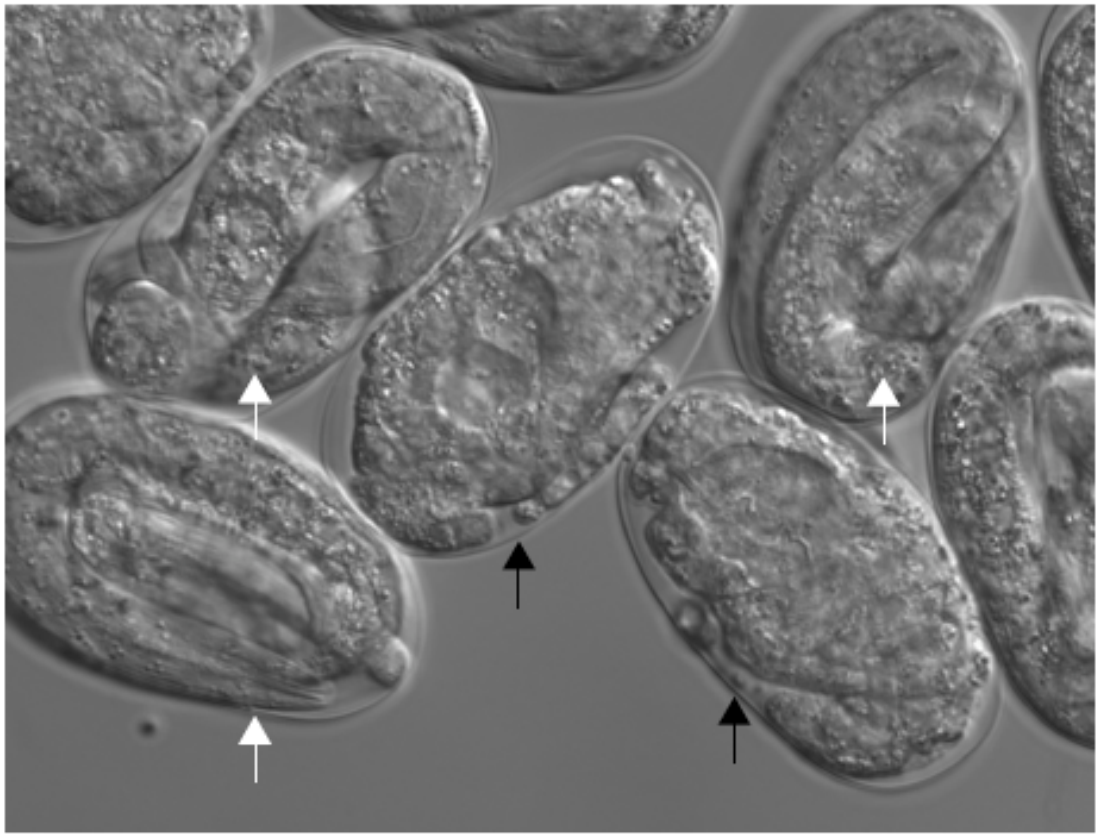

Fig. A.5.3. Approximately a quarter of embryos from *par-2/sC1; rcd-1* are embryonic lethal. A DIC image of five embryos from *par-2/sC1; rcd-1* that were allowed to develop at 16C for about 20hrs. The black arrows point to embryos that have failed embryogenesis while the white arrows point to sibling embryos that have nearly completed embryogenesis.

BIBLIOGRAPHY

Aceto, D., Beers, M. and Kemphues, K. J. (2006). Interaction of PAR-6 with CDC-42 is required for maintenance but not establishment of PAR asymmetry in C. elegans. *Dev Biol* **299**, 386-97.

Albertson, R. and Doe, C. Q. (2003). Dlg, Scrib and Lgl regulate neuroblast cell size and mitotic spindle asymmetry. *Nat Cell Biol* **5**, 166-70.

Atwood, S. X. and Prehoda, K. E. (2009). aPKC phosphorylates Miranda to polarize fate determinants during neuroblast asymmetric cell division. *Curr Biol* **19**, 723-9.

Beatty, A., Morton, D. and Kemphues, K. (2010). The C. elegans homolog of Drosophila Lethal giant larvae functions redundantly with PAR-2 to maintain polarity in the early embryo. *Development* **137**, 3995-4004.

Benton, R. and St Johnston, D. (2003). Drosophila PAR-1 and 14-3-3 inhibit Bazooka/PAR-3 to establish complementary cortical domains in polarized cells. *Cell* **115**, 691-704.

Betschinger, J., Eisenhaber, F. and Knoblich, J. A. (2005). Phosphorylation-induced autoinhibition regulates the cytoskeletal protein Lethal (2) giant larvae. *Curr Biol* **15**, 276-82.

Betschinger, J., Mechtler, K. and Knoblich, J. A. (2003). The Par complex directs asymmetric cell division by phosphorylating the cytoskeletal protein Lgl. *Nature* **422**, 326-30.

Bilder, D. (2004). Epithelial polarity and proliferation control: links from the Drosophila neoplastic tumor suppressors. *Genes Dev* **18**, 1909-25.

Bilder, D., Li, M. and Perrimon, N. (2000). Cooperative regulation of cell polarity and growth by Drosophila tumor suppressors. *Science* **289**, 113-6.

Boyd, L., Guo, S., Levitan, D., Stinchcomb, D. T. and Kemphues, K. J. (1996). PAR-2 is asymmetrically distributed and promotes association of P granules and PAR-1 with the cortex in C. elegans embryos. *Development* **122**, 3075-84.

Brenner, S. (1974). The genetics of Caenorhabditis elegans. *Genetics* **77**, 71-94.

Cheeks, R. J., Canman, J. C., Gabriel, W. N., Meyer, N., Strome, S. and Goldstein, B. (2004). C. elegans PAR proteins function by mobilizing and stabilizing asymmetrically localized protein complexes. *Curr Biol* **14**, 851-62.

Chen, J., Rappsilber, J., Chiang, Y. C., Russell, P., Mann, M. and Denis, C. L.

(2001). Purification and characterization of the 1.0 MDa CCR4-NOT complex identifies two novel components of the complex. *J Mol Biol* **314**, 683-94.
Cheng, N. N., Kirby, C. M. and Kemphues, K. J. (1995). Control of cleavage spindle orientation in Caenorhabditis elegans: the role of the genes par-2 and par-3. *Genetics* **139**, 549-59.

Cowan, C. R. and Hyman, A. A. (2004). Centrosomes direct cell polarity independently of microtubule assembly in C. elegans embryos. *Nature* **431**, 92-6.

Cuenca, A. A., Schetter, A., Aceto, D., Kemphues, K. and Seydoux, G. (2003). Polarization of the C. elegans zygote proceeds via distinct establishment and maintenance phases. *Development* **130**, 1255-65.

Doerflinger, H., Vogt, N., Torres, I. L., Mirouse, V., Koch, I., Nusslein-Volhard, C. and St Johnston, D. (2010). Bazooka is required for polarisation of the Drosophila anterior-posterior axis. *Development* **137**, 1765-73.

Etemad-Moghadam, B., Guo, S. and Kemphues, K. J. (1995). Asymmetrically distributed PAR-3 protein contributes to cell polarity and spindle alignment in early C. elegans embryos. *Cell* **83**, 743-52.

Fichelson, P., Jagut, M., Lepanse, S., Lepesant, J. A. and Huynh, J. R. (2010). Lethal giant larvae is required with the par genes for the early polarization of the Drosophila oocyte. *Development* **137**, 815-24.

Fire, A., Xu, S., Montgomery, M. K., Kostas, S. A., Driver, S. E. and Mello, C. C. (1998). Potent and specific genetic interference by double-stranded RNA in Caenorhabditis elegans. *Nature* **391**, 806-11.

Garapaty, S., Mahajan, M. A. and Samuels, H. H. (2008). Components of the CCR4-NOT complex function as nuclear hormone receptor coactivators via association with the NRC-interacting Factor NIF-1. *J Biol Chem* **283**, 6806-16.

Garces, R. G., Gillon, W. and Pai, E. F. (2007). Atomic model of human Rcd-1 reveals an armadillo-like-repeat protein with in vitro nucleic acid binding properties. *Protein Sci* **16**, 176-88.

Gateff, E. (1978). Malignant neoplasms of genetic origin in Drosophila melanogaster. *Science* **200**, 1448-59.

Goehring, N. W., Hoege, C., Grill, S. W. and Hyman, A. A. (2011). PAR proteins diffuse freely across the anterior-posterior boundary in polarized C. elegans embryos. *J Cell Biol* **193**, 583-94.

Goldstein, B. and Hird, S. N. (1996). Specification of the anteroposterior axis in Caenorhabditis elegans. *Development* **122**, 1467-74.

Goldstein, B. and Macara, I. G. (2007). The PAR proteins: fundamental players in animal cell polarization. *Dev Cell* **13**, 609-22.

Gonczy, P. (2008). Mechanisms of asymmetric cell division: flies and worms pave the way. *Nat Rev Mol Cell Biol* **9**, 355-66.

Goodrich, L. V. and Strutt, D. (2011). Principles of planar polarity in animal development. *Development* **138**, 1877-92.

Gotta, M., Abraham, M. C. and Ahringer, J. (2001). CDC-42 controls early cell polarity and spindle orientation in C. elegans. *Curr Biol* **11**, 482-8.

Guo, S. and Kemphues, K. J. (1995). par-1, a gene required for establishing polarity in C. elegans embryos, encodes a putative Ser/Thr kinase that is asymmetrically distributed. *Cell* **81**, 611-20.

Haas, M., Siegert, M., Schurmann, A., Sodeik, B. and Wolfes, H. (2004). c-Myb protein interacts with Rcd-1, a component of the CCR4 transcription mediator complex. *Biochemistry* **43**, 8152-9.

Hannak, E., Kirkham, M., Hyman, A. A. and Oegema, K. (2001). Aurora-A kinase is required for centrosome maturation in Caenorhabditis elegans. *J Cell Biol* **155**, 1109-16.

Hao, Y., Boyd, L. and Seydoux, G. (2006). Stabilization of cell polarity by the C. elegans RING protein PAR-2. *Dev Cell* **10**, 199-208.

Hattendorf, D. A., Andreeva, A., Gangar, A., Brennwald, P. J. and Weis, W. I. (2007). Structure of the yeast polarity protein Sro7 reveals a SNARE regulatory mechanism. *Nature* **446**, 567-71.

Hoege, C., Constantinescu, A. T., Schwager, A., Goehring, N. W., Kumar, P. and Hyman, A. A. (2010). LGL can partition the cortex of one-cell Caenorhabditis elegans embryos into two domains. *Curr Biol* **20**, 1296-303.

Hung, T. J. and Kemphues, K. J. (1999). PAR-6 is a conserved PDZ domain-containing protein that colocalizes with PAR-3 in Caenorhabditis elegans embryos. *Development* **126**, 127-35.

Hutterer, A., Betschinger, J., Petronczki, M. and Knoblich, J. A. (2004). Sequential roles of Cdc42, Par-6, aPKC, and Lgl in the establishment of epithelial polarity during Drosophila embryogenesis. *Dev Cell* **6**, 845-54.

Hyenne, V., Desrosiers, M. and Labbe, J. C. (2008). C. elegans Brat homologs regulate PAR protein-dependent polarity and asymmetric cell division. *Dev Biol* **321**, 368-78.

Jenkins, N., Saam, J. R. and Mango, S. E. (2006). CYK-4/GAP provides a localized cue to initiate anteroposterior polarity upon fertilization. *Science* **313**, 1298-301.

Kay, A. J. and Hunter, C. P. (2001). CDC-42 regulates PAR protein localization and function to control cellular and embryonic polarity in C. elegans. *Curr Biol* **11**, 474-81.

Kemphues, K. J., Priess, J. R., Morton, D. G. and Cheng, N. S. (1988). Identification of genes required for cytoplasmic localization in early C. elegans embryos. *Cell* **52**, 311-20.

Kirby, C.M. (1992). Cytoplasmic Reorganization and the Generation of Asymmetry in Caenorhabditis Elegans, with an Emphasis on par-3, a Maternal-Effect Gene Essential for both Processes. Thesis Dissertation. Cornell University.

Knoblich, J. A. (2008). Mechanisms of asymmetric stem cell division. *Cell* **132**, 583-97.

Kumfer, K. T., Cook, S. J., Squirrell, J. M., Eliceiri, K. W., Peel, N., O'Connell, K. F. and White, J. G. (2010). CGEF-1 and CHIN-1 regulate CDC-42 activity during asymmetric division in the Caenorhabditis elegans embryo. *Mol Biol Cell* **21**, 266-77.

Lee, M. and Vasioukhin, V. (2008). Cell polarity and cancer--cell and tissue polarity as a non-canonical tumor suppressor. *J Cell Sci* **121**, 1141-50.

Levitan, D. J., Boyd, L., Mello, C. C., Kemphues, K. J. and Stinchcomb, D. T. (1994). par-2, a gene required for blastomere asymmetry in Caenorhabditis elegans, encodes zinc-finger and ATP-binding motifs. *Proc Natl Acad Sci U S A* **91**, 6108-12.

Li, J., Kim, H., Aceto, D. G., Hung, J., Aono, S. and Kemphues, K. J. (2010). Binding to PKC-3, but not to PAR-3 or to a conventional PDZ domain ligand, is required for PAR-6 function in C. elegans. *Dev Biol* **340**, 88-98.

Liu, J., Maduzia, L. L., Shirayama, M. and Mello, C. C. (2010). NMY-2 maintains cellular asymmetry and cell boundaries, and promotes a SRC-dependent asymmetric cell division. *Dev Biol* **339**, 366-73.

Maduro, M. and Pilgrim, D. (1995). Identification and cloning of unc-119, a gene expressed in the Caenorhabditis elegans nervous system. *Genetics* **141**, 977-88.

Mayer, M., Depken, M., Bois, J. S., Julicher, F. and Grill, S. W. (2010). Anisotropies in cortical tension reveal the physical basis of polarizing cortical flows. *Nature* **467**, 617-21.

Moore, R. and Boyd, L. (2004). Analysis of RING finger genes required for embryogenesis in C. elegans. *Genesis* **38**, 1-12.

Morton, D. G., Shakes, D. C., Nugent, S., Dichoso, D., Wang, W., Golden, A. and Kemphues, K. J. (2002). The Caenorhabditis elegans par-5 gene encodes a 14-3-3 protein required for cellular asymmetry in the early embryo. *Dev Biol* **241**, 47-58.

Motegi, F. and Seydoux, G. (2007). Revisiting the role of microtubules in C. elegans polarity. *J Cell Biol* **179**, 367-9.

Motegi, F. and Sugimoto, A. (2006). Sequential functioning of the ECT-2 RhoGEF, RHO-1 and CDC-42 establishes cell polarity in Caenorhabditis elegans embryos. *Nat Cell Biol* **8**, 978-85.

Munro, E. and Bowerman, B. (2009). Cellular symmetry breaking during Caenorhabditis elegans development. *Cold Spring Harb Perspect Biol* **1**, a003400.

Munro, E., Nance, J. and Priess, J. R. (2004). Cortical flows powered by asymmetrical contraction transport PAR proteins to establish and maintain anterior-posterior polarity in the early C. elegans embryo. *Dev Cell* **7**, 413-24.

Musch, A., Cohen, D., Yeaman, C., Nelson, W. J., Rodriguez-Boulan, E. and Brennwald, P. J. (2002). Mammalian homolog of Drosophila tumor suppressor lethal (2) giant larvae interacts with basolateral exocytic machinery in Madin-Darby canine kidney cells. *Mol Biol Cell* **13**, 158-68.

Nakayama, Y., Shivas, J. M., Poole, D. S., Squirrell, J. M., Kulkoski, J. M., Schleede, J. B. and Skop, A. R. (2009). Dynamin participates in the maintenance of anterior polarity in the Caenorhabditis elegans embryo. *Dev Cell* **16**, 889-900.

Nance, J., Munro, E. M. and Priess, J. R. (2003). C. elegans PAR-3 and PAR-6 are required for apicobasal asymmetries associated with cell adhesion and gastrulation. *Development* **130**, 5339-50.

Nance, J. and Zallen, J. A. (2011). Elaborating polarity: PAR proteins and the cytoskeleton. *Development* **138**, 799-809.

Nilsson, L., Conradt, B., Ruaud, A. F., Chen, C. C., Hatzold, J., Bessereau, J. L., Grant, B. D. and Tuck, S. (2008). Caenorhabditis elegans num-1 negatively regulates endocytic recycling. *Genetics* **179**, 375-87.

Okazaki, N., Okazaki, K., Watanabe, Y., Kato-Hayashi, M., Yamamoto, M. and Okayama, H. (1998). Novel factor highly conserved among eukaryotes controls sexual development in fission yeast. *Mol Cell Biol* **18**, 887-95.

Ohshiro, T., Yagami, T., Zhang, C. and Matsuzaki, F. (2000). Role of cortical tumour-suppressor proteins in asymmetric division of Drosophila neuroblast. *Nature* **408**, 593-6.

Peng, C. Y., Manning, L., Albertson, R. and Doe, C. Q. (2000). The tumour-

suppressor genes lgl and dlg regulate basal protein targeting in Drosophila neuroblasts. *Nature* **408**, 596-600.

Pereira-Leal, J. B. and Seabra, M. C. (2001). Evolution of the Rab family of small GTP-binding proteins. *J Mol Biol* **313**, 889-901.

Piekny, A. J. and Mains, P. E. (2002). Rho-binding kinase (LET-502) and myosin phosphatase (MEL-11) regulate cytokinesis in the early Caenorhabditis elegans embryo. *J Cell Sci* **115**, 2271-82.

Plant, P. J., Fawcett, J. P., Lin, D. C., Holdorf, A. D., Binns, K., Kulkarni, S. and Pawson, T. (2003). A polarity complex of mPar-6 and atypical PKC binds, phosphorylates and regulates mammalian Lgl. *Nat Cell Biol* **5**, 301-8.

Praitis, V., Casey, E., Collar, D. and Austin, J. (2001). Creation of low-copy integrated transgenic lines in Caenorhabditis elegans. *Genetics* **157**, 1217-26.

Prehoda, K. E. and Bowerman, B. (2010). Cell polarity: keeping worms LeGaL. *Curr Biol* **20**, R646-8.

Riento, K. and Ridley, A. J. (2003). Rocks: multifunctional kinases in cell behaviour. *Nat Rev Mol Cell Biol* **4**, 446-56.

Schneider, S. Q. and Bowerman, B. (2003). Cell polarity and the cytoskeleton in the Caenorhabditis elegans zygote. *Annu Rev Genet* **37**, 221-49.

Schonegg, S., Constantinescu, A. T., Hoege, C. and Hyman, A. A. (2007). The Rho GTPase-activating proteins RGA-3 and RGA-4 are required to set the initial size of PAR domains in Caenorhabditis elegans one-cell embryos. *Proc Natl Acad Sci U S A* **104**, 14976-81.

Schonegg, S. and Hyman, A. A. (2006). CDC-42 and RHO-1 coordinate acto-myosin contractility and PAR protein localization during polarity establishment in C. elegans embryos. *Development* **133**, 3507-16.

Schubert, C. M., Lin, R., de Vries, C. J., Plasterk, R. H. and Priess, J. R. (2000). MEX-5 and MEX-6 function to establish soma/germline asymmetry in early C. elegans embryos. *Mol Cell* **5**, 671-82.

Schumacher, J. M., Ashcroft, N., Donovan, P. J. and Golden, A. (1998). A highly conserved centrosomal kinase, AIR-1, is required for accurate cell cycle progression and segregation of developmental factors in Caenorhabditis elegans embryos. *Development* **125**, 4391-402.

Semotok, J. L., Cooperstock, R. L., Pinder, B. D., Vari, H. K., Lipshitz, H. D. and Smibert, C. A. (2005). Smaug recruits the CCR4/POP2/NOT deadenylase complex to trigger maternal transcript localization in the early Drosophila embryo. *Curr Biol* **15**,

284-94.

Sonnichsen, B., Koski, L. B., Walsh, A., Marschall, P., Neumann, B., Brehm, M., Alleaume, A. M., Artelt, J., Bettencourt, P., Cassin, E. et al. (2005). Full-genome RNAi profiling of early embryogenesis in Caenorhabditis elegans. *Nature* **434**, 462-9.

Sripathy, S., Lee, M. and Vasioukhin, V. (2011). Mammalian Llgl2 Is Necessary for Proper Branching Morphogenesis during Placental Development. *Mol Cell Biol* **31**, 2920-33.

Stenmark, H. (2009). Rab GTPases as coordinators of vesicle traffic. *Nat Rev Mol Cell Biol* **10**, 513-25.

Strand, D., Jakobs, R., Merdes, G., Neumann, B., Kalmes, A., Heid, H. W., Husmann, I. and Mechler, B. M. (1994). The Drosophila lethal(2)giant larvae tumor suppressor protein forms homo-oligomers and is associated with nonmuscle myosin II heavy chain. *J Cell Biol* **127**, 1361-73.

Strand, D., Unger, S., Corvi, R., Hartenstein, K., Schenkel, H., Kalmes, A., Merdes, G., Neumann, B., Krieg-Schneider, F., Coy, J. F. et al. (1995). A human homologue of the Drosophila tumour suppressor gene l(2)gl maps to 17p11.2-12 and codes for a cytoskeletal protein that associates with nonmuscle myosin II heavy chain. *Oncogene* **11**, 291-301.

St Johnston, D. and Ahringer, J. (2010). Cell polarity in eggs and epithelia: parallels and diversity. *Cell* **141**, 757-74.

Suzuki, A. and Ohno, S. (2006). The PAR-aPKC system: lessons in polarity. *J Cell Sci* **119**, 979-87.

Tabuse, Y., Izumi, Y., Piano, F., Kemphues, K. J., Miwa, J. and Ohno, S. (1998). Atypical protein kinase C cooperates with PAR-3 to establish embryonic polarity in Caenorhabditis elegans. *Development* **125**, 3607-14.

Tanentzapf, G. and Tepass, U. (2003). Interactions between the crumbs, lethal giant larvae and bazooka pathways in epithelial polarization. *Nat Cell Biol* **5**, 46-52.

Tenlen, J. R., Molk, J. N., London, N., Page, B. D. and Priess, J. R. (2008). MEX-5 asymmetry in one-cell C. elegans embryos requires PAR-4- and PAR-1-dependent phosphorylation. *Development* **135**, 3665-75.

Tian, A. G. and Deng, W. M. (2008). Lgl and its phosphorylation by aPKC regulate oocyte polarity formation in Drosophila. *Development* **135**, 463-71.

Timmons, L. and Fire, A. (1998). Specific interference by ingested dsRNA. *Nature* **395**, 854.

Tsai, M. C. and Ahringer, J. (2007). Microtubules are involved in anterior-posterior axis formation in C. elegans embryos. *J Cell Biol* **179**, 397-402.

Vasioukhin, V. (2006). Lethal giant puzzle of Lgl. *Dev Neurosci* **28**, 13-24.

Velarde, N., Gunsalus, K. C. and Piano, F. (2007). Diverse roles of actin in C. elegans early embryogenesis. *BMC Dev Biol* **7**, 142.

Wallenfang, M. R. and Seydoux, G. (2000). Polarization of the anterior-posterior axis of C. elegans is a microtubule-directed process. *Nature* **408**, 89-92.

Warming, S., Costantino, N., Court, D. L., Jenkins, N. A. and Copeland, N. G. (2005). Simple and highly efficient BAC recombineering using galK selection. *Nucleic Acids Res* **33**, e36.

Watts, J. L., Etemad-Moghadam, B., Guo, S., Boyd, L., Draper, B. W., Mello, C. C., Priess, J. R. and Kemphues, K. J. (1996). par-6, a gene involved in the establishment of asymmetry in early C. elegans embryos, mediates the asymmetric localization of PAR-3. *Development* **122**, 3133-40.

Watts, J. L., Morton, D. G., Bestman, J. and Kemphues, K. J. (2000). The C. elegans par-4 gene encodes a putative serine-threonine kinase required for establishing embryonic asymmetry. *Development* **127**, 1467-75.

Wirtz-Peitz, F. and Knoblich, J. A. (2006). Lethal giant larvae take on a life of their own. *Trends Cell Biol* **16**, 234-41.

Wirtz-Peitz, F., Nishimura, T. and Knoblich, J. A. (2008). Linking cell cycle to asymmetric division: Aurora-A phosphorylates the Par complex to regulate Numb localization. *Cell* **135**, 161-73.

Yamanaka, T., Horikoshi, Y., Sugiyama, Y., Ishiyama, C., Suzuki, A., Hirose, T., Iwamatsu, A., Shinohara, A. and Ohno, S. (2003). Mammalian Lgl forms a protein complex with PAR-6 and aPKC independently of PAR-3 to regulate epithelial cell polarity. *Curr Biol* **13**, 734-43.

Zonies, S., Motegi, F., Hao, Y. and Seydoux, G. (2010). Symmetry breaking and polarization of the C. elegans zygote by the polarity protein PAR-2. *Development* **137**, 1669-77.